UNIVERSITY OF CALIFORNIA,
IRVINE

Wildfires in California's Sierra Nevada Mountains: Fuels, Emissions, and Management Strategies

DISSERTATION

submitted in partial satisfaction of the requirements
for the degree of

DOCTOR OF PHILOSOPHY

in Earth System Science

by

Audrey Odwuor

Dissertation Committee:
Professor James T. Randerson, co-Chair
Professor Claudia I. Czimczik, co-Chair
Distinguished Professor, Ellen R.M. Druffel
Associate Professor, Tirtha Banerjee

2023

DEDICATION

To my mom, my sisters, and Gueli. I would not be here without the support and love they have given me every day. Las quiero mas alla que los limites del amor.

TABLE OF CONTENTS

LIST OF FIGURES

LIST OF TABLES

ACKNOWLEDGEMENTS

I first acknowledge that much of the work included in this dissertation was conducted on the unceded homelands of the Acjachemen and Tongva peoples who, in the face of on-going settler colonialism, maintain stewardship of and enduring relationship with their ancestral lands as they have for the past 8,000 years.

I would like to thank my advisors, Drs. James T. Randerson and Claudia I. Czimczik, for their guidance and support over the course of my PhD. I am especially grateful for their willingness to let me explore creative outreach and professional development opportunities in addition to the activities that would help me develop as a researcher. I hope that the future of academia includes a greater recognition that for PhD students, technical training and intellect are only a fraction of what will make us trusted experts and leaders.

I am also grateful for my thesis committee members, Drs. Ellen R.M. Druffel and Tirtha Banerjee, and advancement committee members Drs. Paulo Brando and Celia Faiola, whose feedback allowed me to think about my work from a new perspective. Thank you to the Czimczik, Randerson, and AMS labs for supporting my analyses and providing feedback on my research.

In addition, I thank Drs. Chelsea Corr-Limoges and Rob Griffin, who advised me as an undergraduate researcher and whose support and patience helped me developed the interest I have today in wildfire science and the belief that I could conduct meaningful research. I also thank Dr. Caroline A. Masiello, who hired me as a post-baccalaureate research assistant. She always fostered a positive work environment and set the example of a great mentor.

My interest in science began at a young age, and the mentorship and community I received as an undergraduate in the Rice Emerging Scholars Program (RESP) continually inspired me to believe in myself and persist through all challenges I would face in academia and STEM. I give a special thanks to Megan McSpedon, who was the director of RESP during my time at Rice University. I am also endlessly grateful for the NASA Student Airborne Research Program, via which I conducted my first Earth science research project, first began considering a PhD, and have met many of the colleagues and friends whose support has truly been critical to my experience as a grad student. In addition, I thank CLEAN, UCI Graduate Division, the American Geophysical Union Voices for Science Program, KUCI, the team at Earth Calling Show, and the ADDSTEAM Foundation for helping me engage with my community, explore my creative side, and develop into the science communicator I am today.

I would like to thank my labmates past and current – especially the Lab Girls – my cohort, my fellow ESS graduate students, my collaborators, and my friends and colleagues at other institutions, without whose support and solidarity I could not have completed this degree.

Lastly, I would like to express my deepest appreciation for my friends, partner, and family for their love, patience, and support. Thank you to all my friends all around the world – especially Christine, Yvette, Javi, Romeo, Peter, Ariana, Niky, Kyle, Liz, Adrien, Alex, Dani, Ben, Shivani, Dean, and Jo – for always being supportive and good friends despite the huge geographical distances between

some of us. I'm especially thankful for Liz and Luna being great roommates for almost three years. Thank you to my partner Joe for being there when I needed encouragement and support. Thank you to Tio, Minda, Alix, Matthew, Lauren, Ivy, and my extended family for being supportive and sharing how proud they are of me. I am especially grateful for my mom, my sisters, and Gueli for always believing in me, often more than I believed in myself. I thank them for supporting my big move to Houston for college, and then even bigger move to California to continue pursuing what I love. It's been challenging to be apart from my family in pursuit of my career and their unwavering support allows me to truly feel good about the work I do.

This work was funded in part by the Jenkins Foundation Fellowship, UCI Graduate Division fellowships and awards, NSF Grant DGE-1839285, and the ADDSTEAM Foundation.

Chapter 3 of this dissertation was adapted from the 2023 text "Evidence for multi-decadal fuel buildup in a large California wildfire from smoke measurements" *Environmental Research Letters* 18(9), 094030. doi: 10.1088/1748-9326/aced17, with permission from IOP Publishing. The co-authors listed on this publication are Yañez, C., Moreno, A., Chen, Y., Xu, X., Hopkins, F.M., Czimczik, C. I., Randerson, J. T.

The co-authors James T. Randerson and Claudia I. Czimczik directed and supervised research which forms the basis for the dissertation.

VITA

Audrey Odwuor (she, her, hers)
University of California, Irvine Department of Earth System Science

Education

2018 - 2023	**Ph.D., Earth System Science**, University of California, Irvine Dissertation: Wildfires in California's Sierra Nevada Mountains: Fuels, Emissions, and Management Strategies Advisors: Claudia I. Czimczik, James T. Randerson
2018 - 2020	**M.S., Earth System Science,** University of California, Irvine
2013 - 2017	**B.S., Earth Science** (Geochemistry Concentration), Rice University

Fellowships, Honors, and Awards

2023	**Scholar,** ADDSTEAM Foundation
2023	**Second Place Winner,** University of California, Irvine Grad Slam 2023
2022	**Graduate Student Engagement Fellow,** California Wildfire and Forest Resilience Task Force
2022	**Voices for Science Media/Communications Advocate,** American Geophysical Union
2022	**Finalist,** University of California, Irvine Grad Slam 2022
2020	**Outstanding Contributions to the Department,** Univ. of California, Irvine Dept. of Earth System Science
2020	**Graduate Research Fellowship,** National Science Foundation
2018	**Eugene Cota Robles Fellowship,** University of California, Irvine
2018	**Nevin Graduate Endowment Fellowship,** University of California, Irvine
2018	**Diversity Recruitment Fellowship,** University of California, Irvine
2017	**Mae C. Jemison Award for Academic Achievement and Public Service,** Rice University
2017	**Eugene Merten Memorial Prize in Geophysics,** Rice University
2016	**Outstanding Student Paper Award – Namais Travel Grant**, American Geophysical Union
2016	**Best Earth Science Presentation,** Gulf Coast Undergraduate Research Symposium
2014	**Sustaining Excellence in Research Program Scholar,** Rice University
2013	**Rice Emerging Scholars Program Scholar,** Rice University

Peer-Reviewed Publications

Odwuor, A. Welch, A. M., Czimczik, C. I., Randerson, J.T., Xu, X., York, R., Banerjee, T. Large-diameter dead fuel classes as drivers of $PM_{2.5}$ emissions from prescribed fire in California. (in prep)

Odwuor, A., Yañez, C., Moreno, A., Chen, Y., Xu, X., Hopkins, F.M., Czimczik, C. I., Randerson, J. T. (2023) Evidence for multi-decadal fuel buildup in a large California

wildfire from smoke measurements. *Environmental Research Letters, 18(9),* 094030. doi: 10.1088/1748-9326/aced17

Research Experience

Sept 2018- **Graduate Student Researcher,** *University of California, Irvine Department of Earth System Science*
Utilize field, laboratory, and modeling techniques to understand fuel consumption and emissions in wildfires and prescribed fires in California in collaboration with scientists at NASA Langley Research Center, The University of California, Riverside, and Blodgett Forest Research Station

Sept 2017- May 2018 **Research Assistant,** *Masiello Group, Rice University Dept. of Earth, Environmental and Planetary Sciences*
Designed and published group website, mentored undergraduate group members, and assisted with the development and execution of projects in soil science, synthetic microbiology, and indoor air quality

Jun 2017- Aug 2017 **Independent Consultant,** *NASA DEVELOP National Program*
Enhanced the Texas Commission on Environmental Quality's capacity for investigating exceptional air quality events by creating a 3D wildfire aerosol transport map and technical report using NASA Earth Observations on a team of four scientists
Represented NASA Earth Science at 2017 VA/KY District Fair

Aug 2016- May 2017 **Undergraduate Researcher,** *Griffin Group, Rice University Dept. of Civil and Environmental Engineering*
Analyzed data from several NASA airborne missions to investigate the spectral dependence of wildfire-emitted aerosol optical properties

Jun 2016- Aug 2016 **Independent Researcher,** *NASA Student Airborne Research Program*
Collected measurements of atmospheric species aboard NASA DC-8 aircraft, designed a project to investigate the spectral dependence of wildfire aerosol optical properties using airborne data, and presented findings at program closeout

Feb 2015- Aug 2016 **Project Intern,** *Baylor College of Medicine Cardiothoracic Surgery Research Lab*
Investigated signaling pathways in aortic destruction, healing, and remodeling to develop a pharmaceutical treatment for vascular diseases

Communications, Outreach, and Service

Jan 2022- **Peer Mentor,** Rice Engineering Alumni
Mentor undergraduate Rice University engineering students to help launch their professional careers

Jan 2021- **Peer Mentor,** *Science Champions for Change*
Provide individual mentoring in bi-weekly meetings with community college STEM student pursuing transfer to the University of California and aid in the transition to a four-year university while maintaining personal, social, and academic wellbeing

Jun 2022- Jun 2023 **Professional Development Lead,** *University of California, Irvine Dept. of Earth System Science*

	Worked with co-lead to integrate role into department Graduate Student Leadership Team and tracked campus-wide professional development opportunities and disseminated among department
Sept 2020-Jun 2023	**Executive Board Member,** *Climate Literacy, Empowerment and iNquiry (501(c)(3) non-profit organization)* Collaboratively created and led monthly virtual presentations and interactive activities with STEM teachers, other board members, and student members for underserved middle school students (~25 students per class)
Aug 2022-April 2023	**Co-Host and Producer,** *Earth Calling Radio Show on KUCI 88.9 FM, Irvine* Produced show centered around topics in climate change/environmental justice Co-managed show social media accounts, recruited guest speakers and collaborated with two co-hosts to create weekly show schedule, conduct interviews, broadcast live shows, and edit and disseminate recorded shows Trained in audio equipment operation, Federal Communications Commission rules and regulations, and live broadcasting
Mar 2022-Mar 2023	**Media/Communications Advocate**, *American Geophysical Union Voices for Science* Communicated the value of Earth and space science research and science-based policy to decision-makers, journalists, and the public by engaging in regular outreach activities and creating content for digital media/multimedia
Sept 2021-Sept 2022	**Trainee Council Member,** *Graduate Professional Success for PhD Students and Postdocs in STEM* Developed and executed career and professional development programming with faculty leadership and fellow Trainees
Sept 2018-Sept 2020	**Student Member,** *Climate Literacy, Empowerment and iNquiry (CLEAN) Education* Co-led in-person and virtual lessons on climate change (~monthly) to underserved middle school students (~25 students per class) and led scientific demonstrations as part of 2019 Annual Earth Science Day for local students and members of the community
Aug 2019-June 2020	**Peer Mentor,** *University of California Dept. of Earth System Science* Advised first-year graduate students via monthly meetings to ensure personal, social, and academic wellbeing
April 2019-Jun 2020	**Graduate Student Representative,** *University of California, Irvine Dept. of Earth System Science* Collaborated regularly with other graduate student representatives and department faculty and staff to coordinate the department peer mentoring program, hosted quarterly graduate student body townhall meetings, lead department tours/information sessions, and organized weekly to quarterly social/bonding events for the department and graduate student body
Dec 2016-May 2017	**Chair of Scholarly Activities Committee,** *Texans for Climate Change Action* Led committee in researching and disseminating information about climate science and policy and engaged with university faculty, political officials, and other organizations focused on climate research and activism
May 2016-	**Education Assistant,** *Rice University Emergency Medical Services (EMS)*

May 2017	Provided mentorship and academic assistance to students (~36 per class) enrolled in EMT-Basic training at Rice University and assisted in planning and execution of large-scale practice drills and national certification exams
Sept 2015- May 2017	**Rice Firsts Mentor,** *Rice University First Year Programs* Mentored first-year students attending Rice University who self-identified as first-generation college students
Jun 2015- Aug 2015	**Head Fellow,** *Rice Emerging Scholars Program* Mentored 26 incoming first-year STEM students, aiding in social and academic transitions to the depth, rigor, and pace of STEM at Rice; organized and led tutoring sessions, study groups, and social events; and worked with Rice faculty and other STEM educators to adjust student workload and gauge performance throughout the program

Teaching Experience

Sept 2019- Jun 2020	**Teaching Assistant,** *Univ. of California, Irvine Dept. of Earth System Science* Trained in pedagogy, best practices for teaching STEM, diversity issues in STEM fields, and distance learning to help design and lead in-person and virtual laboratory experiments for undergraduates (~30 per session) in Earth system biology and chemistry and physical geology and provide individual and group academic assistance for students
Dec 2016- May 2017	**Teaching Assistant,** *Rice University Student Success Initiatives* Co-instructed course entitled "Foundations for Self-Discovery and Lifelong Learning" and helped create curriculum with staff from Rice Student Success Initiatives to help first-year students navigate resources at Rice while maintaining personal, social, and academic wellbeing

Other Professional Experience

Oct 2015- May 2018	**Special Events EMT,** *Rice University EMS* Responded to emergencies during special events (sporting events, Baker Institute for Public Policy events, etc.)
Jun 2015- May 2018	**CPR and Basic Life Support Instructor,** *Rice University EMS* Taught American Heart Association CPR and basic life support to Rice students, faculty/staff and members of the community (up to 36 students per class)
Oct 2014- May 2017	**Duty Crew EMT,** *Rice University EMS* Volunteered as an EMT with Rice EMS, providing coverage in 12-hour shifts and responding to emergencies on campus

Workshops, Certificates, etc.

2022	**Emotional Intelligence for Management,** University of California, Irvine Graduate Division
2022	**Science Communication Skills for STEM Scientists**, University of California, Irvine GPS-STEM/Loh Down on Science

2021	**Inclusive Excellence Certificate,** University of California, Irvine Office of Inclusive Excellence
2020	**R Programming for Data Science,** edX
2019	**Using Satellite Observations to Advance Climate Models**, NASA's Earth Observations Summer School
2019	**Radiocarbon in Ecology and Earth System Science Short Course,** Univ. of California, Irvine Dept. of Earth System Science

Academic and Professional Society Membership

2022-23	**Member,** International Association of Wildland Fire
2021-	**Member,** Association for Women in Science
2021-22	**Executive Board Member,** UCI Graduate Professional Success for PhD Students and Postdocs in STEM
2018-	**Member,** UCI Diverse Educational Community and Doctoral Experience
2017-	**Member,** Earth Science Women's Network
2016-	**Member,** American Geophysical Union
2016-17	**Treasurer,** Rice Undergraduate Geosciences Society

Conference and Seminar Presentations

Odwuor, A., Yañez, C., Moreno, A., Chen, Y., Xu, X., Hopkins, F.M., Czimczik, C. I., Randerson, J. T. "Evidence for multi-decadal fuel buildup in a large California wildfire from smoke measurements." International Association of Wildland Fire, Fire and Climate 2022, June 2022. (poster)

Odwuor, A., Anderson, B., Czimczik, C. I., Randerson, J. T., Wiggins, E. B., Xu, X. "Using radiocarbon as a constraint on fuel consumption during the 2019 western U.S. fire season." American Geophysical Union Fall Meeting 2021, Dec 2021. (oral)

Odwuor, A., Anderson, B., Czimczik, C. I., Randerson, J. T., Wiggins, E. B., Xu, X. "Using radiocarbon measurements of PM2.5 to constrain fuel consumption in western U.S. wildfires." UCI Department of Earth System Science Half-Baked Seminar, Nov 2021. (oral)

Odwuor, A., Anderson, B., Czimczik, C. I., Randerson, J. T., Wiggins, E. B., Xu, X. "Using radiocarbon measurements of PM2.5 to constrain fuel consumption in western U.S. wildfires." AirUCI Internal Seminar, Nov 2021. (oral)

Odwuor, A., Czimczik, C. I., Randerson, J. T., Xu, X. "Characterizing carbonaceous aerosol in the Brazilian Amazon using isotopic analyses". 2nd Annual Radiocarbon Summit, NASA Jet Propulsion Laboratory Carbon Cycle and Ecosystems Group, Feb 2020. (oral)

Odwuor, A., Czimczik, C. I., Randerson, J. T., Xu, X. "Characterizing carbonaceous aerosol in the Brazilian Amazon using isotopic analyses". NASA Jet Propulsion Laboratory Earth Observations Summer School, Aug 2019. (oral)

Odwuor, A., Corr, C. A., Griffin, R. J., Pusede, S., Anderson, B. E., Beyersdorf, A. J., Campuzano-Jost, P., Chen, G., Day, D.A., DiGangi, J., Diskin, G., Jimenez, J., Moore, R. H., Nault, B. A., Schwarz, J. P., Shook, M., Thornhill, K. L., Winstead, E., Wisthaler, A., and Ziemba, L. D. "Utilizing NASA Airborne Data to Investigate the Influence of Fuel Type on Biomass Burning Aerosol Properties". 2018 Graduate Climate Conference, Nov 2018. (poster)

Odwuor, A., Griffin, R. J., Pusede, S., Anderson, B. E., Beyersdorf, A. J., Campuzano-Jost, P., Chen, G., Day, D.A., DiGangi, J., Diskin, G., Jimenez, J., Moore, R. H., Nault, B. A., Schwarz, J. P., Shook, M., Thornhill, K. L., Winstead, E., Wisthaler, A., and Ziemba, L. D. "Utilizing NASA Airborne Data to Investigate the Influence of Fuel Type on Biomass Burning Aerosol Properties". American Geophysical Union Fall Meeting 2017, Dec 2017. (poster)

White, E., Colley, B., Kolandaivelu, K., **Odwuor, A.** "Monitoring Exceptional Air Pollution Events in Texas Using NASA Earth Observations". American Geophysical Union Fall Meeting 2017, Dec 2017. (poster)

White, E., Colley, B., Kolandaivelu, K., **Odwuor, A.** "Monitoring Exceptional Air Pollution Events in Texas Using NASA Earth Observations". 2017 NASA Annual Earth Science Applications Showcase. Aug 2017. (poster)

Odwuor, A. Corr, C., Griffin, R. J. "Investigating the Spectral Dependence of Biomass Burning Aerosol Optical Properties". American Geophysical Union Fall Meeting 2016, Dec 2016. (poster)

Odwuor, A. Corr, C., Kotsakis, A., Pusede, S., "Investigating the Spectral Dependence of Biomass Burning Aerosol Optical Properties". 2016 Gulf Coast Undergraduate Research Symposium, Oct 2016. (oral)

Other Presentations

Odwuor, A. "Fighting Fire With Fire" University of California, Irvine Grad Slam 2023. Mar 2023. (oral). https://vimeo.com/event/2866620#t=3448

Odwuor, A. "Clearing the air: What's actually burning in our wildfires?" St. Margaret's Episcopal School Girls in STEAM Symposium. Mar 2022. (oral)

Odwuor, A. "Clearing the air: What's actually burning in our wildfires?" University of California, Irvine Grad Slam 2022. Feb 2022. (oral). https://vimeo.com/678440946#t=1096946

Schlatterer, J.; Howell, M.; Masterson, J.; **Odwuor, A.**; "Tips for applying to the NSF Graduate Research Program (GRFP)". ACS Student & Postdoctoral Scholars Office Webinar, Jun 2020. (webinar)

Media and Press Coverage

Blakemore, Erin (2023, Oct 1). "Large trees fueled massive Calif. wildfire that killed giant sequoias." *The Washington Post.* https://www.washingtonpost.com/science/2023/10/01/old-large-trees-knp-wildfire-fuel/

Joel, Lucas (2023, Sept 25). "UC Irvine scientists reveal what fuels wildfires in Sierra Nevada Mountains." *UCI Physical Sciences News.* https://news.uci.edu/2023/09/25/uc-irvine-scientists-reveal-what-fuels-wildfires-in-sierra-nevada-mountains/

UCI Graduate Division (2023, May 31). "Grad Hooding Q&A – Audrey Odwuor." https://grad.uci.edu/2023/05/31/grad-hooding-qa-audrey-odwuor/

Zhong, Raymond (2022, Sept 07). "How to Save a Forest by Burning It." *The New York Times*. https://www.nytimes.com/2022/09/07/climate/california-wildfire prescribed-burn.html/

Odwuor, Audrey (2022, Aug 03). Interview with Fire Scientist Audrey Odwuor. Earth Calling on KUCI 88.9 FM, Irvine [Radio Broadcast]. https://www.earthcallingshow.org/shows

Joel, Lucas (2021, Sept 03). "UCI Science Delivery: Audrey Odwuor and the Caldor Fire." *UCI Physical Sciences News*. https://ps.uci.edu/news/2474

Computer Skills

Software/Languages: MATLAB, qGIS, Microsoft Office, Adobe Photoshop, Illustrator, and Audition

Technical Skills

Instrument operation: Sunset OC/EC Analyzer, MetOne Remote Dust Monitor, PurpleAir sensor, Picarro G2401, Picarro G2123
Laboratory techniques: Vacuum line gas extraction, Cryogenic gas trapping, SWISS_4S thermal-optical analysis, Sample preparation for elemental analysis and accelerator mass spectrometry, Glass tube preparation, Gas torch operation, Combustion oven operation
Other: Field work, Independent research, Collaborative research, Data analysis

Social, Business, and Other Skills

Spanish (advanced speaking, reading, writing proficiency), Public speaking, Oral communication, Written communication, Science communication, Social media management, Interviewing subjects, Live broadcasting, Project management, Peer mentoring, Independent research, Teamwork, Emotional intelligence, Advanced life support, CPR and first aid instruction, Emergency management

ABSTRACT OF THE DISSERTATION

Wildfires in California's Sierra Nevada Mountains:

Fuels, Emissions, and Management Strategies

by

Audrey Odwuor

Doctor of Philosophy in Earth System Science

University of California, Irvine, 2023

Professor James T. Randerson, co-Chair

Professor Claudia I. Czimczik, co-Chair

Over the last several decades, increasing wildfire activity across California has put the state's communities and ecosystems at risk. Effective wildfire management is critical to achieving social and ecological goals, which include protecting public health and safety, the economy, and natural resources. However, wildfire management is complicated by uncertainties related to the amount and composition of fuels and emissions from California's landscape fires.

In this dissertation, I explored some of the challenges to wildfire management in the Sierra Nevada mountains of California. By investigating fire growth, weather, firefighting resources, and damages during the 2021 fire season in the second chapter of this dissertation, I found that broad-scale weather caused extreme fire growth in multiple large fires at once in the Sierra Nevada, creating a strain on already-limited resources and influencing the magnitude and timing of damages from the fires. In my third chapter, I characterized the total carbon and radiocarbon (^{14}C) composition of fine particulate matter ($PM_{2.5}$) emissions from the 2021 KNP Complex Fire in the

southern Sierra Nevada. I combined these observations with a Keeling plot approach and a box model to estimate the mean age of fuels that were combusted. I concluded that fuel buildup over several decades drove emissions in the KNP Complex Fire, supporting the idea that a legacy of fire suppression has contributed to increased fire severity in the Sierra Nevada by promoting the accumulation of fuels. For my fourth chapter, I estimated fuel consumption and characterized the composition of fuels and $PM_{2.5}$ emissions for a prescribed (Rx) fire in the central Sierra Nevada in 2022 as part of the Smart Practices and Architectures for Rx Fire in California campaign. I found that larger-diameter dead fuels contributed significantly to total fuel consumption in the prescribed fire, indicating that prescribed fire in landscapes with similar fuel composition might result in elevated $PM_{2.5}$ concentrations associated with the combustion of larger fuels. Further, agreement in the observed ^{14}C signature of fire-emitted $PM_{2.5}$ and the ^{14}C signature estimated using my ^{14}C and fuel consumption measurements provides confidence that ^{14}C measurements of atmospheric $PM_{2.5}$ in the background atmosphere near fire-affected areas could be used to evaluate the influence of prescribed fire on fuel composition.

Altogether, the results of my research provide insight into the potential for large wildfires to overwhelm fire suppression capacity, highlight the importance of effective wildfire management, and identify a method by which prescribed fire can be monitored.

Chapter 1

Introduction

1.1. Changing drivers of fire activity in California

Fire is a natural and critical process in many ecosystems (Andreae, 1991), but a combination of human activities and climate change has created conditions that many fire-adapted ecosystems and communities can no longer support (Bowman *et al.*, 2009; Miller *et al.*, 2012; Safford *et al.*, 2022). Specifically, California's coniferous forests, like those in the Sierra Nevada mountains (Fig. 1.1) evolved with fire. They can withstand low- to moderate- intensity fires (Miller and Safford, 2012) with a mean fire return interval of 12 years (van de Water and Safford, 2011).

Figure 1.1. Map showing the location of the Sierra Nevada in California, USA. The Sierra Nevada is defined according to the US EPA Level III Ecoregions of the Continental United States.

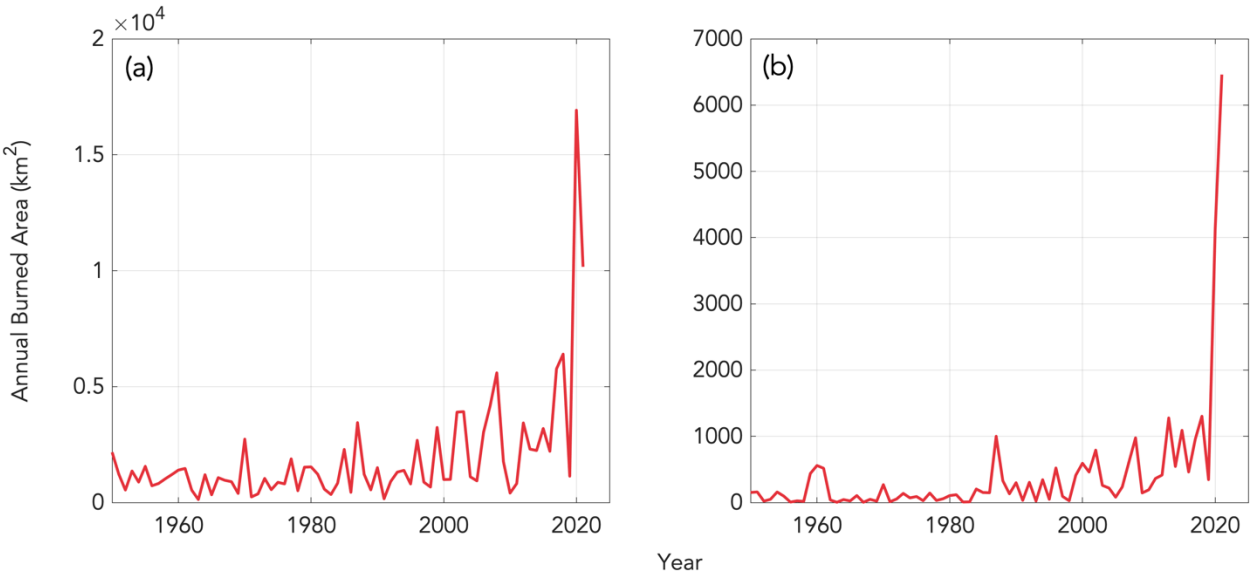

Figure 1.2. Time series of annual burned area in (a) California and (b) the Sierra Nevada mountains of California from 1950 to 2021 using data from the California Department of Forestry and Fire Protection Fire Resource Assessment Program (available at: https://www.fire.ca.gov/what-we-do/fire-resource-assessment-program)

However, since the late 19th century, the mean fire return interval in the Sierra Nevada has increased to about 84 years (Safford and Van de Water, 2013), and the Sierra Nevada now experiences higher-severity fires (Miller and Safford, 2012), more frequent large fires (Dennison *et al.*, 2014; Taylor *et al.*, 2016), and a higher level of annual burned area (Fig. 1.2) (Miller *et al.*, 2012; Dennison *et al.*, 2014; Williams *et al.*, 2019).

Long-term changes in fire regimes can be strongly linked to multiple socioecological phases, including Indigenous land management, depopulation of Indigenous people by Euro-American settlers, logging, widespread grazing and deforestation during the Gold Rush era, and, more

recently, the cumulative effects of fire suppression (Fig. 1.3) (Taylor *et al.*, 2016). Each of these phases is characterized by different land management activities that influence fuel amount and structure, and, thereby, fire behavior. More recently, climate-change-driven increases in summer temperatures and drought stress have further modified fuel moisture levels, the length of the fire season, and regional fire dynamics (Abatzoglou and Williams, 2016; Westerling, 2016; Williams *et al.,* 2019).

Indigenous land management in the Sierra Nevada can be traced back as far as 1300 A.D. (Anderson and Moratto, 1996). By means of cultural burning, fires were ignited frequently for various reasons, including to reduce hazardous fuel loads (Anderson and Moratto, 1996; Quinn-Davidson and Varner, 2012). These frequent, low-intensity surface fires resulted in low fuel continuity (i.e., less dense, more open forests) (Hagmann *et al.*, 2021) and prevented fuel buildup (McKelvey and Busse, 1996). Then, the fire return interval in the Sierra Nevada was 5-50 years (Stephens *et al.*, 2009; Safford and Van de Water, 2013). Low fire return intervals are associated with finer fuels, lower tree mortality, little accumulation of understory vegetation, and thereby, lower intensity surface fires (Gorte, 2009; Steel *et al.*, 2015).

In the late 18th century, during the Spanish-Mexican colonial phase following the depopulation of Indigenous people (Taylor *et al.*, 2016), fire activity increased as fuels became more continuous with the reduction in cultural burning. Greater fuel availability led to more frequent fires and a

stronger relationship between fire and climate as ignition and fire spread became the limiting factors to fire activity (Stephens *et al.*, 2009; Steel, Safford and Viers, 2015; Taylor *et al.*, 2016).

Following Euro-American settlement and the Gold Rush in California in the late 19th century (~1866-1903), fire activity returned to pre-colonial levels (Taylor *et al.*, 2016). Logging and grazing accompanying population growth in the Sierra Nevada reduced fuel continuity. Therefore, fire activity decreased, and the relationship between fire and climate weakened as fuels became the limiting factor to fire activity.

Fire management since the 20th century can be characterized by widespread fire suppression. Fire suppression policy began around 1903 (Agee and Skinner, 2005; Taylor *et al.*, 2016). By the 1930s, cultural burning had essentially been banned and an aggressive fire suppression policy was applied to most forested ecosystems (Agee and Skinner, 2005). The widespread suppression of low- to moderate-intensity fires has allowed for greater fuel continuity and a buildup of fuels, including an increase in understory vegetation and ladder fuels that contribute to the less frequent but more severe wildfires that occur in today's climate-limited regime (McKelvey and Busse, 1996; Stephens *et al.*, 2009; Taylor *et al.*, 2016; Pausas and Keeley, 2019).

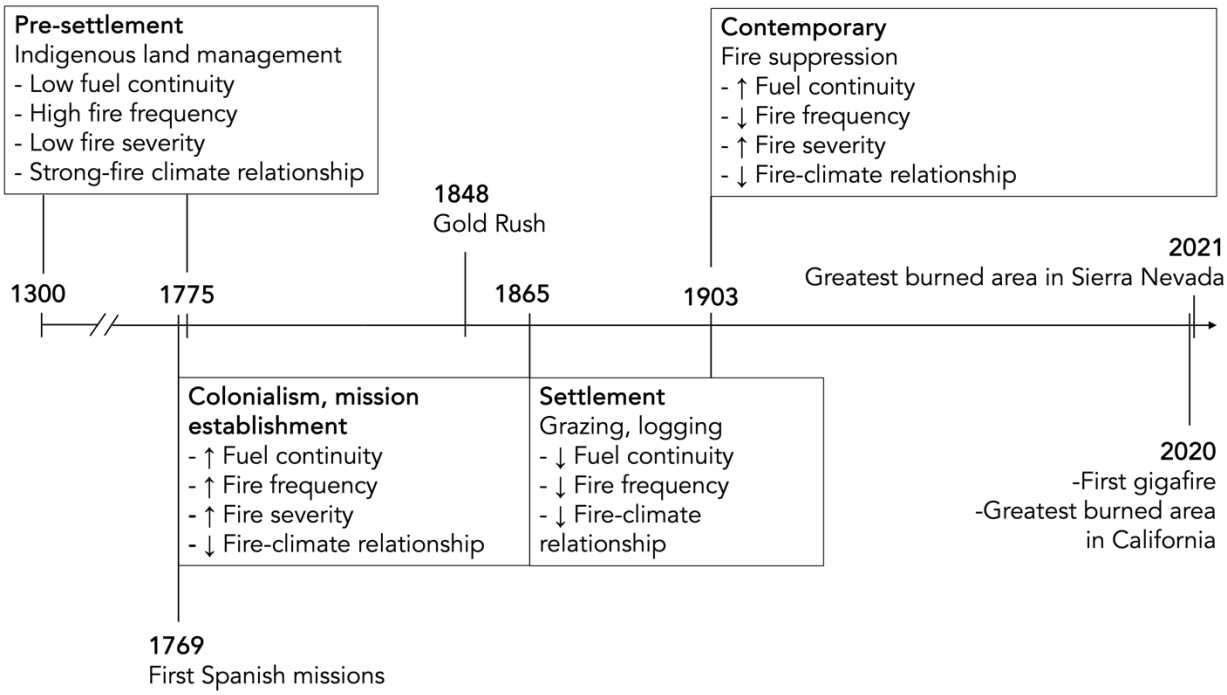

Figure 1.3. Summary of major socioecologial shifts and accompanying changes to fire activity and the fire-climate relationship as described by Taylor *et al.* (2016) and supplemented by information from Anderson and Moratto (1996).

In addition to fuel buildup from the legacy of 20th century forest management, the Sierra Nevada is expected to continue experiencing warmer, drier summers in the coming decades, which is predicted to increase both the likelihood and extent of fires (Safford and Van de Water, 2013; Williams *et al.*, 2019; Gutierrez *et al.*, 2021; Hagmann *et al.*, 2021). Higher summer temperatures drive increases in vapor-pressure deficit, contributing to drier and more flammable fuels, earlier snowmelt, and, thereby, longer fire seasons (Westerling *et al.*, 2006; Riley *et al.*, 2019). During periods of extreme heat, drier fuels contribute to a higher probability that a wildfire ignition will

escape initial containment, highlighting the role of climate in increasing fire occurrence from both lightning and human ignition sources (Gutierrez *et al.*, 2021). Considering expected increases in summer air temperatures alone and no significant changes to fire suppression or forest management, annual burned area is projected to increase by 59 ± 33% by the 2040s (Gutierrez *et al.*, 2021). Because fuels are abundant and climate conditions are conducive to rapid fire growth, the area burned by wildfires in the Sierra Nevada is becoming increasingly tied to the ignition and rapid expansion of just a few megafires.

1.2. The effects of wildfires on the environment and society

Although California's coniferous forests are largely fire-adapted, they are made especially vulnerable by today's high-intensity crown fires that contrast with lower-intensity surface fires they experienced in the past. The contemporary fire regime has decreased the average size and age of trees and increased stand density and surface fuels in California's conifer forests (Agee and Skinner, 2005; Stephens *et al.*, 2009; North *et al.*, 2021), thereby increasing the probability of high-intensity fire and destabilizing landscape-scale carbon storage (Collins, Everett and Stephens, 2011; Hurteau *et al.*, 2019). Increased fire intensity influences vegetation composition and distribution in ecosystems, which impacts the habitats of sensitive plant and animal species and increases vulnerability to drought, disease, insects, and even greater fire intensity (McKenzie *et al.*, 2004; Collins, Everett and Stephens, 2011; Goodwin *et al.*, 2020). Specifically, larger fire-adapted trees and some endangered endemic species like the ancient giant sequoia (*Sequoiadendron giganteum* (LINDL.) J.T. BUCHHOLZ) in old-growth forests are made vulnerable

by the growth of younger, smaller trees in the understory that provide ladder fuels enabling high-intensity crown fires (Hurteau *et al.*, 2019; Goodwin *et al.*, 2020; Shive *et al.*, 2022). Further, soil erosion following wildfires can negatively impact downstream aquatic ecosystems and water quality and supply (Sankey *et al.*, 2017).

The 2020 fire season burned over 17,000 km^2 (4.3 million acres) of California's wildlands, corresponding to an estimated 0.1 Pg of carbon dioxide (CO_2) emitted, equivalent to almost 30% of California's 2020 emissions (CAL FIRE, 2020; California Air Resources Board, 2020; California Air Resources Board, 2022). In addition to CO_2, wildfires produce other gaseous pollutants like nitrous oxides, ozone, methane, etc., and particulate matter (PM) and its precursors (Akagi *et al.*, 2011; Andreae *et al.,* 2019). Of special concern is fine airborne PM ($PM_{2.5}$), which encompasses most of the aerosol produced by landscape fires. Some aerosol types contributing to fire-emitted $PM_{2.5}$ in different settings include nitrate and sulfate aerosol and mineral aerosols associated with combustion and the entrainment of soil particles in fire plumes (Hand *et al*., 2013). Additionally, $PM_{2.5}$ has carbonaceous fractions that are commonly differentiated according to thermo-optical properties, from light-scattering organic carbon (OC) to light-absorbing black carbon (BC) (Andreae and Gelencsér, 2006), which is especially important for climate warming, atmospheric visibility, and public health (Bond *et al.*, 2013; Reisen *et al.*, 2018; Burke *et al.*, 2021)

$PM_{2.5}$ is associated with increased premature mortality. At the end of the last decade, premature deaths due to $PM_{2.5}$ exposure in the U.S. increased by an estimated 9500 persons or about $134

billion, 43% of which is attributed to changes in air quality within California (Clay *et al.*, 2021). In addition to increased mortality, wildfire smoke exposure has been linked to increased respiratory-related hospitalizations and increased adverse health outcomes related to restricted activity and days of work lost (Kochi *et al.*, 2010). Because wildfires often occur near highly populated areas, voluntary and forced evacuations can cause hundreds to tens of thousands of people to flee their homes, assuming safe evacuation routes and access to reliable emergency information (Safford *et al.*, 2012; Tubbesing *et al.*, 2021). The potential for smoke to affect communities is further influenced by the composition and concentration of pollutants, which are partly determined by fire processes that regulate fuel consumption (May *et al.*, 2015; Williamson *et al.*, 2016).

Wildfires also negatively affect the economy. In 2021, structures damaged and destroyed during California's fire season cost over $500 million (CAL FIRE, 2021a). In addition to long-term health effects, indirect costs of wildfires include environmental cleanup, lost business and tax revenue, and infrastructure repairs (Thomas *et al.*, 2017; Wang *et al.*, 2021). Direct costs of wildfire include fire suppression and property losses. In the 2020 fire season, emergency fire suppression cost California over $1.7 billion, almost four times the average amount spent annually by the state in the previous decade (CAL FIRE, 2021b). Further, over half of the federal budget for fire suppression is spent in California alone (Taylor *et al.*, 2016). Approximately 10,000 structures were destroyed in the 2020 fire season, and a recent study estimated that last decade, structures destroyed cost an average of $1 billion annually to replace, a value that is over twice as high as

during the previous decade and expected to continue rising as burned area increases this decade (CAL FIRE, 2020; Buechi *et al.*, 2021).

1.3. Fuel treatments as a wildfire management strategy

Fuels can be reduced using mechanical treatments and/or burning. Mechanical fuel treatments include crown thinning, thinning from below, and mastication (i.e., grinding, chipping, etc.) (Stephens and Moghaddas, 2005), while prescribed burning involves intentionally applying fire to a landscape under certain conditions to achieve specific goals (Kalies and Kent, 2016). Depending on the desired outcome, trees may be thinned from the canopy before being thinned from below to increase canopy spacing and reduce tree density (Stephens and Moghaddas, 2005). Individual trees are cut down and either left as logs, masticated in place, or chipped and removed from the site for processing for timber products (Stephens and Moghaddas, 2005; Stephens *et al.*, 2012). The cost of chipping and removing smaller trees can be prohibitive, and as a result, these trees are often left as logs, adding to the surface fuel load (Stephens *et al.*, 2012). Mechanical treatments alone have been found to reduce fire hazard in part by lowering stand density and ladder fuels (Johnston *et al.*, 2021). They are often followed by prescribed fire to enhance their effectiveness (Kalies and Kent, 2016).

Prescribed burning can be similar to cultural burning. In more recent decades, prescribed fire policy was reintroduced to western U.S. forests (Stephens *et al.*, 2012), and there is strong evidence that, especially when combined with mechanical treatments, it can effectively reduce fuel loads

and, thereby, fire intensity and severity (Stephens and Moghaddas, 2005; Stephens *et al.*, 2012; Kalies and Kent, 2016; Levine *et al.*, 2020; Johnston *et al.*, 2021). An estimated 2.4 million ha of forested area in the Sierra Nevada are under high fire hazard in dire need of restoration (Levine *et al.*, 2020). In California, a key management goal is to expand use of prescribed fire each year by a factor or ten or more (California Wildfire and Forest Resilience Task Force, 2021). The rapid and widespread expansion of prescribed fire will involve streamlining the review and approval process for burns, growing and training the state's prescribed fire workforce, tracking burns, and optimizing smoke management programs (California Wildfire and Forest Resilience Task Force, 2021).

1.4. Radiocarbon as a tool for understanding fire activity

Radiocarbon (^{14}C) is a radioactive isotope of carbon with a half-life of about 5730 years that is naturally produced in the atmosphere, primarily in the lower stratosphere and upper troposphere. It is created when cosmic radiation interacts with nitrogen atoms in nitrogen gas. Over a period of several months, the ^{14}C is oxidized to ^{14}CO and then to $^{14}CO_2$. Radiocarbon enters the biosphere when plants fix atmospheric $^{14}CO_2$ during photosynthesis. Living biomass and emissions from its combustion are labeled with the ^{14}C content of the atmosphere at the time of photosynthesis so that annual plants have a ^{14}C signature closely matching the contemporary atmosphere while the ^{14}C signature of perennial plants reflects the integrated atmospheric ^{14}C content over their lifetimes.

The ^{14}C content of a sample can be reported as $\Delta^{14}C$ in units of per mille (‰), and the relationship between $\Delta^{14}C$ and the widely-used fraction modern (F) measurement is shown in equation (1), where y is the year of ^{14}C sampling (in this dissertation, 2021 and 2022); F is the ^{14}C /^{12}C ratio of the sample divided by 95% of the ^{14}C /^{12}C ratio of the oxalic acid I (OX-I) standard measured in 1950 (^{14}C /$^{12}C_{OX1} = 1.176 \pm 0.010 \times 10^{-12}$) corrected for mass-dependent fractionation; 8267 years is the mean lifetime of ^{14}C; and 1950 is the reference year:

$$\Delta^{14}C = \left(F \times e^{\frac{1950-y}{8267}} - 1\right) \times 1000 \qquad \text{(Eqn. 1.1)}$$

The $^{14}C/^{12}C$ measurements collected via accelerator mass spectrometry are normalized to a common $\delta^{13}C$ so that differences in $\Delta^{14}C$ do not reflect isotopic fractionation (Stuiver and Polach 1977).

Atmospheric $\Delta^{14}CO_2$ has changed considerably over the past 70 years (Fig. 1.4) because of the Earth system's response to the production of "bomb" ^{14}C from aboveground nuclear weapons testing during the late 1950s and early 1960s (Nydal, 1963; Levin *et al.*, 2010). This bomb carbon approximately doubled the number of ^{14}C atoms of Northern hemispheric CO_2 but was rapidly diluted by mixing throughout the biosphere since the cessation of aboveground nuclear weapons testing. Dilution by fossil fuel emissions, which are essentially ^{14}C-free, now controls the decline in atmospheric ^{14}C content. For the period from 1950 to present day, the age of a plant (e.g., fuel) is determined by comparing its ^{14}C content to atmospheric $\Delta^{14}CO_2$.

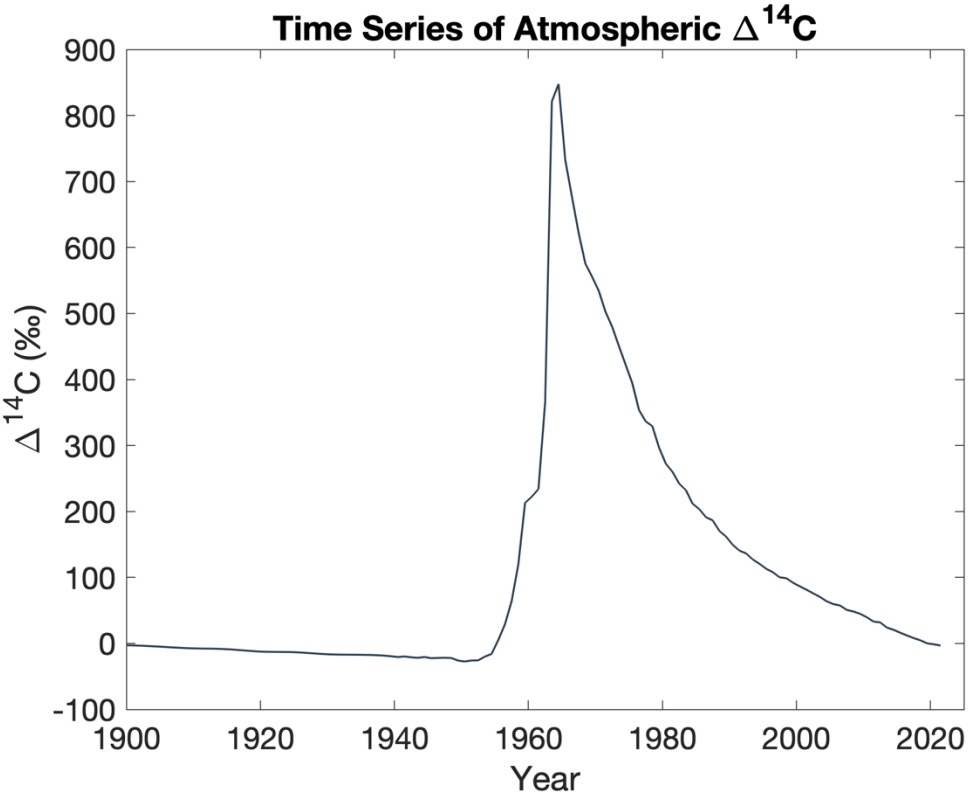

Figure 1.4. Time series of atmospheric radiocarbon content ($^{14}CO_2$) for the Northern hemisphere derived from observations by Hua *et al*. (2022; for the region from about 45ºN to the position of the summer intertropical convergence zone) and X. Xu (personal communication, 2021; from Pt. Barrow, AK, USA). The $^{14}CO_2$ in the atmosphere is taken up during photosynthesis along with $^{13}CO_2$ and $^{12}CO_2$. As a result, organic matter produced after the 1950s contains some degree of bomb-derived ^{14}C, and these samples are considered "modern." Plant biomass is labeled with the $^{14}C/^{12}C$ ratio of the atmosphere at the time of fixation, and as this plant material cycles through the biosphere, this ^{14}C signature is retained, although it is slowly modified by radioactive decay.

1.5. Organization of dissertation

This research aims to understand some of the challenges to wildfire management in California's Sierra Nevada and enhance our understanding of the different fuel types contributing to emissions for both prescribed and wildland fires.

In Chapter 2, I investigated the relationships among wildfire growth, weather, firefighting resources, and damages during California's 2021 wildfire season to highlight some of the challenges to fire suppression in the Sierra Nevada mountains (Odwuor *et al.,* in prep). To do this, I analyzed a satellite-derived dataset of active fire line length and burned area (Liu *et al*., in review) and data on firefighting resources and damages from reports maintained by the U.S. National Incident Management System. I focused my analyses on the Dixie, Caldor, and KNP Complex Fires, three of the largest fires that occurred that year, but compared them to the 8 other largest 2021 fires. In this study, I found that fires in the Sierra Nevada responded to similar broad-scale weather, synchronizing fire growth. Further, the number of structures destroyed responded to increases in fire growth, creating a strain on firefighting resources, but the KNP Complex Fire, which burned through more forested, less populated areas, received fewer firefighting resources per unit active fire line length. I also identified three periods of greatest stress to firefighting efforts, which corresponded to the destruction of two towns and the threat of destruction of another. The results from Chapter 2 suggest that climate contributes to fires that are harder to contain, straining already-limited firefighting resources and emphasizing the need for fuel treatments to manage wildfires.

I further investigated the 2021 wildfire season in Chapter 3 by characterizing the composition of fire-emitted $PM_{2.5}$ from KNP Complex Fire to estimate the mean age of combusted fuels (Odwuor *et al.,* 2023). I first collected fire-emitted $PM_{2.5}$ samples from smoke downwind of the fire over a period of 26 hours. Then, I measured the total carbon and ^{14}C content of the samples and used a

Keeling plot approach combined with a steady-state, one-box ecosystem model to determine the mean $\Delta^{14}C$ and age of the combusted fuel. I found that the mean age of combusted fuels in the KNP Complex Fire was about 40 years, suggesting that the legacy of fire suppression contributed to high fire intensity by promoting the accumulation of fuels over several decades and providing insight into the influence of fuel composition on the composition of fire-emitted $PM_{2.5}$.

In Chapter 4, I estimated fuel consumption and characterized the composition of emissions and fuels in a 2022 prescribed fire in the central Sierra Nevada mountains to further constrain the influence of fuel composition on emissions. I conducted inventories of surface fuels to estimate mass consumed by difference before and after the fire. In addition to measuring the total carbon and ^{14}C content of fire-emitted $PM_{2.5}$ following the methods used in Chapter 3, I also measured the $\Delta^{14}C$ of surface fuels collected before the fire for direct comparison with the $\Delta^{14}C$ of $PM_{2.5}$ emissions. Here, I found that the combustion of larger-diameter fuels contributed significantly to total fuel consumption and $PM_{2.5}$ emissions. Further, the ^{14}C signature of $PM_{2.5}$ estimated from the fuel consumption and $\Delta^{14}C$ measurements in this study was similar to the observed $\Delta^{14}C$ of fire-emitted $PM_{2.5}$. The findings from this chapter help us constrain fuel consumption and composition during prescribed fire and understand its influence on $PM_{2.5}$ emissions. Further, these results suggest the potential for our methods to evaluate the effectiveness of prescribed fire.

In Chapter 5, I summarize my conclusions from this research, explore the broader implications of these findings for wildfire management, and propose future study directions, including field and laboratory techniques in this area of research.

1.6. References

Abatzoglou, J. T. and Williams, A. P. (2016) 'Impact of anthropogenic climate change on wildfire across western US forests', *Proceedings of the National Academy of Sciences,* 113(42), 11770-11775. doi: 10.1073/pnas.1607171113.

Agee, J. K. and Skinner, C. N. (2005) 'Basic principles of forest fuel reduction treatments', *Forest Ecology and Management*, 211(1–2), pp. 83–96. doi: 10.1016/j.foreco.2005.01.034.

Akagi, S. K. *et al.* (2011) 'Emission factors for open and domestic biomass burning for use in atmospheric models', *Atmospheric Chemistry and Physics*, 11(9), pp. 4039–4072. doi: 10.5194/acp-11-4039-2011.

Anderson, M. K. and Moratto, M. J. (1996) *Native American Land-Use Practices and Ecological Impacts*. In *Sierra Nevada ecosystem project: final report to Congress* (Vol. 2, pp. 187-206). Davis, CA: University of California, Centers for Water and Wildland Resources Davis.

Andreae, M. O. (1991) 'Biomass burning: Its history, use, and distribution and its impact on environmental quality and global climate, in Global Biomass Burining: Atmospheirc, Climate and Biospheric implications, edited by J, S. Levine', *MIT Press, Cambridge, Mass.*, (October), pp. 3–21.

Andreae, M. O. and Gelencsér, A. (2006) 'Atmospheric Chemistry and Physics Black carbon or brown carbon? The nature of light-absorbing carbonaceous aerosols', *Atmos. Chem. Phys*, 6, pp. 3131–3148. doi: 10.5194/acp-6-3131-2006

Andreae, M. O. (2019). Emission of trace gases and aerosols from biomass burning–an updated assessment. *Atmospheric Chemistry and Physics*, *19*(13), 8523-8546.Bond, T. C. *et al.* (2013) 'Bounding the role of black carbon in the climate system: A scientific assessment', *Journal of Geophysical Research Atmospheres*, 118(11), pp. 5380–5552. doi: 10.1002/jgrd.50171.

Bowman, D. M. J. S. *et al.* (2009) 'Fire in the earth system', *Science*, 324(5926), pp. 481–484. doi: 10.1126/science.1163886.

Buechi, H. *et al.* (2021) 'Long-term trends in wildfire damages in California', *International Journal of Wildland Fire*, 30(10), pp. 757–762. doi: 10.1071/WF21024.

Burke, M. *et al.* (2021) 'The changing risk and burden of wildfire in the United States', *Proceedings of the National Academy of Sciences of the United States of America*, 118(2), pp. 1–6. doi: 10.1073/PNAS.2011048118.

California Air Resources Board (2020) *Greenhouse Gas Emissions of Contemporary Wildfire, Prescribed Fire, and Forest Management Activities* (available at: https://ww2.arb.ca.gov/sites/default/files/classic/cc/inventory/pubs/ca_ghg_wildfire_forestmanagement.pdf) (Accessed 2 November 2023)

California Air Resources Board (2022) *Current California GHG Emission Inventory Data* (available at: https://ww2.arb.ca.gov/ghg-inventory-data) (Accessed 2 Noember 2023)

California Wildfire and Forest Resilience Task Force (2022) *California's Strategic Plan for Expanding the Use of Beneficial Fire* (available at: https://wildfiretaskforce.org/wp-content/uploads/2022/05/californias-strategic-plan-for-expanding-the-use-of-beneficial-

fire.pdf) (Accessed 3 November 2023)
CAL FIRE (2020) *2020 Wildfire Activity Statistics* (available at: https://34c031f8-c9fd-4018-8c5a-4159cdff6b0d-cdn-endpoint.azureedge.net/-/media/calfire-website/our-impact/fire-statistics/2020_redbook_final.pdf?rev=72030b4d2cb7466aa573754ecb4f656e&hash=337DB407876BE384081C7D722D82B1BF) (Accessed 2 November 2023)
CAL FIRE (2021a) *2021 Wildfire Activity Statistics.* (available at: https://34c031f8-c9fd-4018-8c5a-4159cdff6b0d-cdn-endpoint.azureedge.net/-/media/calfire-website/our-impact/fire-statistics/2021_redbook_final.pdf?rev=525959073bbe4bbe816d67624911e4c3&hash=CFD17F879B2CE984AB5BA9FEA4F73A56) Accesssed 2 November 2023)
CAL FIRE (2021b) *Emergency Fund Fire Suppression Expenditures* (available at: www.fire.ca.gov/media/px5lnaaw/suppressioncos tsonepage1.pdf) (Accessed 20 February 2023)
Clay, K., Muller, N. Z. and Wang, X. (2021) 'Recent Increases in Air Pollution : Evidence and Implications for Mortality', *Review of Environmental Economics and Policy,* 15(1). doi: 10.3386/w26381
Collins, B. M., Everett, R. G. and Stephens, S. L. (2011) 'Impacts of fire exclusion and recent managed fire on forest structure in old growth Sierra Nevada mixed-conifer forests', *Ecosphere*, 2(4). doi: 10.1890/ES11-00026.1.
Dennison, P. E. *et al.* (2014) 'Geophysical Research Letters', *Geophysical Research Letters*, (April), pp. 6413–6419. doi: 10.1002/2014GL061184.Received.
Goodwin, M. J. *et al.* (2020) 'Changing climate reallocates the carbon debt of frequent-fire forests', *Global Change Biology*, 26(11), pp. 6180–6189. doi: 10.1111/gcb.15318.
Gorte, R. W. (2009) 'Wildfire fuels and fuel reduction', *Congressional Research Service, Library of Congress*, pp. 1–16.
Gutierrez, A. A. *et al.* (2021) 'Wildfire response to changing daily temperature extremes in California's Sierra Nevada', *Science Advances*, 7(47), pp. 1–11. doi: 10.1126/sciadv.abe6417.
Hagmann, R. K. *et al.* (2021) 'Evidence for widespread changes in the structure, composition, and fire regimes of western North American forests', *Ecological Applications*, 31(8). doi: 10.1002/eap.2431.
Hand, J. L., B. A. Schichtel, M. Pitchford, W. C. Malm, and N. H. Frank (2012), Seasonal composition of remote and urban fine particulate matter in the United States, *J. Geophys. Res*., *117*, D05209, doi:10.1029/2011JD017122.
Huang, X. *et al.* (2023) 'Smoke-weather interaction affects extreme wildfires in diverse coastal regions', *Science*, 379(6631), pp. 457–461. doi: 10.1126/science.add9843.
Hurteau, M. D. *et al.* (2019) 'Managing for disturbance stabilizes forest carbon', *Proceedings of the National Academy of Sciences of the United States of America*, 116(21), pp. 10193–10195. doi: 10.1073/pnas.1905146116.
Johnston, J. D. *et al.* (2021) 'Mechanical thinning without prescribed fire moderates wildfire behavior in an Eastern Oregon, USA ponderosa pine forest', *Forest Ecology and Management*. Elsevier B.V., 501, p. 119674. doi: 10.1016/j.foreco.2021.119674.
Kalies, E. L. and Kent, L. L. Y. (2016) 'Tamm Review: Are fuel treatments effective at

achieving ecological and social objectives? A systematic review', *Forest Ecology and Management*. Elsevier B.V., 375, pp. 84–95. doi: 10.1016/j.foreco.2016.05.021.
Kochi, I. *et al.* (2010) 'The economic cost of adverse health effectsfrom wildfire-smoke exposure: A review', *International Journal of Wildland Fire*, 19(7), pp. 803–817. doi: 10.1071/WF09077.
Levin, I. *et al.* (2010) 'Observations and modelling of the global distribution and long-term trend of atmospheric 14CO2', *Tellus, Series B: Chemical and Physical Meteorology*, 62(1), pp. 26–46. doi: 10.1111/j.1600-0889.2009.00446.x.
Levine, J. I. *et al.* (2020) 'Forest stand and site characteristics influence fuel consumption in repeat prescribed burns', *International Journal of Wildland Fire*, 29(2), pp. 148–159. doi: 10.1071/WF19043.
May, A. A. *et al.* (2015) 'Observations and analysis of organic aerosol evolution in some prescribed fire smoke plumes', *Atmospheric Chemistry and Physics*, 15(11), pp. 6323–6335. doi: 10.5194/acp-15-6323-2015.
McKelvey, K. S. and Busse, K. K. (1996) 'Twentieth-century fire patterns on Forest Service lands', *Sierra Nevada Ecosystem Project: Final report to Congress*, II, pp. 1119–1138.
McKenzie, D. *et al.* (2004) 'Climatic change, wildfire, and conservation', *Conservation Biology*, 18(4), pp. 890–902. doi: 10.1111/j.1523-1739.2004.00492.x.
Miller, J. D. *et al.* (2012) 'Differences in wildfires among ecoregions and land management agencies in the Sierra Nevada region, California, USA', *Ecosphere*, 3(9), p. art80. doi: 10.1890/es12-00158.1.
Miller, J. D. and Safford, H. (2012) 'Trends in wildfire severity: 1984 to 2010 in the Sierra Nevada, Modoc Plateau, and southern Cascades, California, USA', *Fire Ecology*, 8(3), pp. 41–57. doi: 10.4996/fireecology.0803041.
North, M. P. *et al.* (2021) 'Pyrosilviculture Needed for Landscape Resilience of Dry Western United States Forests', *Journal of Forestry*, 119(5), pp. 520–544. doi: 10.1093/jofore/fvab026.
Nydal, R. (1963) 'Increase in radiocarbon from the most recent series of thermonuclear tests', *Nature*, pp. 212–214. doi: 10.1038/200212a0
Pausas, J. G. and Keeley, J. E. (2019) 'Wildfires as an ecosystem service', *Frontiers in Ecology and the Environment*, 17(5), pp. 289–295. doi: 10.1002/fee.2044.
Quinn-Davidson, L. N. and Varner, J. M. (2012) 'Impediments to prescribed fire across agency, landscape and manager: An example from northern California', *International Journal of Wildland Fire*, 21(3), pp. 210–218. doi: 10.1071/WF11017.
Reisen, F. *et al.* (2018) 'Ground-Based Field Measurements of PM2.5 Emission Factors From Flaming and Smoldering Combustion in Eucalypt Forests', *Journal of Geophysical Research: Atmospheres*, 123(15), pp. 8301–8314. doi: 10.1029/2018JD028488.
Riley, K. L. *et al.* (2019) 'Will Landscape Fire Increase in the Future? A Systems Approach to Climate, Fire, Fuel, and Human Drivers', *Current Pollution Reports*. Current Pollution Reports, 5(2), pp. 9–24. doi: 10.1007/s40726-019-0103-6.
Safford, H. D. *et al.* (2012) 'Fuel treatment effectiveness in California yellow pine and mixed conifer forests', *Forest Ecology and Management*. Elsevier B.V., 274, pp. 17–28. doi:

10.1016/j.foreco.2012.02.013.
Safford, H. D. *et al.* (2022) 'The 2020 California fire season: A year like no other, a return to the past or a harbinger of the future?', *Global Ecology and Biogeography*, 31(10), pp. 2005–2025. doi: 10.1111/geb.13498.
Safford, H. D. and Van de Water, K. M. (2013) 'Using Fire Return Interval Departure (FRID) analysis to map spatial and temporal changes in fire frequency on National Forest lands in California', *Pacific Southwest Research Station - Research Paper PSW-RP-266*, (January), pp. 1–59. (available at: http://www.fs.fed.us/psw/publications/documents/psw_rp266/psw_rp266.pdf.) (Accessed 9 November 2023)
Sankey, J. B. *et al.* (2017) 'Climate, wildfire, and erosion ensemble foretells more sediment in western USA watersheds', *Geophysical Research Letters*, 44(17), pp. 8884–8892. doi: 10.1002/2017GL073979.
Shive, K. L. *et al.* (2022) 'Ancient trees and modern wildfires: Declining resilience to wildfire in the highly fire-adapted giant sequoia', *Forest Ecology and Management*. Elsevier B.V., 511(October 2021), p. 120110. doi: 10.1016/j.foreco.2022.120110.
Steel, Z. L., Safford, H. D. and Viers, J. H. (2015) 'The fire frequency-severity relationship and the legacy of fire suppression in California forests http://www.esajournals.org/doi/pdf/10.1890/ES14-00224.1', *Ecosphere*, 6(1). doi: 10.1890/ES14-00224.1.
Stephens, S. L. *et al.* (2009) 'Fire treatment effects on vegetation structure, fuels, and potential fire severity in western U.S. forests', *Ecological Applications*, 19(2), pp. 305–320. doi: 10.1890/07-1755.1.
Stephens, S. L. *et al.* (2012) 'The effects of forest fuel-reduction treatments in the United States', *BioScience*, 62(6), pp. 549–560. doi: 10.1525/bio.2012.62.6.6.
Stephens, S. L. and Moghaddas, J. J. (2005) 'Experimental fuel treatment impacts on forest structure, potential fire behavior, and predicted tree mortality in a California mixed conifer forest', *Forest Ecology and Management*, 215(1–3), pp. 21–36. doi: 10.1016/j.foreco.2005.03.070.
Taylor, A. H. *et al.* (2016) 'Socioecological transitions trigger fire regime shifts and modulate fire-climate interactions in the Sierra Nevada, USA, 1600-2015 CE', *Proceedings of the National Academy of Sciences of the United States of America*, 113(48), pp. 13684–13689. doi: 10.1073/pnas.1609775113.
Thomas, D. *et al.* (2017) 'The Costs and Losses of Wildfires: A Literature Survey (NIST Special Publication 1215)', (November). doi: 10.6028/NIST.SP.1215.
Tubbesing, C. L., Martinez, D. J. and Smith, J. (2021) 'Recommendations from the Science Advisory Panel to the Forest Management Task Force'
Wang, D. *et al.* (2021) 'Economic footprint of California wildfires in 2018', *Nature Sustainability*. Springer US, 4(3), pp. 252–260. doi: 10.1038/s41893-020-00646-7.
van de Water, K. M. and Safford, H. D. (2011) 'A summary of fire frequency estimates for California vegetation before Euro-American settlement', *Fire Ecology*, 7(3), pp. 26–58. doi: 10.4996/fireecology.0703026.

Westerling, A. L. *et al.* (2006) 'Warming and earlier spring increase western U.S. forest wildfire activity', *Science*, 313(5789), pp. 940–943. doi: 10.1126/science.1128834

Westerling, A.L.R. (2016) 'Increasing western US forest wildfire activity: sensitivity to changes in the timing of spring', *Phil. Trans. R. Soc. B, 371*, 20150178. doi: 10.1098/rstb.2015.0178

Williams, A. P. *et al.* (2019) 'Observed Impacts of Anthropogenic Climate Change on Wildfire in California', *Earth's Future*, 7(8), pp. 892–910. doi: 10.1029/2019EF001210.

Williamson, G. J. *et al.* (2016) 'A transdisciplinary approach to understanding the health effects of wildfire and prescribed fire smoke regimes', *Environmental Research Letters*. IOP Publishing, 11(12). doi: 10.1088/1748-9326/11/12/125009.

Chapter 2

Investigating the progression of large wildfires and allocation of firefighting resources during the 2021 California wildfire season

Odwuor, A., Liu, T., Delgado, A., Randerson, J.T., and Czimczik, C.I.

2.1. Introduction

Over the last several decades, wildfire activity, including burned area, the occurrence of large fires, and fire severity has increased across much of California (Dennison *et al.*, 2014; Williams *et al.*, 2019; Keeley and Syphard, 2021). In part due to rapid population growth in the wildland urban interface, California is experiencing unprecedented losses of life and property from wildfires (Radeloff *et al.*, 2018; Keeley and Syphard, 2021; Marks-Block and Tripp, 2021). Firefighting efforts by federal government agencies such as the USDA Forest Service and National Park Service and state agencies like the California Department of Forestry and Fire Protection (CAL FIRE) aim to protect life, property, and natural resources. Specifically, CAL FIRE is tasked with maintaining California's resilience against wildfires and responding when wildfires occur. The CAL FIRE budget for fire prevention and protection and resource management in 2021-2022 had increased by almost five times since 2005, reaching approximately $3.8 billion, including $800 million for emergency fire suppression (California Legislative Analyst's Office, 2022). Emergency fire suppression expenditures, typically associated with large wildfires that exceed CAL FIRE's containment capacity, have more almost quadrupled in the last decade (CAL FIRE, 2021a). These costs rival federal expenditures of approximately $4.4 billion for fire suppression across the entire

country in 2021 (National Interagency Fire Center, 2023), half of which is spent on fighting fires in California (Taylor *et al.*, 2016).

The 2021 fire season burned over 10,000 km^2 (2.5 million acres) across California and is second only to the 2020 fire season in terms of annual area burned (CAL FIRE, 2021b). Specifically, over 12% of the Sierra Nevada burned in 2021, compared to an annual average of less than 1% for the period from 1950-2020 (CAL FIRE, 2023). The 2021 fire season occurred during the hottest summer recorded in California and was preceded by two years of below average precipitation and early spring snowmelt (Taylor *et al.*, 2022).

With limited personnel and equipment and competing priorities, agencies tasked with fire protection must decide how to best allocate resources for effective fire suppression. Many fires can occur simultaneously across various landscapes and socioeconomic regions, threatening life, property, and natural resources. In 2021, 3560 structures were destroyed, contributing to losses of over $500 million (CAL FIRE, 2021b). Three firefighters died in the 2021 fire season, while the 2020 fire season resulted in at least 33 fatalities (CAL FIRE, 2020, 2021b). The California Air Resources Board (2022b) estimates that almost 0.09 $PgCO_2$ were emitted by 2021 fires, equivalent to approximately 25% of the state's total 2020 CO_2 emissions (California Air Resources Board, 2022a), and the National Park Service reports that the 2020 Castle and 2021 KNP Complex Fires killed 13-17% of the endangered ancient giant sequoia trees of the southern Sierra Nevada (Shive *et al.,* 2023).

In this study, we analyzed the relationships among fire growth, weather, firefighting resources, and damages during the 2021 California wildfire season. Specifically, we analyzed active fire line length, burned area, and personnel deployed for the 11 largest 2021 fires. Further, we quantified the relationships among temperature, vapor pressure deficit (VPD), wind speed, active fire line length, burned area, structures threatened, and structures destroyed throughout the course of the 2021 Dixie, Caldor, and KNP Complex Fires, which accounted for 50% of 2021 burned area. We also compared these relationships for the Dixie, Caldor, and KNP Complex Fires to the number of personnel, engines, and helicopters deployed to investigate how firefighting resources were allocated when wildfires occurred simultaneously or with little temporal separation. We expected to observe more resources devoted to the Caldor Fire, whose final area was smaller than the Dixie Fire but burned closer to more highly-populated areas.

2.2. Methods

2.2.1. Study fires

We focused our analyses on the Dixie, Caldor, and KNP Complex Fires partly because they were three of the largest fires in 2021 and co-occurred within the Sierra Nevada region. Further, the Dixie and Caldor Fires grew simultaneously during our study period. The KNP Complex Fire ignited within four days after the Dixie and Caldor Fires reached their final sizes, but during that time, containment was incomplete and considerable resources and personnel remained dedicated to these earlier fires.

The Dixie Fire, the largest 2021 fire and the second-largest fire ever recorded in California, began on 13 July and was 100% contained by 25 October mainly via CAL FIRE efforts. The fire burned 3898 km^2 (963,309 acres) primarily on federal lands and was the first wildfire in California's history to exceed $500 million in fire suppression expenditures (Taylor *et al.*, 2022).

The Caldor Fire burned 898 km^2 (221,835 acres) across 3 counties between its ignition on 14 August and containment on 21 October. CAL FIRE and the U.S. Department of Agriculture Forest Service were primarily responsible for fire suppression efforts. It became only the second fire in recorded history to cross the Sierra Nevada mountains (Sion *et al.*, 2023). The Caldor Fire was responsible for over 1000 structures destroyed, similar to the Dixie Fire, despite being about 75% smaller in total burned area (CAL FIRE, 2021b).

Over its course from 10 September to 16 October, the KNP Complex Fire burned 357 km^2 (88,307 acres). The National Park Service was primarily responsible for the KNP Complex Fire suppression efforts, which occurred mainly on forested land in Sequoia and Kings Canyon National Parks. The fire burned through groves of the endangered giant sequoia (*Sequoiadendron giganteum* (LINDL.) J.T. BUCHHOLZ), killing an estimated 3-5% (Stephenson and Brigham, 2021; Odwuor *et al.*, 2023).

We also analyzed fire growth and personnel for eight additional 2021 fires listed in Table 2.1.

Figure 2.1 shows the area of the Dixie, Caldor, and KNP Complex Fires relative to the eight other 2021 fires analyzed in this study and the Sierra Nevada region.

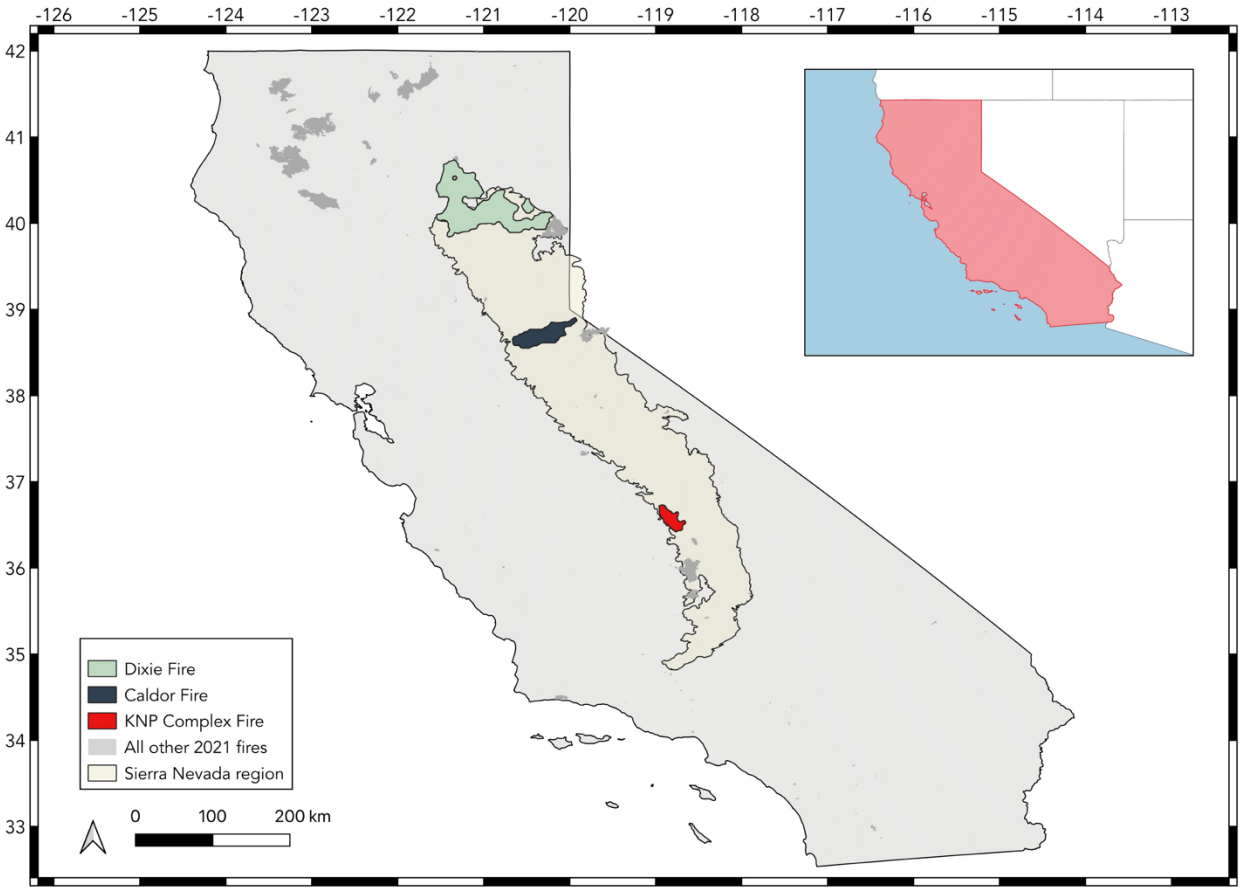

Figure 2.1. Map showing the final perimeters of the 2021 California wildfires. The Dixie, Caldor, and KNP Complex Fire final fire perimeters depicted by the green, blue, and red shaded areas, respectively, are derived from the GOES-Observed Fire Event Representation (GOFER) data product (Liu *et al*., in review). Specifically, the GOFER-W data product, derived from GOES-West active fire detections, was used in our analysis. Final fire perimeters for all other 2021 fires are shown using historical fire perimeter data from the CAL FIRE Fire Resource and Assessment Program (CAL FIRE, 2023).

Table 2.1. Summary table of the 2021 fires analyzed in this study ordered from smallest to largest area burned. Area burned was derived from the CAL FIRE 2021 Wildfire Activity Statistics (CAL FIRE 2021b).

Fire	Area burned (km^2)
Dixie Fire	3898
Monument Fire	903
Caldor Fire	898
River Complex Fire	807
Antelope fire	589
McFarland Fire	496
Beckwourth Complex Fire	428
Windy Fire	395
McCash Fire	384
KNP Complex Fire	357
Tamarack Fire	278
Total	**9433**

2.2.3. Fire growth

Hourly active fire line length and burned area for the 2021 fires were obtained using the GOES-Observed Fire Event Representation (GOFER) dataset (Liu *et al*., in review). The GOFER algorithm derives hourly perimeters of large fires using GOES satellite detections of active fires after correcting parallax effects in complex terrain and using a set of optimized parameters derived from comparison with higher resolution imagery (Liu *et al*., in review). The GOFER-W dataset, derived from GOES-West satellite detections, was used in this analysis. Daily active fire line length

was defined as the concurrent active fire line length from the GOFER-W dataset at 1 pm local time. The concurrent active fire line length represents the sum of perimeter segments that overlap with active fire pixels in the same hour and are actively burning (and potentially spreading into new areas). We also calculated daily burned area growth as the increase difference in burned area from midnight on the day of interest and midnight on the following day.

2.2.4. Climate

Mean temperature, VPD, and wind speed data for the Dixie, Caldor, and KNP Complex Fires were derived from the ERA5-Land reanalysis data product, the fifth generation of European Centre for Medium-Range Weather Forecasts atmospheric reanalysis of the global climate (Hersbach *et al*., 2020). Data were obtained at an hourly, 0.1º x 0.1º resolution and represented the average of grid cells overlapping with the active fire line within a 5 km buffer. To compare with the 1 pm active fire line length and daily burned area, daily we also extracted daily climate variables at 1 pm local time.

2.2.5. Resources

Data for the number of personnel, structures threatened, structures destroyed, engines, and helicopters were obtained from the Incident Command System Incident Status Summary Form 209 (ICS-209 report), reports prepared by the U.S. National Incident Management System to capture regular information about incident development and response (St. Denis *et al.*, 2023). Because the reporting intervals and times of ICS-209 reports are irregular, ranging from 1 to 24 h, we

interpolated data from the ICS-209 reports to hourly time resolution using the interp1 function in Matlab. Daily data were defined as the values for each variable observed at 1 pm local time. The total number of engines and helicopters are reported as the sum of all engine and helicopter categories in the ICS-209 reports. The number of structures threatened is estimated as the number of potentially threatened by the fire within the next 72 hours using currently available information and the number of structures destroyed is defined as those damaged beyond repair.

2.3. Results

We found that the Dixie Fire was actively growing at the time the Caldor Fire began and that the KNP Complex Fire began growing about 2 days after the Dixie Fire and reached its final fire size and 2 days after the Caldor Fire reached its final fire size (Fig. 2.2). Concurrent expansion of the Dixie and Caldor Fires occurred for approximately 23 days between 15 August and 6 September. Neither the Dixie Fire nor Caldor Fire had reached full containment when the KNP Complex Fire began.

We observed an apparent influence of the start of a new fire on the resources assigned to existing fires that were being actively managed (Fig. 2.2b). As the number of personnel rapidly increased with the growth of the Caldor Fire by 13 times between 15-31 August, the number of personnel assigned to the Dixie Fire decreased by about 50%. During this period, the Dixie Fire, which had been burning for approximately 27 days nearly doubled in size, increasing from approximately 2860 km^2 on 15 August to 4110 km^2 on 31 August. The number of personnel assigned to the Dixie

and Caldor Fires decreased sharply as more personnel were deployed to the KNP Complex Fire beginning 12 September.

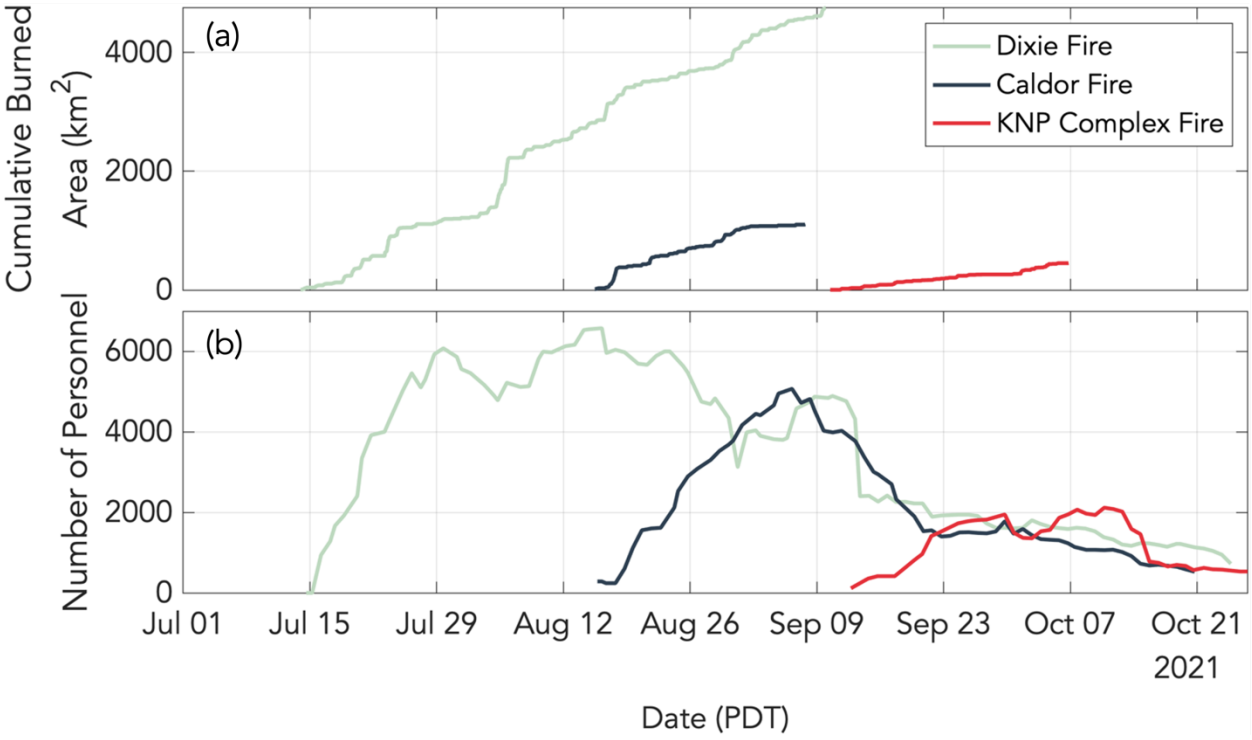

Figure 2.2. Cumulative burned area and total personnel for the Dixie, Caldor, and KNP Complex Fires. (a) Cumulative burned area derived from the GOFER-W data product at an hourly resolution. (b) Total personnel derived from the Incident Command Summary (ICS) Form 209 at variable time resolution (1 to 24 h).

Stress on the availability of fire suppression resources during this period is also evident from comments made by incident command for the Caldor and Dixie Fires and recorded in the ICS-209 reports. For the Caldor fire, comments include:

> "The organization is stretched due to staffing shortages supporting other incidents. This combined with the complexity of this incident, there is a critical concern for diminishing ability to assure firefighter and public safety."

> "Steep and rugged terrain, critically dry fuel conditions, and lack of adequate resources have presented control challenges, limiting the ability for direct attack."

For the Dixie Fire, incident commanders noted the strain on resources:

> "Fire continues to rapidly spread through communities challenging crews in the WUI [wildland urban interface] setting with shortage of overhead and suppression resources."

Even though the fires were separated by hundreds of kilometers, fire weather was highly synchronized across the region. Daily mean surface air temperature variability was correlated between the Dixie and Caldor fires with a Pearson correlation coefficient of 0.97. Daily VPD was

also highly correlated for these two fires with a correlation coefficient of 0.85 (Fig. 2.3). Wind speed had a lower (but still highly significant) correlation of 0.61.

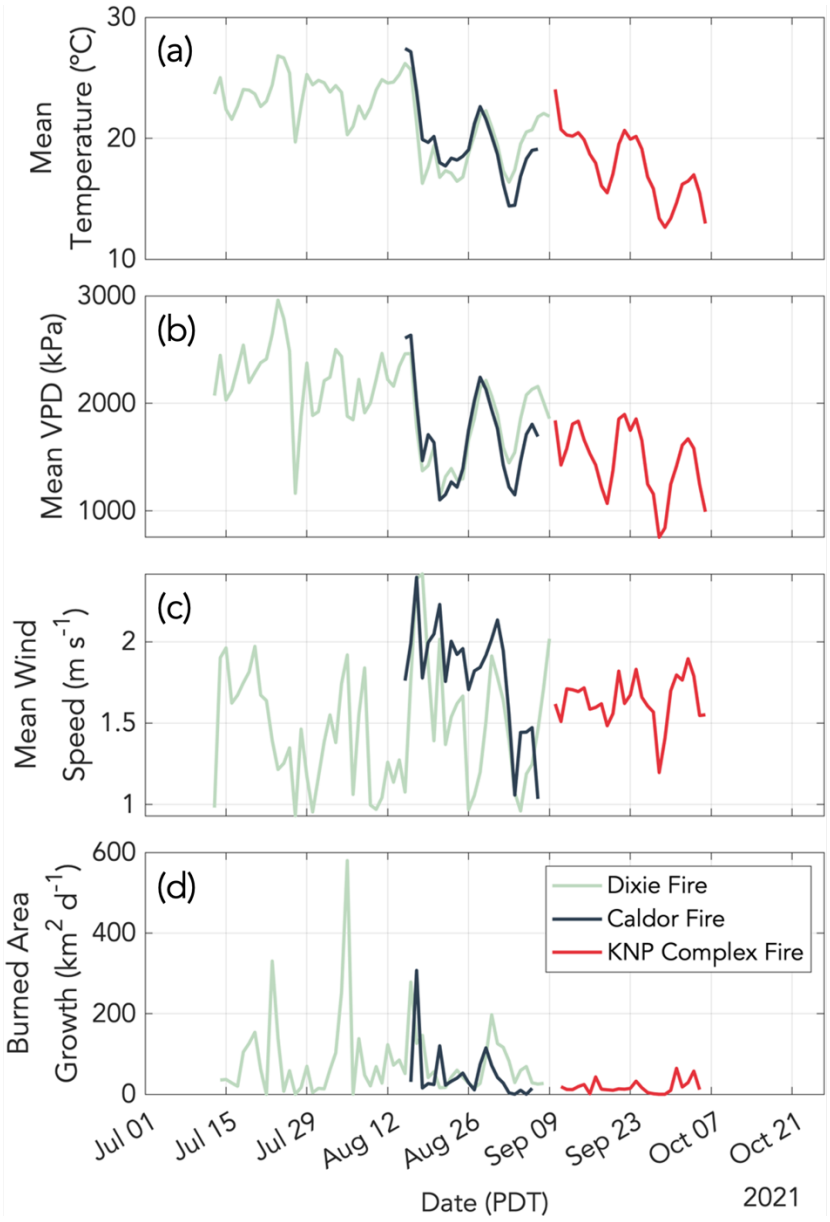

Figure 2.3. Climate variables and burned area growth for the Dixie, Caldor, and KNP Complex Fires. (a) Mean temperature, (b) vapor pressure deficit (VPD), and (c) mean wind speed derived from fifth generation European Centre for Medium-Range Weather Forecasts atmospheric reanalysis of the global climate. Data shown are values for 1pm local time. (d) Burned area growth calculated as the difference between midnight burned area from GOFER-W data product for each date and the following date.

In response to the synchronized fire weather, daily fire growth covaried across the Dixie and Caldor Fires. During their period of overlap, daily fire growth was correlated at a level of 0.97. Both fires experienced periods of rapid expansion on 16-17 and 29-30 August (Fig. 2.4a, b). The first interval occurred during a period of high VPD and mean wind speed, and the second period corresponded to a more moderate peak in fire weather. Active fire line length also appeared synchronized across the two fires, particularly near the end of the overlap period (after a period extremely rapid growth for the Caldor Fire).

Day-by-day estimates of structures threatened provide insight about the proximity to the fire front to the wildland urban interface and the potential for fire growth from the available weather forecast. A comparison across fires reveals several features (Fig. 2.4c, d). First, the threat of the Caldor Fire to the community of South Lake Tahoe is visible with the high number of structures threatened between 29 August and 10 September. Second, the more remote terrain surrounding the KNP Complex Fire in the Sequoia and Kings Canyon National Parks is consistent with the low number of structures threatened compared to the other two fires. Third, structures threatened did not seem to be a particularly effective variable in explaining structures destroyed. This may be expected as a consequence of a successful fire suppression strategy and the more temporally integrated nature of the modeling system used to predict this variable.

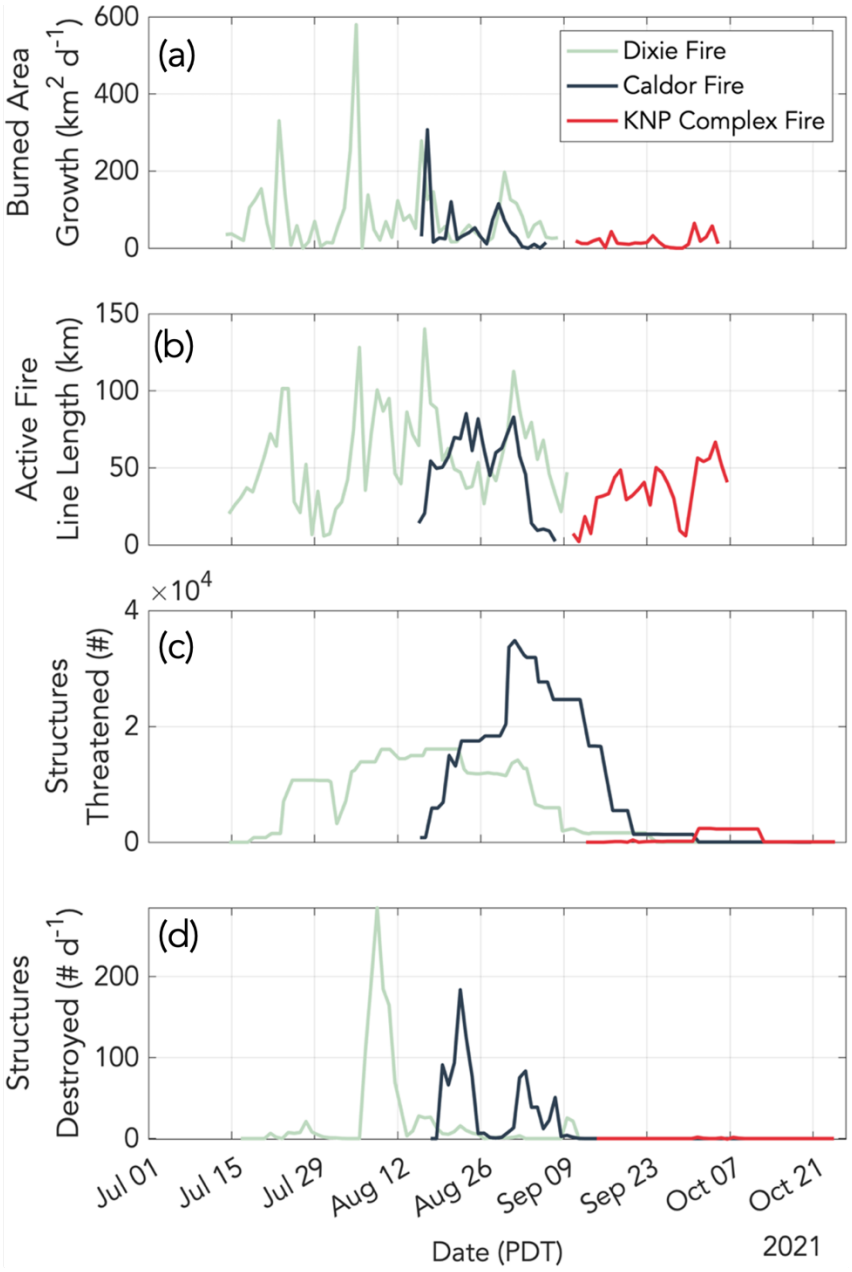

Figure 2.4. Fire growth and structures threatened and destroyed for the Dixie, Caldor, and KNP Complex Fires. (a) Burned area growth calculated as the difference between midnight burned area from GOFER-W data product for each date and the following date. (b) Active fire line length from GOFER-W data product at 1pm local time. (c) Cumulative number of structures threatened from ICS form 209 at variable time resolution (1 to 24 h). (d) Number of structures destroyed per day calculated from ICS Form 209 cumulative structures destroyed averaged to daily resolution.

Days with a high number of structures destroyed were closely tied to intervals of rapid daily fire growth and tended to occur closer to the time of ignition than to the time of final fire size. The dates with greatest structures destroyed roughly coincided with the destruction of Greenville by the Dixie Fire (4 August) and Grizzly Flats by the Caldor Fire (15 August) and the approach of the Caldor Fire at Lake Tahoe (29 August). Structures destroyed were positively correlated with burned area growth for the Caldor and KNP Complex Fires and negatively correlated for the Dixie Fire (Fig. 2.3). We observed a lag in structures destroyed after intervals of rapid fire growth, with the increase in structures destroyed occurring 3-8 days after peaks in fire growth. This may be a consequence of reporting delays, as fire personnel must wait before safely accessing areas immediately behind the fire front.

The number of engines and helicopters deployed to the Dixie and Caldor Fires increased sharply at the beginning of each fire (Fig. 2.5). The maximum number of engines observed for the Caldor Fire (523) nearly approached the maximum for the Dixie Fire (569). Normalized by the active fire line length, the number of engines per unit length active fire line was generally greater for the Dixie Fire. The number of engines at the Dixie Fire decreased simultaneously with increased engines at the Caldor Fire between 16 August and 2 September. The number of helicopters at the Dixie and Caldor Fires increased concurrently, with the Caldor Fire reaching a greater maximum number of helicopters (38) than the Dixie Fire (28), The number of helicopters per km active fire line length was similar for the two fires (Fig. 2.6).

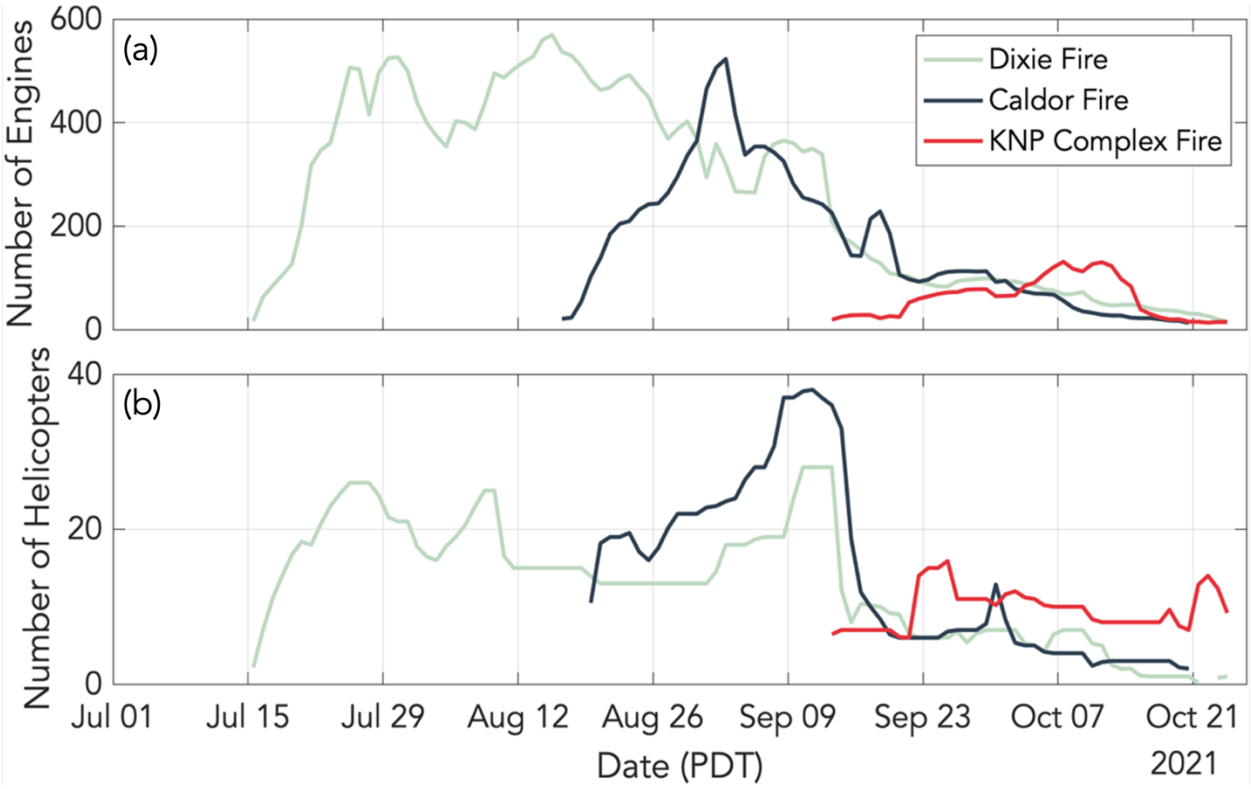

Figure 2.5. Number of engines and helicopters deployed to the Dixie, Caldor, and KNP Complex Fires. Number of (a) engines and (b) helicopters from ICS-209 reports.

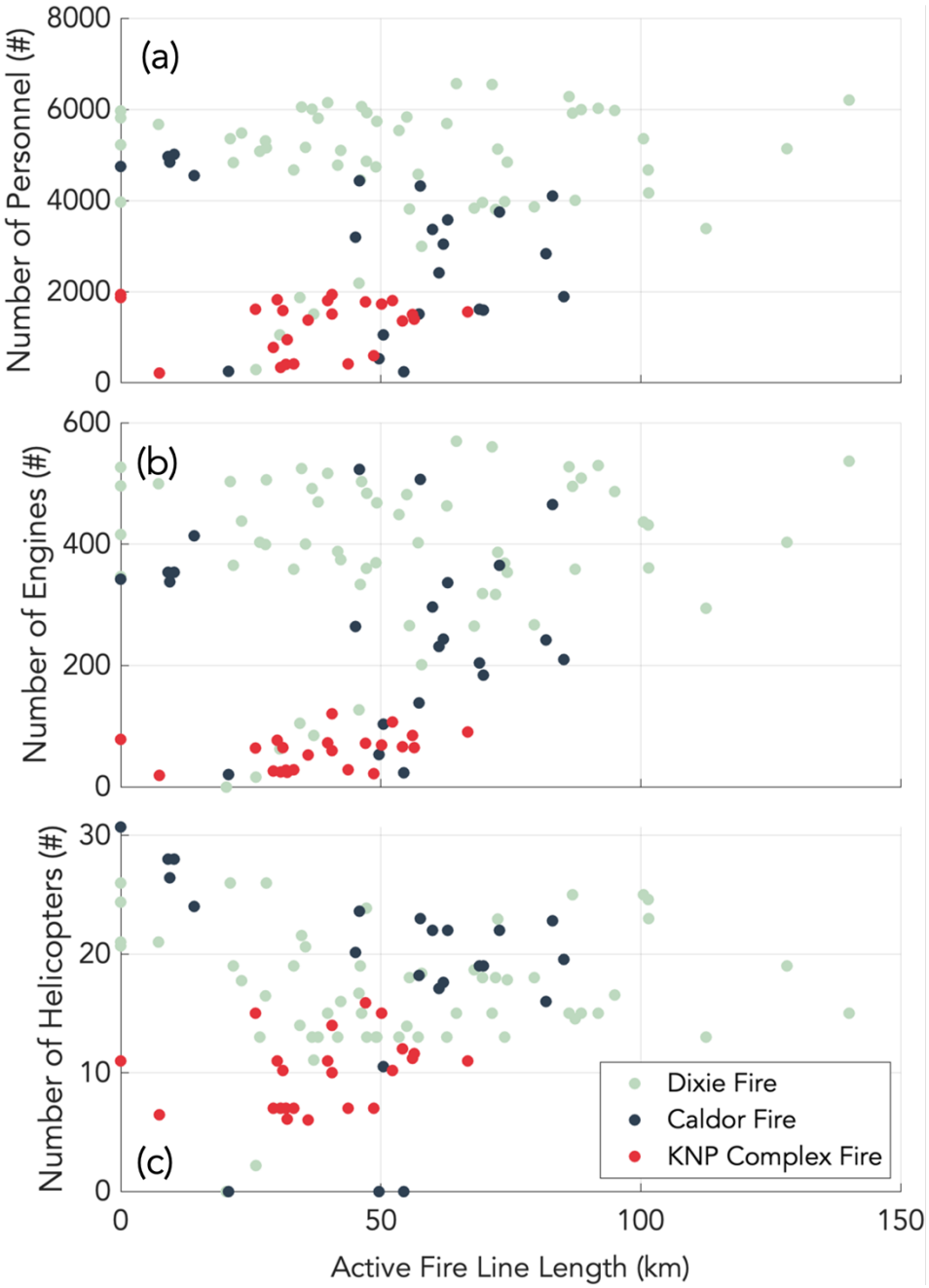

Figure 2.6. Daily resources for the Dixie, Caldor, and KNP Complex Fires as a function of daily active fire line length. Total number of (a) personnel, (b) engines, and (c) helicopters from the ICS-209 reports interpolated to daily resolution and plotted against active fire line length from the GOFER-W data product.

We found that the periods of greatest burned area growth, active fire line length, and personnel deployed for all 2021 fires observed in this study occurred around the 5th, 15th, and 30th of August, which we had identified as the periods of greatest fire growth for the Dixie and Caldor Fires.

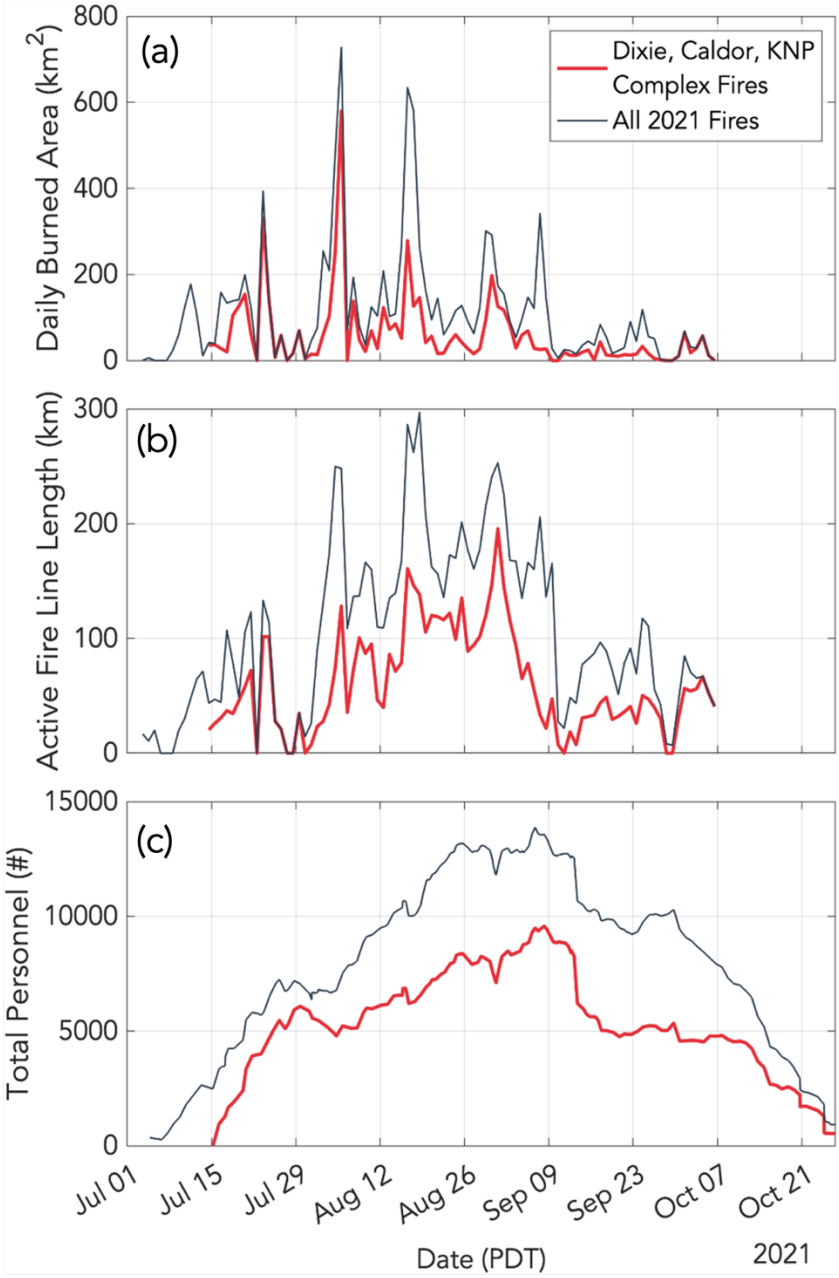

Figure 2.7. Daily burned area, active fire line length, and total personnel for all 2021 fires analyzed inn this study (blue line) and the Dixie, Caldor, and KNP Complex Fires (red line) summed. (a) Daily burned area calculated as the difference between midnight burned area from GOFER-W data product for each date and the following date. (b) Active fire line length from GOFER-W data product at 1pm local time. (c) Total personnel at variable time resolution (1 to 24 h) from ICS-209 reports.

2.4. Discussion

In agreement with previous work on the relationship between climate and fire behavior (Abatzoglou and Williams, 2016; Westerling, 2016; Williams *et al.*, 2019; Gutierrez *et al.*, 2021; Brown *et al.*, 2023), we found that daily fire growth was driven by increases in temperature and VPD. Synchrony between the greatest growth in burned area for the Dixie and Caldor Fires further suggests that fires burning simultaneously, even across different landscapes, are driven by the same climate variables across the Sierra Nevada, which may create challenges for the allocation of firefighting resources.

Whereas we hypothesized that we would see a higher concentration of firefighting resources at the Caldor Fire, which burned through or near areas with a higher density of homes and greater property values, we found instead that resources were distributed relatively evenly across the two fires. The KNP Complex Fire had lower numbers of personnel, engines, and helicopters, which may be explained by the fact that this fire burned through more remote, forested area in Sequoia and Kings Canyon National Parks that was harder to access and had fewer structures threatened. Further, the KNP Complex Fire occurred toward the end of the fire season, when funding and staffing were more depleted. Altogether, this highlights the potential for future fire suppression and treatment efforts to consider weighing the value of natural resources, like the endangered giant sequoia, more heavily. An estimated 3-5% of giant sequoias were estimated to have been killed by the KNP Complex Fire (Stephenson and Brigham, 2021). We propose that multiple large fires occurring at once, driven by the same warm, dry, synchronized weather, create a stress on already-

limited fire suppression resources in California that must be distributed to protect life, property, and natural resources.

We identified the 5th, 15th, and 30th of August as the periods of greatest stress during the 2021 fire season, when the Dixie Fire destroyed the town of Greenville (4 August) and when the Caldor Fire destroyed Grizzly Flats (15 August) and approached Lake Tahoe (29 August). The town of Greenville, with a population of approximately 1000 people, was placed under mandatory evacuation orders days ahead of the Dixie Fire arrived and eventually destroyed an estimated 75% of structures (Kasakove, 2021). Investigative reporting found that that after an aggressive initial attack on the Caldor Fire, extreme fire growth in its first two days of burning caused resources to be extracted in an effort to maintain firefighters' safety (Wildfire Today, 2022).Specifically, crew were ordered off of the fire just a few hours after fire suppression began and on the second day of the fire, CAL FIRE removed several hand crews and engines (Wildfire Today, 2022). In addition to firefighter safety, the available budget is an important factor in the availability of resources.

CAL FIRE's annual budget for emergency fire suppression (E-fund) is primarily used for responding to large wildfires that exceed the agency's ability for containment using the base budget for fire protection (California Legislative Analyst's Office, 2022). In some instances, CAL FIRE might preemptively extend staffing levels or other resources in anticipation of a more severe fire season. However, the majority of the E-fund expenditures in 2021 were for unplanned costs, meaning that wildfires exceeded CAL FIRE's containment capacity unexpectedly during the

course of the wildfire season (California Legislative Analyst's Office, 2023). One factor contributing to CAL FIRE's limited capacity for wildfire response is the recent reduction in the availability of personnel for hand crews, which are responsible for various fire mitigation and suppression activities and are typically largely staffed by inmate populations. Inmate populations have decreased by over 25% in the last decade (California Legislative Analyst's Office, 2021), resulting in a decline in staffing for hand crews. The State of California proposes to increase CAL FIRE's budget to hire more professional firefighters to expand hand crews, anticipating that this increased staffing would primarily be used for wildfire response (California Legislative Analyst's Office, 2021). However, increased staffing also implies that more wildland firefighters will be exposed to extreme occupational hazards.

During wildfire response, wildland firefighters endure heavy physical demands (Vincent *et al.*, 2018) and are exposed to concentrations of many pollutants exceeding the limits deemed safe by the Occupational Safety and Health Administration (Rothman *et al.*, 1991), making them more vulnerable to other respiratory diseases (Navarro *et al.*, 2021) and cardiovascular disease, as well as certain cancers (Navarro *et al.*, 2019). Wildland firefighters also suffer higher incidences of mental illness (Stanley *et al.*, 2018). Although the State of California plans to expand staff for wildland firefighters, an important consideration is protecting their safety and wellbeing. In California, $400 million in 2021 was budgeted to improve the health and wellness of CAL FIRE firefighters to meet the demands of emergency fire response in a changing climate (California Governor's Office, 2022).

Climate warming in the Sierra Nevada is predicted to continue increasing in the coming decades (Williams *et al.*, 2019; Gutierrez *et al.*, 2021). In part because of an over-abundance of fuels, the contemporary fire regime in the Sierra Nevada can be characterized as climate-limited, meaning that fuel abundance is not limiting and that fire occurrence and spread respond directly to warming and drying trends that influence fuel moisture and the likelihood that initial fire starts will escape containment (Steel, Safford and Viers, 2015; Abatzoglou and Williams, 2016). Although additional warming and drying are already in the pipeline from the past history of greenhouse gas accumulation in the atmosphere, humans can modulate the effect of climate on wildfires via fuel treatments like mechanical thinning and prescribed fire. There is strong evidence that, especially when combined with mechanical treatments, it can effectively reduce fuel loads and, thereby, fire intensity and severity (Kalies and Kent, 2016). We emphasize the need not just for not enhanced fire suppression efforts, but also for fuel treatments as means to mitigate wildfire severity and protect natural resources and both public and firefighter health and safety.

2.5. Conclusions

In this study, we used a satellite-derived dataset for tracking the progression of wildfires and the incident command forms maintained by the U.S. National Incident Management System to analyze the relationships among fire growth, weather, firefighting resources, and damages during the 2021 California wildfire season. We found that broad-scale weather patterns drove growth in wildfire burned area, synchronizing the periods of greatest growth for the Dixie and Caldor Fires, two of the largest 2021 fires. The number of structures destroyed increased following periods of rapid fire

growth. We identified the periods of greatest stress to fire suppression efforts as the 5th, 15th, and 30th of August, corresponding to the greatest burned area growth in the Dixie and Caldor Fires and highest associated number of damages. These periods also coincided with the destruction of two towns and the threat of destruction of another. We propose that the control by climate conditions on fire growth causes multiple large fires to become synchronized in their periods of extreme growth, creating a strain on already limited firefighting resources and resulting in the destruction of more structures. Our work identifies some constraints on wildland firefighting efforts, including staffing and competition between the protection of life and property versus natural resources, and highlight the need for fuel management to mitigate fire severity, thereby reducing the demand placed on fire suppression efforts during wildfires in a warming climate.

2.6. References

Abatzoglou, J. T. and Williams, A. P. (2016) 'Impact of anthropogenic climate change on wildfire across western US forests'. doi: 10.1073/pnas.1607171113.

Brown, P. T. *et al.* (2023) 'Climate warming increases extreme daily wildfire growth risk in California', *Nature*. Springer US, 621(July 2022). doi: 10.1038/s41586-023-06444-3.

St. Denis, L. A. *et al.* (2023) 'All-hazards dataset mined from the US National Incident Management System 1999–2020', *Scientific Data*, 10(1), pp. 1–23. doi: 10.1038/s41597-023-01955-0.

California Air Resources Board (2022a) *Current California GHG Emission Inventory Data* (available at: https://ww2.arb.ca.gov/ghg-inventory-data) (Accessed 2 November 2023)

California Air Resources Board (2022b) *Wildfire Emissions Estimates for 2021* (available at: https://ww2.arb.ca.gov/sites/default/files/classic/cc/inventory/Wildfire%20Emission%20Estimates%202000-2021.pdf) (Accessed 2 November 2023)

CAL FIRE (2020) *2020 Wildfire Activity Statistics* (available at: https://34c031f8-c9fd-4018-8c5a-4159cdff6b0d-cdn-endpoint.azureedge.net/-/media/calfire-website/our-impact/fire-statistics/2020_redbook_final.pdf?rev=72030b4d2cb7466aa573754ecb4f656e&hash=337DB407876BE384081C7D722D82B1BF) (Accessed 2 November 2023)

CAL FIRE (2021a) *Emergency Fund Fire Suppression Expenditures* (available at: www.fire.ca.gov/media/px5lnaaw/suppressioncos tsonepage1.pdf) (Accessed 20 February 2023)

CAL FIRE (2021b) *2021 Wildfire Activity Statistics.* (available at: https://34c031f8-c9fd-4018-8c5a-4159cdff6b0d-cdn-endpoint.azureedge.net/-/media/calfire-website/our-impact/fire-statistics/2021_redbook_final.pdf?rev=525959073bbe4bbe816d67624911e4c3&hash=CFD17F879B2CE984AB5BA9FEA4F73A56) Accessed 2 November 2023)

CAL FIRE (2023) Fire and Resource Assessment Program Fire Perimeters (available at: https://frap.fire.ca.gov/mapping/gis-data/on) (Accessed 2 November 2023)

California Governor's Office (2022) *Governor's Budget Summary 2022-23: Emergency Response.* (available at: https://ebudget.ca.gov/2022-23/pdf/BudgetSummary/EmergencyResponse.pdf) (Accessed 3 November 2023)

California Legislative Analyst's Office (2022) *The 2022-23 Budget: Wildfire and Forest Resilience Package* (available at: https://lao.ca.gov/reports/2022/4495/wildfire-forest-resilience-012622.pdf) (Accessed 2 November 2023)

California Legislative Analyst's Office (2023) *The 2023-24 Budget: Improving Legislative Oversight of CalFire's Emergency Fire Protection Budget* (available at: https://lao.ca.gov/reports/2023/4765/CalFire-Emergency-Budget-050123.pdf) (Accessed 3 November 2023)

Dennison, P. E. *et al.* (2014) 'Geophysical Research Letters', *Geophysical Research Letters*, (April), pp. 6413–6419. doi: 10.1002/2014GL061184.Received.

Gabbert, B. (3 October 2022) "60 Minutes investigates the initial attack on Caldor Fire." *Wildfire Today.* https://wildfiretoday.com/2022/10/03/60-minutes-investigates-the-initial-attack-on-caldor-fire/

Gutierrez, A. A. *et al.* (2021) 'Wildfire response to changing daily temperature extremes in California's Sierra Nevada', *Science Advances*, 7(47), pp. 1–11. doi: 10.1126/sciadv.abe6417.

Hantson, S. *et al.* (2022) 'Human-ignited fires result in more extreme fire behavior and ecosystem impacts', *Nature Communications*. Springer US, 13(1), pp. 1–8. doi: 10.1038/s41467-022-30030-2.

Hersbach, H., Bell, B., Berrisford, P., Hirahara, S., Horányi, A., Muñoz-Sabater, J., ... & Thépaut, J. N. (2020). The ERA5 global reanalysis. *Quarterly Journal of the Royal Meteorological Society*, *146*(730), 1999-2049. doi: 10.1002/qj.3803

Juang, C. S. *et al.* (2022) 'Rapid Growth of Large Forest Fires Drives the Exponential Response of Annual Forest-Fire Area to Aridity in the Western United States', *Geophysical Research Letters*, 49(5). doi: 10.1029/2021GL097131.

Kasakove, S., (5 August 2021) "'We lost Greenville': A California town is overrun by the Dixie Fire.*The New York Times.* https://www.nytimes.com/2021/08/05/us/dixie-fire-greenville-california.html#:~:text=Fire%20officials%20estimated%20that%2075,now%20lives%20in%20nearby%20Taylorsville.

Kalies, E. L. and Kent, L. L. Y. (2016) 'Tamm Review: Are fuel treatments effective at achieving ecological and social objectives? A systematic review', *Forest Ecology and Management*. Elsevier B.V., 375, pp. 84–95. doi: 10.1016/j.foreco.2016.05.021.

Keeley, J. E. and Syphard, A. D. (2021) 'Large California wildfires: 2020 fires in historical context', *Fire Ecology*. Fire Ecology, 17(1). doi: 10.1186/s42408-021-00110-7.

Liu, T., Randerson, J.T., Chen, Y., Morton, D.C., Wiggins, E.B., Smyth, P., Foufoula-Georgiou, E., Nadler, R., Nevo, O. (in review) *Systematically tracking the hourly progression of large wildfires using GOES satellite observations*

Marks-Block, T. and Tripp, W. (2021) 'Facilitating prescribed fire in northern California through indigenous governance and interagency partnerships', *Fire*, 4(3). doi: 10.3390/fire4030037.

National Interagency Fire Center *Suppression Costs* (available at: https://www.nifc.gov/fire-information/statistics/suppression-costs) (Accessed 3 Nov 2023)

Shive, K., Brigham, C., Caprio, T., Hardwick, P. (2023) *2021 Fire Season Impacts to Giant Sequoias* (available at: https://www.nps.gov/articles/000/2021-fire-season-impacts-to-giant-sequoias.htm) (Accessed 2 November 2023)

Navarro, K. M. *et al.* (2019) 'Wildland firefighter smoke exposure and risk of lung cancer and cardiovascular disease mortality', *Environmental Research*. Elsevier Inc., 173(November 2018), pp. 462–468. doi: 10.1016/j.envres.2019.03.060.

Navarro, K. M. *et al.* (2021) 'Wildland firefighter exposure to smoke and COVID-19: A new risk on the fire line', *Science of the Total Environment*. Elsevier B.V., 760, p. 144296. doi: 10.1016/j.scitotenv.2020.144296.

Odwuor, A., Yañez, C. C., Chen, Y., Hopkins, F. M., Moreno, A., Xu, X., ... & Randerson, J. T. (2023). Evidence for multi-decadal fuel buildup in a large California wildfire from smoke radiocarbon measurements. *Environmental Research Letters*, *18*(9), 094030. doi: 10.1088/1748-9326/aced17

Radeloff, V. C. *et al.* (2018) 'Rapid growth of the US wildland-urban interface raises wildfire risk', *Proceedings of the National Academy of Sciences of the United States of America*, 115(13), pp. 3314–3319. doi: 10.1073/pnas.1718850115.

Rothman, N. *et al.* (1991) 'Pulmonary Function and Respiratory Symptoms in Wildland Firefighters', *Journal of Occupational Medicine*, 33(11), pp. 1163–1167.

Sion, B. *et al.* (2023) 'Assessment of the Effects of the 2021 Caldor Megafire on Soil Physical Properties, Eastern Sierra Nevada, USA', *Fire*, 6(2). doi: 10.3390/fire6020066.

Stanley, I. H. *et al.* (2018) 'Wildland firefighters and suicide risk: Examining the role of social disconnectedness', *Psychiatry Research*, 266(January), pp. 269–274. doi: 10.1016/j.psychres.2018.03.017.

Steel, Z. L., Safford, H. D. and Viers, J. H. (2015) 'The fire frequency-severity relationship and the legacy of fire suppression in California forests http://www.esajournals.org/doi/pdf/10.1890/ES14-00224.1', *Ecosphere*, 6(1). doi: 10.1890/ES14-00224.1.

Stephenson, N. and Brigham, C. (2021) 'Preliminary Estimates of Sequoia Mortality in the 2020 Castle Fire', *National Park Service*, pp. 1–32.

Taylor, A. H. *et al.* (2016) 'Socioecological transitions trigger fire regime shifts and modulate fire-climate interactions in the Sierra Nevada, USA, 1600-2015 CE', *Proceedings of the National Academy of Sciences of the United States of America*, 113(48), pp. 13684–13689. doi: 10.1073/pnas.1609775113.

Taylor, A. H., Harris, L. B. and Skinner, C. N. (2022) 'Severity patterns of the 2021 Dixie Fire exemplify the need to increase low-severity fire treatments in California's forests', *Environmental Research Letters*, 17(7). doi: 10.1088/1748-9326/ac7735.

Vincent, G. E. *et al.* (2018) 'Sleep in wildland firefighters: What do we know and why does it matter?', *International Journal of Wildland Fire*, 27(2), pp. 73–84. doi: 10.1071/WF17109.

Westerling, A. L. *et al.* (2006) 'Warming and earlier spring increase western U.S. forest wildfire activity', *Science*, 313(5789), pp. 940–943.

Westerling, A. L. R. (2016) 'Increasing western US forest wildfire activity: Sensitivity to changes in the timing of spring', *Philosophical Transactions of the Royal Society B: Biological Sciences*, 371(1696). doi: 10.1098/rstb.2015.0178.

Williams, A. P. *et al.* (2019) 'Observed Impacts of Anthropogenic Climate Change on Wildfire in California', *Earth's Future*, 7(8), pp. 892–910. doi: 10.1029/2019EF001210.

Chapter 3

Evidence for multi-decadal fuel buildup in a large California wildfire from smoke radiocarbon measurements

Adapted from:
Odwuor, A., Yañez, C. C., Chen, Y., Hopkins, F. M., Moreno, A., Xu, X., ... & Randerson, J. T. (2023). Evidence for multi-decadal fuel buildup in a large California wildfire from smoke radiocarbon measurements. *Environmental Research Letters*, *18*(9), 094030. doi: 10.1088/1748-9326/aced17

3.1. Introduction

Wildfire activity in California, including area burned and occurrence of large fires, has increased over the last several decades, with intensifying impacts on society, the economy, and ecosystems (Dennison *et al.,* 2014, Williams *et al.,* 2019, Safford *et al.,* 2022, Wang *et al.,* 2021). During high fire years, mandatory evacuation orders force tens of thousands of people to flee their homes (Safford *et al.,* 2022). Direct costs of wildfires, including fire suppression and property losses, have more than doubled in the last decade (California Department of Forestry and Fire Protection, 2022a). Wildfires also incur significant indirect costs (Wang *et al.,* 2021) related to environmental cleanup, lost business revenue, infrastructure repair, and health impacts. Wildfires account for up to half of the exposure to $PM_{2.5}$ (airborne particulate matter (PM) with diameter <2.5 μm) in the western U.S. (Burke *et al.,* 2021), and smoke exposure has been linked to increased respiratory-related hospitalizations and adverse health outcomes related to restricted activity and days of work lost (Kochi *et al.,* 2010, Reid *et al.,* 2016). California's ecosystems are also negatively affected by intensifying wildfires, which can weaken landscape-scale carbon storage, shift vegetation composition, reduce biodiversity, and threaten water supplies and other ecosystem services (Wu *et al*., 2011;, Stevens, 2017a; Foster *et al*., 2020). These worsening impacts motivate an urgent

need for research aimed at informing and evaluating wildfire management strategies in California and the western U.S.

In the Sierra Nevada mountains of California, burned area has increased by more than seven-fold since the 1980s, mainly as a consequence of the cumulative effects of widespread fire suppression and climate change (Taylor *et al.,* 2016; Williams *et al.,* 2019; Gutierrez *et al.,* 2021; Hagmann *et al.,* 2021). Widespread suppression of low- to moderate- intensity fires has allowed overgrowth of shrubs and small trees, which compete with larger trees for resources (e.g., water) and serve as ladder fuels that facilitate high-intensity crown fires (McKelvey and Busse, 1996, Stephens *et al.,* 2009; Pausas and Keeley, 2019). In addition to fuel buildup, the region has experienced warmer and drier conditions that increase the likelihood of more frequent and extensive wildfires (Williams *et al.,* 2019; Abatzoglou *et al.,* 2021; Gutierrez *et al.,* 2021; Higuera and Abatzoglou, 2021).

Although California's coniferous trees evolved with fire and can withstand low- to moderate-intensity fires with a return interval of about 15 years (Swetnam, 1993; Swetnam *et al.,* 2009), they are vulnerable to today's high-intensity crown fires (Shive *et al.,* 2022). This is especially important to consider in old- growth forests, such as stands of the endangered giant sequoia (*Sequoiadendron giganteum* (LINDL.) J.T. BUCHHOLZ), which have experienced widespread mortality in recent higher-intensity fires (Shive *et al.,* 2022). Specifically, fires like the Castle Fire in 2020 and KNP Complex Fire in 2021 contributed to giant sequoia mortality. The Castle Fire killed an estimated 10-14% of large (>1.2 m dbh) sequoias (Stephenson and Brigham 2021; Shive

et al., 2022). Today's fire regime is unlike what California's forests and communities have experienced in the past (Stevens *et al.,* 2021), motivating greater investments in forest and wildfire management practices, including prescribed fire, to reduce fire severity (Tubbesing *et al.,* 2021).

In this study, we measured the radiocarbon abundance ($\Delta^{14}C$) (Stuiver and Polach, 1977) of $PM_{2.5}$ emitted by the KNP Complex Fire over a 26 h sampling period, along with *in situ* trace gas dry air mole fractions and $PM_{2.5}$ concentrations, which were used to validate the influence of wildfire emissions on variability on variability in observed $PM_{2.5}$ concentrations. We then used this information to constrain the ages (and types) of combusted fuels and explore implications for fire intensity. Radiocarbon (^{14}C) is a radioactive isotope of carbon that is naturally produced in the atmosphere. Still, the $\Delta^{14}C$ of atmospheric carbon dioxide (CO_2) has changed considerably over the past 70 years because of the Earth system's response to the production of 'bomb' ^{14}C from aboveground nuclear weapons testing during the late 1950s and early 1960s (Nydal, 1963; Levin *et al*., 2010). In past work, $\Delta^{14}C$ measurements of fire-emitted PM have been used to identify the depth of burning in organic duff layers in boreal forest ecosystems (Mouteva *et al*., 2015) and the age of combusted peats contributing to severe haze events in Southeast Asia (Wiggins *et al*., 2018). For western U.S. wildfires, Δ^{14} C measurements can provide information about the size classes of combusted fuels because larger-diameter fuels decompose more slowly and, therefore, persist longer within ecosystems (Harmon, 2021).

We hypothesized that fire-emitted $PM_{2.5}$ would be considerably enriched in ^{14}C relative to current atmospheric CO_2 because larger-diameter fuels incorporated ^{14}C via photosynthesis over several decades when the atmosphere had higher bomb ^{14}C values. Older fuels are associated with larger fuel classes that decompose relatively slowly and build up for decades if not removed mechanically or burned. Several methods are commonly used to assess fire severity, including the composite burn index (Key and Benson, 2006) and remotely-sensed indices, like the normalized burn ratio (Miller *et al.,* 2009a). Measuring the $\Delta^{14}C$ of fire emissions may complement these approaches by constraining the age (and therefore, size distribution) of combusted fuels. By sampling the atmosphere down-wind of a large wildfire, our technique also provides a means to obtain a regionally-integrated snapshot across actively burning areas within the fire perimeter.

3.2. Methods

3.2.1. Sampling location

We collected $PM_{2.5}$ samples and measured *in situ* trace gas and $PM_{2.5}$ levels with a ground-based mobile laboratory in the town of Three Rivers, CA, USA (36.453ºN, 118.873ºW, 361 m above sea level) during 2–3 October 2021. We chose this sampling location to be as close to the KNP Complex Fire as possible without being inside a mandatory evacuation zone. This was within a residential community approximately 0.5 km from the town's main road. Traffic was minimal because the area was under an evacuation warning. Our sampling location was about 10 km from two actively burning fire fronts that were located to the north and east and approximately 1000 m lower in elevation. The KNP Complex Fire resulted from two lightning fires (Colony and Paradise

Fires) that merged into one large fire on 17 September 2021 (Stephenson and Brigham, 2021). The fire was 100% contained on 16 December 2021 after reaching a final size of 357 km^2 (88,307 acres) (California Department of Forestry and Fire Protection 2022b). Over the course of the fire, it burned 18 km^2 (4374 acres) of giant sequoia groves (Shive *et al.,* 2022).

Figure 3.1 shows our sampling location and the distribution of Suomi/NPP Visible and Infrared Imaging Radiometer Suite active fires for the 1:30 pm overpass on 2 October. The active fire line and outer fire perimeter for the KNP Complex Fire on 2 October are also mapped using information from the Fire Events Data Suite version 1 (Chen *et al.,* 2022). This fire information is superimposed on an Aqua MODIS 250 m true color image displaying the spatial extent of smoke from the KNP Complex Fire on 2 October. The location of giant sequoia groves is also provided using data from the National Park Service (National Park Service and Sequoia and Kings Canyon National Parks, 2017). Three lines of evidence confirmed our sampling location was downwind of the fire and its plume: (1) elevated and covarying trace gas and $PM_{2.5}$ concentrations (as described in Results), (2) visual inspection of the smoke cloud in Figure 3.1 and (3) back-trajectory analysis conducted with NOAA's HYSPLIT model (data not shown).

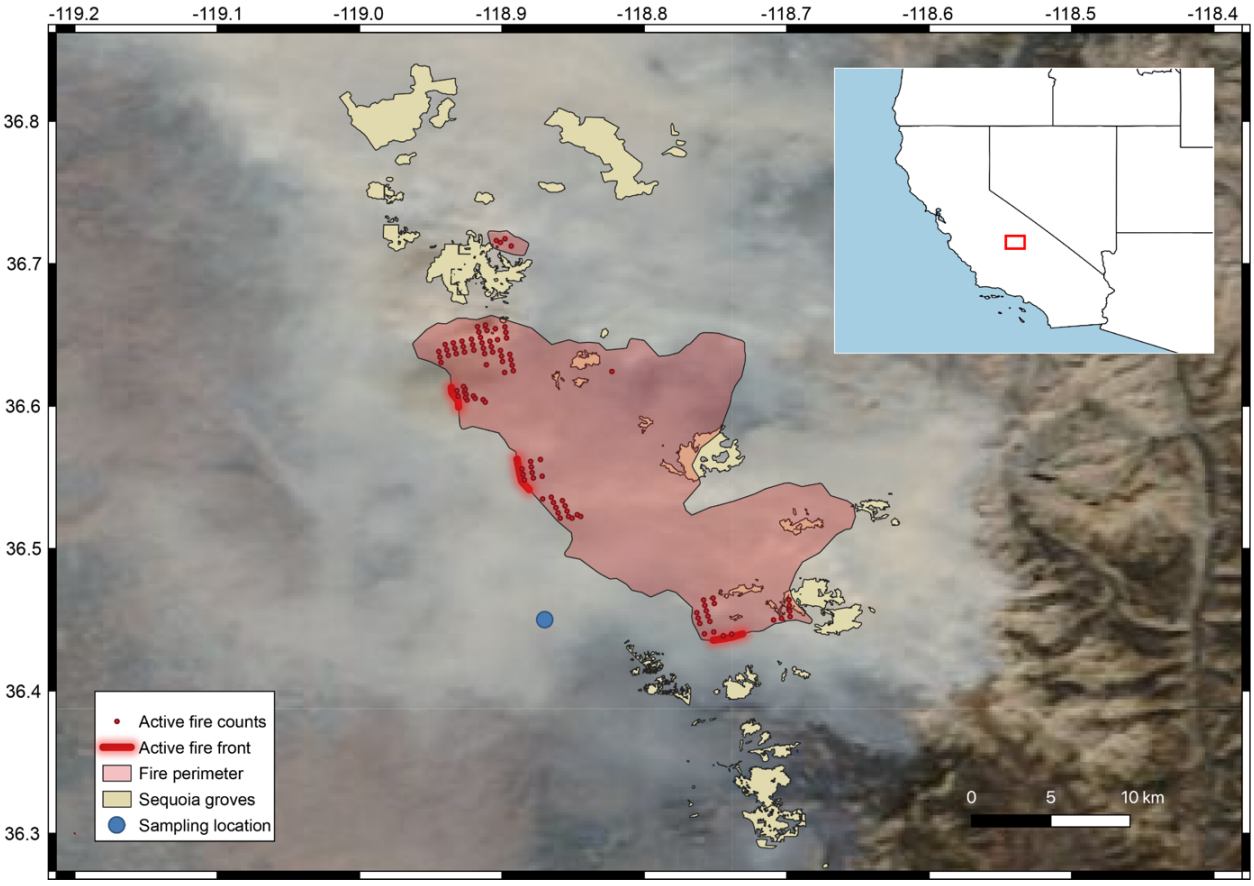

Figure 3.1. Map showing the location of Suomi/NPP Visible and Infrared Imaging Radiometer Suite active fire counts (red circles), the active fire front (red line with red highlight), and fire perimeter (red shading) on 2 October 2021 derived using Fire Events Data Suite version 1. These data are superimposed on an Aqua MODIS 250 m true color image from the same day. The location of giant sequoia groves (tan shading) is shown using the dataset from the National Park Service. Our particulate matter sampling location in the town of Three Rivers, CA, USA is shown with a blue circle.

Air temperature and relative humidity reported here were measured by a compact weather sensor (METSENS500, Campbell Scientific, Logan, UT, USA) mounted on the mobile laboratory approximately 3 m above ground level. The air temperature was 32.0ºC at the beginning of the sampling period at 3:00 pm on 2 October and declined through the evening and night, reaching a

minimum of 17.4ºC at 7:45 am on 3 October. The temperature rose through the morning and afternoon on 3 October, reaching a maximum of 27.2ºC at 2:25 pm. Relative humidity varied from 14% to 26% over the sampling period, within the minimum observed at 3:00 pm on 2 October and the maximum at 26% at 10:30 am on 3 October.

3.2.2. PM2.5 measurement and collection

We measured *in situ* $PM_{2.5}$ mass concentrations (μg $PM_{2.5}$ m^{-3} air) using a PurpleAir PA-II air quality sensor with laser particle counting (PurpleAir, Draper, UT, USA) at a sampling height of approximately 1.2 m above ground. We analyzed the PurpleAir Channel A data, which is appropriate for outdoor conditions and has a 2 min resolution.

Filter samples of $PM_{2.5}$ were collected at an inlet height of 1.2 m above ground level using a low-volume aerosol sampler (MiniVol Tactical Air Sampler, AirMetrics, Springfield, OR, USA) with a $PM_{2.5}$ impactor (#202-100) over periods of 0.5–6.0 h. Sampling duration was determined according to concurrent $PM_{2.5}$ concentration (i.e., sampling duration was inversely related to concurrent $PM_{2.5}$ concentration). To maintain a uniform volume flow, we used ambient temperature and pressure to adjust the sampler's flow rate between 4.50 and 4.75 l min^{-1}. Samples were collected on 47 mm diameter quartz fiber filters (GE Healthcare Life Sciences, #1851-047). Before sampling, filters were pre-combusted at 500ºC for 3 h, wrapped individually in aluminum foil, and stored in plastic bags. Blank filters were mounted on the inside of the sampler housing with no active airflow and collected concurrently with 2 of the 12 $PM_{2.5}$ samples (#253740 and

253744). After collection, filters were wrapped in aluminum foil, sealed in plastic bags, and stored at −20ºC. A total of 12 $PM_{2.5}$ samples and 2 blanks were collected.

3.2.3. Elemental and isotopic analyses of PM2.5

3.2.3.1. Measurement of TC and radiocarbon

Filter samples of $PM_{2.5}$ were analyzed for TC concentration (μg C m^{-3}) and $\Delta^{14}C$ at the W. M. Keck Carbon Cycle Accelerator Mass Spectrometry (KCCAMS) laboratory at the University of California, Irvine. We focused our analysis on the $\Delta^{14}C$ of $PM_{2.5}$ because it is a criteria pollutant for the U.S. Environmental Protection Agency (EPA) and is associated with a wide range of particles generated during combustion (Andreae, 2019). Examining fuel age, $PM_{2.5}$ presents various practical advantages: it is conveniently sampled in the field and in wildfire smoke, and its relatively high signal-to-noise ratio enables a clear differentiation from the background atmosphere.

For each sample, a portion of or the entire filter (depending on estimated TC concentration) was sealed with cupric oxide in pre-combusted 6 mm OD quartz tubes and oxidized to CO2 at 900ºC for 3 h. This TC-derived CO_2 was then extracted and quantified manometrically on a vacuum line, reduced to graphite using a modified sealed-tube zinc reduction method (Walker and Xu, 2019), and its $\Delta^{14}C$ was measured via accelerator mass spectrometry alongside graphitization standards and blanks. The units of $\Delta^{14}C$ are per mille (‰), and the relationship between Δ14C and the widely-used fraction modern (F) measurement is shown in equation (1), where y is the year of ^{14}C

sampling (2021); F is the ^{14}C /^{12}C ratio of the sample divided by 95% of the ^{14}C /^{12}C ratio of the oxalic acid I (OX-I) standard measured in 1950 (^{14}C /$^{12}C_{OX1}$ = 1.176 ± 0.010 × 10−12) corrected for mass-dependent fractionation; 8267 years is the mean lifetime of ^{14}C; and 1950 is the reference year,

$$\Delta^{14}C = \left(F \times e^{\frac{1950-y}{8267}} - 1\right) \times 1000 \quad (1)$$

The ^{14}C data are normalized to a common $\delta^{13}C$ so that differences in $\Delta^{14}C$ do not reflect isotopic fractionation processes (Stuiver and Polach, 1977).

TC and $\Delta^{14}C$ measurements for our $PM_{2.5}$ samples are reported in table 3.1. Error in TC was computed assuming 3% error in sampler flow rate, 0.5% error in sampling duration, and 6% error in our measurement of the filter area. The measured $\Delta^{14}C$ of each sample ($\Delta^{14}C_{meas}$) was corrected for contamination by extraneous carbon associated with handling the filters during field and laboratory work using blank filters and a simple isotopic mass balance equation (equation (2)):

$$\Delta^{14}C_{sample} = \frac{\Delta^{14}C_{meas} \times TC_{meas} - \Delta^{14}C_{blank} \times TC_{blank}}{TC_{meas} - TC_{blank}} \quad (2)$$

where ‘sample’ refers to the sampled filter and ‘blank’ refers to the blank filter. The mean blank TC concentration was 0.1 μg C cm^{-2}, and the blank mean $\Delta^{14}C$ was −278.6 ± 14.3‰. The error (*err*) in $\Delta^{14}C_{sample}$ was calculated according to equation (3):

$$err\ in\ \Delta^{14}C_{sample} = \sqrt{\left(\frac{TC_{meas}}{TC_{sample}} \times err\ in\ \Delta^{14}C_{meas}\right)^2 - \left(\frac{TC_{blank}}{TC_{sample}} \times err\ in\ \Delta^{14}C_{blank}\right)^2} \quad (3)$$

Table 3.1. Summary of total carbon (TC) concentration and $\Delta^{14}C$ of $PM_{2.5}$ collected within the smoke plume of the KNP Complex Fire in Three Rivers, CA, USA. Error in TC_{sample} and $\Delta^{14}C_{sample}$ represent the propagated uncertainty in the collection of these measurements.

Start (PDT)		**End (PDT)**	**TC_{sample} (µg C cm^{-2})**	**TC_{sample} (µg C m^{-3})**		**$\Delta^{14}C_{sample}$ (‰)**		**UCI AMS #**
Date	Time	Time		Mean	Error	Mean	Error	
2-Oct-2021	15:10	15:40	1.5	130.6	± 8.7	-16.8	± 6.9	253731
2-Oct-2021	16:09	17:39	3.3	97.5	± 6.5	-83.6	± 5.6	253734
2-Oct-2021	17:53	19:23	3.8	111.7	± 7.5	-33.7	± 4.9	253735
2-Oct-2021	19:38	21:38	8.4	185.9	± 12.6	34.5	± 3.0	253736
2-Oct-2021	21:49	23:49	18.7	392.4	± 26.6	68.9	± 1.9	253737
3-Oct-2021	00:12	04:12	40.8	427.3	± 28.7	81.0	± 3.1	253738
3-Oct-2021	04:24	07:24	29.0	405.4	± 27.5	78.2	± 1.9	253739
3-Oct-2021	07:38	09:38	21.0	439.8	± 29.6	76.5	± 1.9	253740
3-Oct-2021	09:46	12:16	28.4	475.7	± 32.1	79.9	± 3.8	253743
3-Oct-2021	12:28	14:28	25.2	556.4	± 37.6	72.8	± 1.9	253744
3-Oct-2021	14:43	16:13	16.9	497.1	± 33.5	66.8	± 2.0	253745
3-Oct-2021	16:18	17:48	18.3	539.8	± 36.7	43.4	± 2.1	253746

3.2.3.2. Keeling plot analysis

A Keeling plot regression analysis (Keeling, 1958; Pataki *et al.,* 2003) allows us to estimate the $\Delta^{14}C$ of the wildfire $PM_{2.5}$ end member, separating it from $PM_{2.5}$ in the background atmosphere (Mouteva *et al.,* 2015; Wiggins *et al.,* 2018). Application of the Keeling plot equation (equation (4)) draws upon the linear relationship between $\Delta^{14}C_{sample}$ and $1/TC_{sample}$ and allows for identification of the wildfire $\Delta^{14}C$ end member from the regression intercept:

$$\Delta^{14}C_{sample} = TC_{background} \times \left(\Delta^{14}C_{background} - \Delta^{14}C_{wildfire}\right) \times \frac{1}{TC_{sample}} + \Delta^{14}C_{wildfire} \qquad (4)$$

The 12 sampled filter measurements of 1/TC and $\Delta^{14}C$ were fit using a geometric mean regression, which accounts for errors in both TC and $\Delta^{14}C$ measurements. The regression was calculated using the 'lsqfitgm' function in Matlab developed by E. T. Peltzer at the Monterey Bay Aquarium Research Institute[1]. The standard deviation (SD) of wildfire $\Delta^{14}C$ is the SD of the y-intercept calculated by the regression function. The Keeling plot approach assumes the composition of the wildfire end member and background atmosphere remain constant over the sampling duration.

3.2.3.3. Estimation of combusted fuel mean age

[1] lsqfitgm function by E. T. Peltzer, Monterey Bay Aquarium Research Institute

The mean age of the combusted fuel was determined using a steady-state, one-box ecosystem model forced with $\Delta^{14}C$ of the historical atmosphere using observations by Hua *et al.* (2022) and X. Xu[2]. Given a user-prescribed mean age of the carbon pool, the model simulates the evolving $\Delta^{14}C$ of the pool from 10,000 years before present to 2021 with inputs from photosynthesis and losses from decomposition and radioactive decay each year. We ran the model for a range of mean ages (between 5 and 75 years) to simulate the $\Delta^{14}C$ of the terrestrial carbon pool in 2021. We then matched the mean $\Delta^{14}C$ of combusted fuel end member from the Keeling plot approach described above (section 3.2.3.2) to the mean age from the model corresponding to the closest matching $\Delta^{14}C$ value. We estimated a 1σ uncertainty range for the fuel mean ages by identifying where the measured wildfire $\Delta^{14}C$ end member value minus 1σ intersected the curve of ecosystem model predictions. This approach generated an asymmetric uncertainty range for the fuel age.

3.2.4. Trace gas measurements

Carbon monoxide (CO) and methane (CH_4) dry air mole fractions were measured using a wavelength- scanned cavity ring-down spectrometer (G2401, Picarro, Santa Clara, CA, USA) at an inlet height of approximately 3 m above ground at approximately 1 s resolution. We calibrated measurements before and after the sampling period using two NOAA-certified air standards in

[2] X. Xu, personal communication 2022

compressed gas cylinders with known mole fractions of CO and CH_4 that spanned the range of observed values. Standards were measured for approximately 5 min during the calibration period. Using the linear relationship between known values and values measured during the calibration period, we applied a two-point correction to the CO and CH_4 data obtained during the sampling period (Hopkins *et al*., 2016; Yañez *et al*., 2022). Outliers in the data (values more than three scaled median absolute deviations from the median) were replaced with linear interpolation of neighboring, non-outlier values using the 'filloutliers' function in Matlab[3]. Measurements collected when cavity pressure or temperature in the instrument was unstable (pressure/temperature change between measurements >0) were removed. Calibrated data with outliers removed were then averaged to a 1 min resolution.

3.3. Results

Throughout the 26 h sampling period, CO, CH_4, and $PM_{2.5}$ measurements varied synchronously and were elevated relative to expected background levels (Fig. 3.2). CO near the beginning of the sampling period at 5:10 pm on 2 October was approximately 1330 ppb. CO increased rapidly at first and then more gradually, reaching a level of 6000 ppb around 4:30 am on 3 October (Fig. 3.2a). CO levels varied between 6000 and 5630 ppb from 4:00 am to 11:00 am on 3 October before

[3] filloutliers function Copyright 2016-2021 The MathWorks, Inc.

increasing again in the early afternoon, reaching a maximum of 7890 ppb by 3:10 pm. CH_4 measurements followed a similar temporal pattern with a minimum initial dry air mole fraction of 2090 ppb at 5:10 pm on 2 October and then increasing to a maximum of 2870 ppb at 3:10 pm on 3 October (Fig. 3.2b). $PM_{2.5}$ concentrations increased during the evening of 2 October with similar timing to CO and CH_4. $PM_{2.5}$ remained relatively constant from midnight to 6:15 am on 3 October (Fig. 3.2c). A minimum in $PM_{2.5}$ concentration of 277 μg m^{-3} was observed at 7:20 pm on 2 October and a maximum of 1330 μg m^{-3} was observed at 12:25 pm on 3 October. Compared to CO and CH_4, $PM_{2.5}$ had a much less pronounced rise in the early afternoon on 3 October. The Pearson correlation coefficients for the different trace gas and $PM_{2.5}$ time series were relatively high: 0.99 for CO and CH_4 , 0.91 for CO and $PM_{2.5}$, and 0.90 for CH_4 and $PM_{2.5}$. The simultaneous buildup of fire-emitted $PM_{2.5}$ and trace gases during the evening and night of 2 October is consistent with a collapsing planetary boundary layer and downslope flow from the fire to our lower elevation sampling location, which is typical of a diurnal circulation pattern in mountain regions (Kuwagata and Kondo, 1989; Geerts *et al.,* 2008).

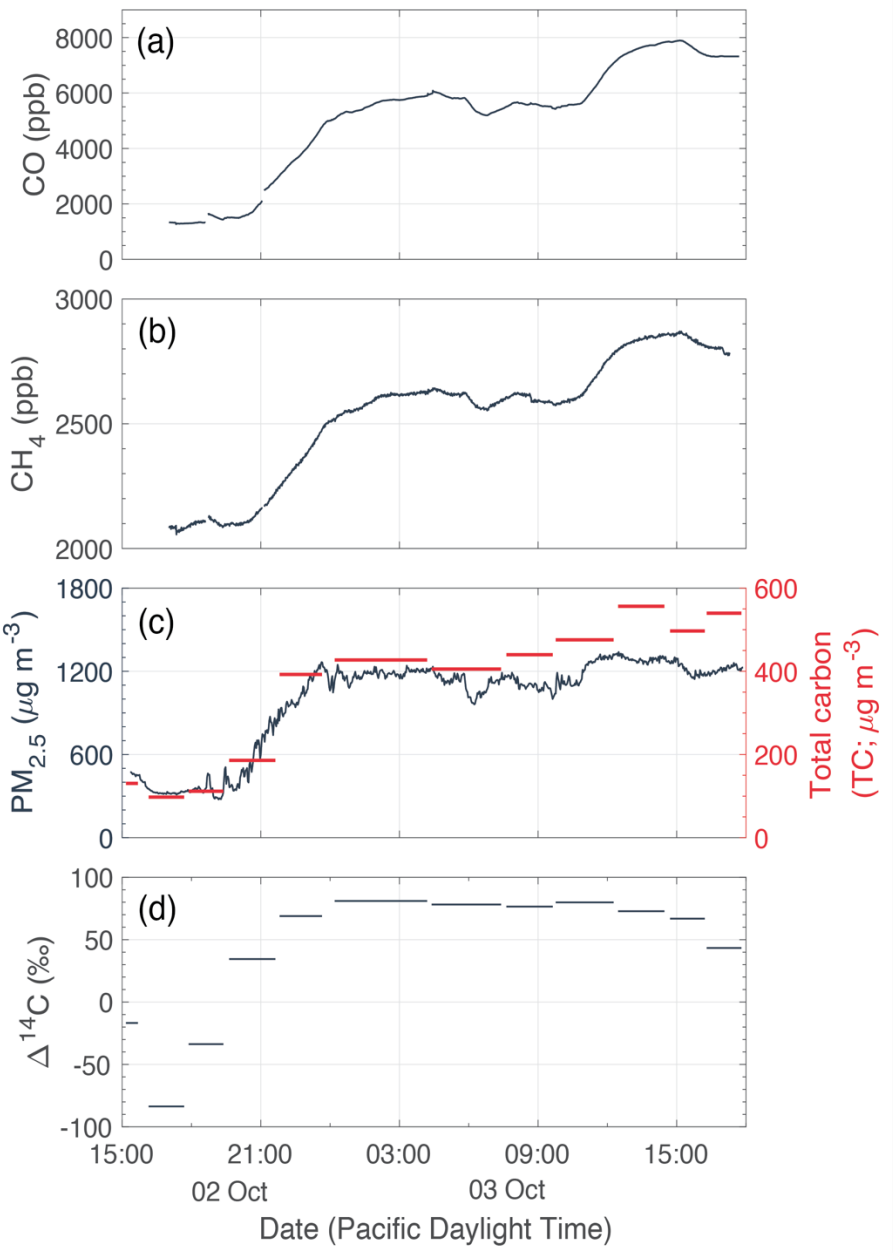

Figure 3.2. Composition of the smoke plume of the KNP Complex Fire on 2–3 October 2021 in Three Rivers, CA, USA. Dry air mole fractions of (a) CO and (b) CH_4 in ppb averaged to one-minute resolution. (c) $PM_{2.5}$ mass concentration (μg m^{-3}) averaged to one-minute resolution on the left axis (blue) and total carbon (TC) mass concentration (μg C m^{-3}) measured for samples on the right axis (red) with sample length represented by the length of each line along the *x*-axis. (d) $\Delta^{14}C$ (‰) of $PM_{2.5}$.

The trace gas and $PM_{2.5}$ time series downwind of the KNP Complex Fire were also considerably elevated relative to expected levels in the background atmosphere. For CO, initial measurements at our sampling site (1330 ppb) were more than 13 times higher than the monthly average 'clean air' level of 98 ppb measured at Cape Kumukahi, HI, USA in October 2021 by the Global Monitoring Laboratory of NOAA's Earth System Research Laboratory (Petron *et al*., 2022). For CH_4, our initial measurement of 2090 ppb was 7% higher than the October 2021 average of 1945 ppb at Cape Kumukahi (Lan *et al*., 2022). Initial $PM_{2.5}$ concentrations of 460 μg m^{-3} far exceeded the limits deemed safe (35 μg m^{-3}) and even hazardous (250 μg m^{-3}) by the U.S. EPA (Aguilera *et al.,* 2021). The high correlation among the different tracers and the elevated atmospheric concentrations relative to expected background levels (Akagi *et al.,* 2011; Andreae, 2019) provided evidence that wildfire emissions were the dominant driver of the variations in atmospheric composition observed during our sampling campaign.

The TC concentration of our filter samples closely tracked the in-situ optical estimates of $PM_{2.5}$ concentration and varied between 97.5 and 556.4 μg C m^{-3} (Fig. 3.2c). The $\Delta^{14}C$ of TC was negative near the beginning of the sampling period (Fig. 3.2d), which is consistent with a substantial contribution from fossil emissions in the background atmosphere (Mouteva *et al.,* 2015, 2017). During the evening on 2 October, $\Delta^{14}C$ increased concurrently with the rise in trace gas mole fractions and $PM_{2.5}$ concentrations, reaching a maximum of 81.0 ± 3.1‰ for the sample collected between midnight and 4:00 am on 3 October. From 4:00 am to mid-afternoon on 3 October, $\Delta^{14}C$ values were relatively constant, varying between 66.8 ± 2.0‰ and 83.6 ± 5.6‰

before declining to 43.4 ± 2.1‰ during the last sampling interval. The $\Delta^{14}C$ of TC increased at higher $PM_{2.5}$ concentrations, suggesting that fire-emitted $PM_{2.5}$, which we expect to be enriched in ^{14}C, drove variability in emissions.

Using the Keeling plot approach described in section 3.2.3.2, we estimated that the mean $\Delta^{14}C$ of the wildfire end member was 111.6 ± 7.7‰ (Fig. 3.3). The $\Delta^{14}C$ of emissions was enriched relative to the northern hemisphere atmospheric CO_2 background in 2021 of −3.2 ± 1.4‰, indicating the combusted fuels likely accumulated over a period of many decades, during a time when the atmosphere was more enriched in bomb ^{14}C (Fig. 3.4a).

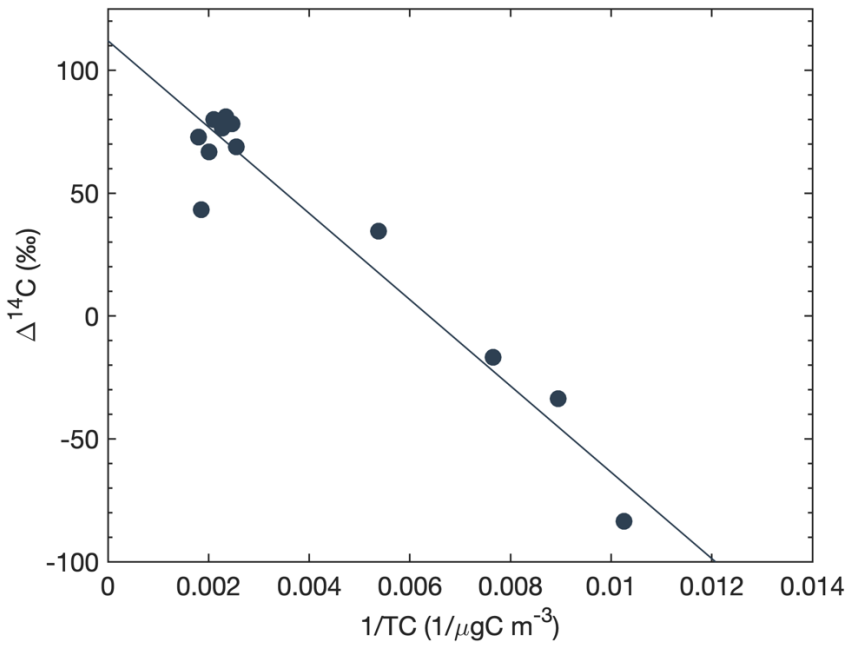

Figure 3.3. Keeling plot showing the $\Delta^{14}C$ of $PM_{2.5}$ as a function of its inverse total carbon (TC) concentration. The *y*-intercept of the regression represents the mean observed $\Delta^{14}C$ of the combusted fuel in the KNP Complex Fire (111.6‰). The standard deviation of the *y*-axis is 7.7‰. The regression coefficient for the linear fit was 0.96.

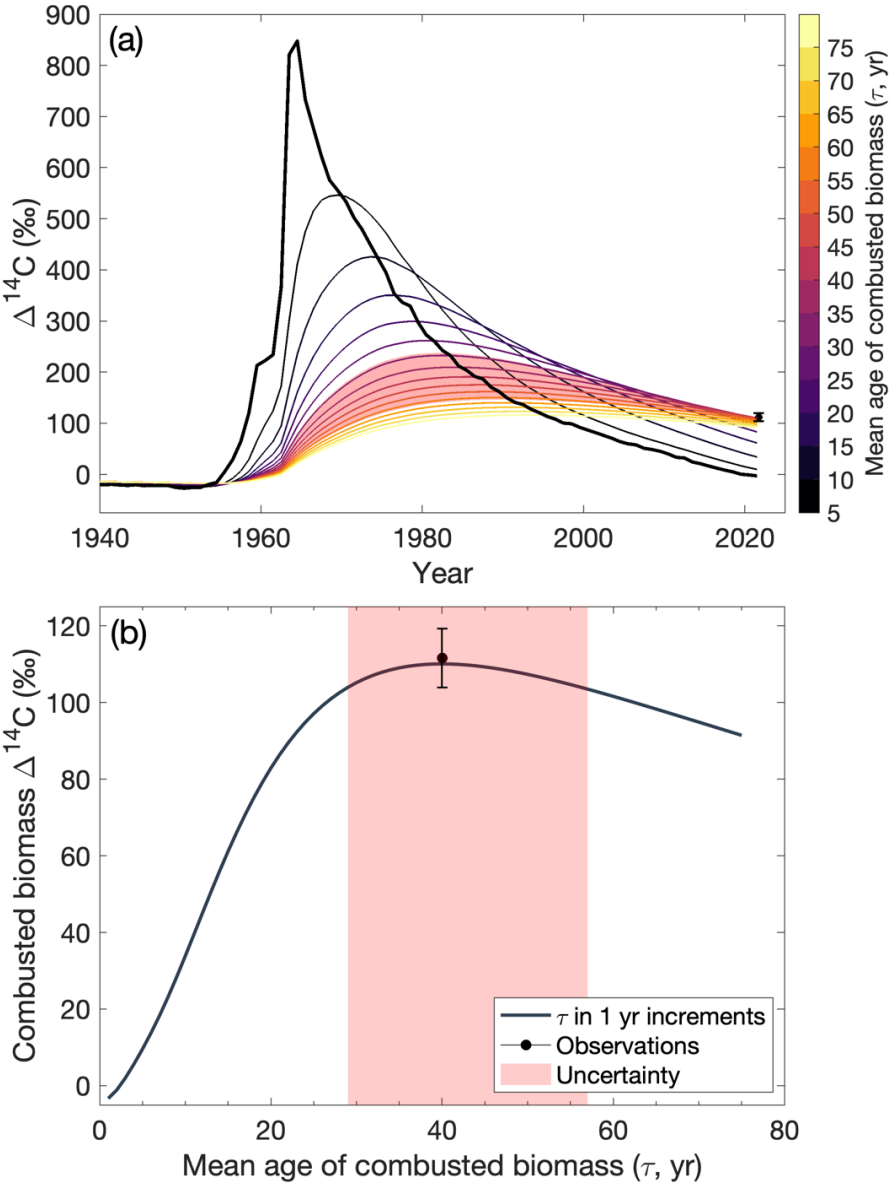

Figure 3.4. Analysis of fuel age using a steady-state one-box ecosystem model. (a) Atmospheric $\Delta^{14}C$ (black line) and modeled $\Delta^{14}C$ of combusted fuel (colored lines) over time from 1940 to 2021. Combusted fuel $\Delta^{14}C$ is modeled here given mean ages ranging from 5 to 75 years, visualized every 1 year. The black filled circle represents the modeled combusted fuel $\Delta^{14}C$ for a mean age of 40 years, estimated by the model to correspond to the mean observed $\Delta^{14}C$ of 111.6 ± 7.7‰. (b) Expected $\Delta^{14}C$ of combusted fuel given mean ages ranging from 5 to 75 years. The red shading corresponds to potential mean ages that are consistent with a 1σ uncertainty on the $\Delta^{14}C$ of fire-emitted $PM_{2.5}$.

To further constrain the age range of the wildfire $PM_{2.5}$ emissions, we used the steady-state one-box ecosystem model described in section 3.2.3.3, in which the mean transit time of the carbon is equal to its mean age. With the uncertainty range of our observed combusted fuel $\Delta^{14}C$ (111.6 ± 7.7‰), we attained a best-fit for fuel age of 40 years, with an asymmetrical uncertainty range of 29–57 years, corresponding to 1σ uncertainty of the mean $\Delta^{14}C$ (Fig. 3.4b). In 2021, a fuel class with a relatively young mean age (5 years) would have a $\Delta^{14}C$ of 9.5‰, which is only slightly enriched relative to the contemporary atmosphere in 2021 (Fig. 3.4a). Needles and leaf litter may be examples of materials in this fuel class. Since these materials decompose relatively quickly, very little retain the high degree of bomb labeling from the 1950s and 1960s. As the age of fuels increases from 5 to 40 years, the predicted $\Delta^{14}C$ of combusted fuel from the model rises to approximately 110.0‰. Fuels with a 40 year mean age may encompass larger- diameter woody detritus and other woody biomass like live shrubs and small trees.

3.4. Discussion

The diameter of woody fuels influences the length of time required for decomposition in forest ecosystems. Fine fuels (i.e., needles, leaf litter, and small- diameter woody detritus) decompose relatively rapidly over several years. In contrast, fuels with a larger diameter decompose relatively slowly and can remain in the understory and on the forest floor for decades (Harmon 2021). Lower-intensity fires, including prescribed fires, typically consume only fine fuel classes because larger-diameter fuels generally have a higher moisture content and require more energy to ignite and support high-intensity fires (Chuvieco *et al.,* 2002; Gorte, 2009). High rates of energy release from

the consumption of large-diameter fuels, in turn, can contribute to longer flame lengths and increase probability that ground fires will jump into the over- story and develop into crown fires (Stephens *et al.,* 2022). High-intensity crown fires are a major concern with respect to preservation of giant sequoias because thick bark near the base of tree makes sequoias nearly impervious to ground fires, yet scorch in the upper canopy can damage foliage and more vulnerable vascular tissues (Shive *et al.,* 2022).

Our $\Delta^{14}C$ measurements provide evidence that the KNP Complex Fire burned through larger-diameter fuels, likely with a considerably higher intensity than what would be expected for surface fires. It is also possible that the combustion of deeper organic soil (Pellegrini *et al.,* 2021) that has a similar mean age to the woody detritus in some forests (Mouteva *et al.,* 2015), also contributed to emissions. However, our study does not include depth of burn measurements, which would allow us to apportion the relative contributions from woody detritus and soil. Still, our measurements are broadly consistent with previous studies documenting how the accumulation of fuel in California's coniferous forests (including the buildup of shrubs, small trees, and woody detritus on multi-decadal timescales) con- tributes to high fire intensity (Miller *et al.,* 2009b; Safford and Stevens 2017; Stevens *et al.,* 2017b). Notably, the KNP Complex Fire led to the mortality of about 5900 giant sequoias, meaning that 3-5% of all giant sequoias in the Sierra Nevada mountains were killed or are expected to die within 5 years (Stephenson and Brigham, 2021). This compounds giant sequoia mortality from the 2020 Castle Fire, which killed an estimated 10-14% of large giant sequoias (Stephenson and Brigham, 2021). The native range of

giant sequoias does not extend beyond the western slope of the Sierra Nevada, therefore a loss of approximately 15% in such a short period is a major threat to this endangered species.

Fuel treatments, including mechanical thinning and prescribed fire, have historically been used to decrease fuel loads in forests. Legislation was recently passed in California that will expand the use of prescribed fire across the state with a goal of one million acres treated per year by 2025 (California Wildfire and Forest Resilience Task Force, 2022). If they are successful, we expect fuel treatments to gradually reduce the mean age of combusted fuels because under- story vegetation and larger-diameter woody detritus should be removed (Harmon, 2021). Regional PM sampling during periods with prescribed fire might be an effective way to monitor the success of this pro- gram. Specifically, after a sustained effort, the $\Delta^{14}C$ of combusted fuel should more closely match the contemporary atmosphere because finer fuel classes have younger mean ages. Eventually, wildfires would also be expected to have lower intensities and more closely track the $\Delta^{14}C$ of atmospheric CO_2.

Apart from evaluating the effectiveness of prescribed burning, PM $\Delta^{14}C$ monitoring in California may be helpful for understanding the role of wildfire in influencing air quality across the state. For instance, the San Joaquin Valley of California is a serious non-attainment area for $PM_{2.5}$ and other pollutants with adverse health effects. It often exceeds both state and national air quality standards for harmful pollutants (Huang *et al.,* 2021). Pollution in the San Joaquin Valley is primarily anthropogenic due to both local emissions and those transported from surrounding urban areas,

but wildfires play a variable and often significant role in elevated pollutant levels (Schweizer and Cisneros, 2017; Burke *et al.,* 2021; Frausto-Vicencio *et al.,* 2023). Disentangling contributions to observed $PM_{2.5}$ levels from prescribed fire, wildfire, and urban sources will be critical for creating effective policy to improve air quality in the San Joaquin Valley and simultaneously meet the State's forest management goals.

Future directions for this work include building a longer time series of observations from multiple fires, which will provide information about a broader range of burning conditions. The length of our time series was constrained by rapidly changing conditions and challenges securing a safe sampling location that was both near the smoke and outside of the mandatory evacuation zone. Future analyses should be conducted over longer sampling intervals on a variety of wildland fire types, including grass and shrub fires and prescribed fire, to more broadly understand the effects of climate, fuel, and fuel treatments on the composition of PM emissions across California and other fire-prone forests. Fire emissions contain many carbonaceous components (Olsen *et al.,* 2020), so another important research direction is to simultaneously measure the $\Delta^{14}C$ of black and organic carbon (BC and OC) $PM_{2.5}$ fractions and carbon-containing trace gases (CO and CO_2) to understand better the linkages between fuel age (and type), flaming and smoldering combustion, and the composition of fire emissions. In past work, for example, fire-emitted EC has been shown to have higher levels of $\Delta^{14}C$ than OC, likely due to a different mixture of fuels (Mouteva *et al.,* 2015).

3.5. Conclusions

In this study, we measured the $\Delta^{14}C$ of $PM_{2.5}$ from the KNP Complex Fire and used these observations to infer that fuel buildup over multiple decades was a dominant contributor to $PM_{2.5}$ emissions in smoke. Our analysis is consistent with past work showing that cessation of Indigenous burning practices and implementation of fire suppression in the Sierra Nevada mountains are important contributors to recent increases in fire intensity. We also propose that our measurement techniques can be used to assess the efficacy of prescribed fire and other fuel treatments planned for California in the near future and to identify fire impacts on air quality in remote urban areas. Altogether, fuel management and an enhanced understanding of emissions associated with California's wildfires can help mitigate their social, economic, and ecosystem impacts.

3.6. Data availability statement

The data that support the findings of this study are openly available at the following URL/DOI: https:// doi.org/10.7280/D1498P (Odwuor 2023).

3.7. Acknowledgments

This work was conducted on the unceded lands of the Mono (Monache), Yokut, Tübatulabal, Paiute, and Western Shoshone people (National Park Service 2021). This material is based upon work supported by the National Science Foundation Graduate Research Fellowship under Grant No. DGE-2039655 to AO. J T R received funding support from the NASA's Modeling, Analysis, and Prediction (MAP) and Earth Information System—Fire research pro- grams and the U.S.

Department of Energy Office of Science's RUBISCO Science Focus Area. Funding from the Ralph J and Carol. M Cicerone Chair in the Department of Earth System Science supported the field campaign and laboratory measurements.

We thank the KCCAMS staff for supporting the elemental and isotopic analyses and A Ocampo and C McCormick for assisting with data collection.

3.8. References

Abatzoglou, J.T., Battisti, D.S., Williams, A.P. *et al.* (2021) 'Projected increases in western US forest fire despite growing fuel constraints', *Commun. Earth Environ.,* **2** *227* 10.1038/s43247-021-00299-0

Aguilera, R., Corringham, T., Gershunov, A., & Benmarhnia, T. (2021). 'Wildfire smoke impacts respiratory health more than fine particles from other sources: observational evidence from Southern California', *Nature communications*, *12*(1), 1493. doi: 10.1038/s41467-021-21708-0

Akagi, S. K. *et al.* (2011) 'Emission factors for open and domestic biomass burning for use in atmospheric models', *Atmospheric Chemistry and Physics*, 11(9), pp. 4039–4072. doi: 10.5194/acp-11-4039-2011

Andreae, M. (2019) 'Emission of trace gases and aerosols from biomass burning. Global Biogeochemical', *Atomospheric Chemistry and Physics*, 15(4)(April), pp. 955–966. 10.5194/acp-2019-303

Burke, M. *et al.* (2021) 'The changing risk and burden of wildfire in the United States', *Proceedings of the National Academy of Sciences of the United States of America*, 118(2), e2011048118. doi: 10.1073/PNAS.2011048118

California Department of Forestry and Fire Protection 2022a *Emergency Fund Fire Suppression Expenditures* (available at: www.fire.ca.gov/media/px5lnaaw/suppressioncostsonepage1.pdf) (Accessed 20 February 2023)

California Department of Forestry and Fire Protection 2022b *Fire and Resource Assessment Program Fire Perimeters* (available at: https://frap.fire.ca.gov/mapping/gis-data/on) (Accessed 20 February 2023)

California Wildfire and Forest Resilience Task Force 2022 *California's Strategic Plan for Expanding the Use of Beneficial Fire* (available at: www.fire.ca.gov/media/xcqjpjmc/californias-strategic-plan-for-expanding-the-use-of-beneficial-fire-march-16_2022.pdf) (Accessed 20 February 2023)

Chen, Y. *et al.* (2022) 'California wildfire spread derived using VIIRS satellite observations and an object-based tracking system', *Scientific Data*. Springer US, 9(1), 249. doi: 10.1038/s41597-022-01343-0

Chuvieco, E. *et al.* (2002) 'Estimation of fuel moisture content from multitemporal analysis of Landsat Thematic Mapper reflectance data: Applications in fire danger assessment', *International Journal of Remote Sensing*, 23(11), pp. 2145–2162. doi: 10.1080/01431160110069818

Dennison, P. E. *et al.* (2014) 'Large wildfire trends in the western United States, 1984–2011', *Geophysical Research Letters*, 41(8), pp. 6413–6419. doi: 10.1002/ecs2.3198

Frausto-Vicencio, I., Heerah, S., Meyer, A. G., Parker, H. A., Dubey, M., & Hopkins, F. M. (2023). Ground solar absorption observations of total column CO, CO 2, CH 4, and aerosol optical depth from California's Sequoia Lightning Complex Fire: Emission factors and modified combustion efficiency at large scales. *Atmospheric Chemistry and Physics Discussions*, 1-35. doi: 10.5194/acp-23-4521-2023

Geerts, B., Miao, Q., & Demko, J. C. (2008). Pressure perturbations and upslope flow over a heated, isolated mountain. *Monthly weather review*, 136(11), 4272-4288. doi: 10.1175/2008MWR2546.1

Gorte R W 2009 Wildfire fuels and fuel reduction (Report no. R40811) *Congressional Research Service, Library of Congress* pp 1–16 (available at: https://crsreports.congress.gov/product/pdf/R/R40811/12on) (Accessed 20 February 2023)

Gutierrez, A. A. *et al.* (2021) 'Wildfire response to changing daily temperature extremes in California's Sierra Nevada', *Science Advances*, 7(47), e2905-E2911. doi: 10.1126/sciadv.abe6417

Hagmann, R. K. *et al.* (2021) 'Evidence for widespread changes in the structure, composition, and fire regimes of western North American forests', *Ecological Applications*, 31(8), e0243. doi: 10.1002/eap.2431

Harmon, M. E. (2021) 'The role of woody detritus in biogeochemical cycles: past, present, and future', *Biogeochemistry*. Springer International Publishing, 154(2), pp. 349–369. doi: 10.1007/s10533-020-00751-x

Higuera, P. E. and Abatzoglou, J. T. (2021) 'Record-setting climate enabled the extraordinary 2020 fire season in the western United States', *Global Change Biology*, 27(1), pp. 1–2. doi: 10.1111/gcb.15388

Hopkins, F. M. *et al.* (2016) 'Mitigation of methane emissions in cities: How new measurements and partnerships can contribute to emissions reduction strategies', *Earth's Future*, 4(9), pp. 408–425. doi: 10.1002/2016EF000381

Huang, L. *et al.* (2021) 'Strategies to reduce PM2.5 and O3 together during late summer and early fall in San Joaquin Valley, California', *Atmospheric Research*, 258(3), p. 105633. doi: 10.1016/j.atmosres.2021.105633

Keeling, C. D. (1958) 'The concentration and isotopic abundances of atmospheric carbon dioxide in rural areas', *Geochimica et Cosmochimica Acta*, 13, pp. 322–334. doi: 10.1016/0016-7037(58)90033-4.

Key, C.H. and Benson, N.C. (2006) 'Landscape Assessment (LA) Sampling and Analysis Methods' *FIREMON: Fire effects monitoring and inventory system* (RMRS-GTR-164). Eds D.C. Lutes, R.E. Keane, J.F. Caratti, C.H. Key, N.C. Benson, S. Sutherland, L.J. Gangi. (Ogden, UT: U.S. Department of Agriculture Forest Service, Rocky Mountain Research Station)

Kochi, I. *et al.* (2010) 'The economic cost of adverse health effectsfrom wildfire-smoke exposure: A review', *International Journal of Wildland Fire*, 19(7), pp. 803–817. doi: 10.1071/WF09077.

Kuwagata, T., & Kondo, J. (1989). Observation and modeling of thermally induced upslope flow. *Boundary-layer meteorology*, 49, 265-293. doi: 10.1007/BF00120973

Lan, X., Dlugokencky, E.J., Mund, J.W., Crotwell, A.M., Crotwell, M.J., Moglia, E., Madronich, M., Neff, D., Thoning, K.W. (2022). Atmospheric Methane Dry Air Mole Fractions from the NOAA GML Carbon Cycle Cooperative Global Air Sampling Network, 1983-2021, Version: 2022-11-21, doi: 10.15138/VNCZ-M766

Levin, I. *et al.* (2010) 'Observations and modelling of the global distribution and long-term trend of atmospheric 14CO2', *Tellus, Series B: Chemical and Physical Meteorology*, 62(1), pp. 26–46. doi: 10.1111/j.1600-0889.2009.00446.x.

McKelvey, K. S. and Busse, K. K. (1996) 'Twentieth-century fire patterns on Forest Service lands', *Sierra Nevada Ecosystem Project: Final report to Congress*, II, pp. 1119–1138.

Miller, J. D., Knapp, E. E., Key, C. H., Skinner, C. N., Isbell, C. J., Creasy, R. M., & Sherlock, J. W. (2009a) 'Calibration and validation of the relative differenced Normalized Burn Ratio (RdNBR) to three measures of fire severity in the Sierra Nevada and Klamath Mountains, California, USA', *Remote Sensing of Environment*. Elsevier B.V., 113(3), pp. 645–656. doi: 10.1016/j.rse.2008.11.009

Miller, J. D., Safford, H. D., Crimmins, M., & Thode, A. E. (2009b) 'Quantitative evidence for increasing forest fire severity in the Sierra Nevada and southern Cascade Mountains, California and Nevada, USA', *Ecosystems*, 12(1), pp. 16–32. doi: 10.1007/s10021-008-9201-9.

Mouteva, G. O., Czimczik, C. I., Fahrni, S. M., Wiggins, E. B., Rogers, B. M., Veraverbeke, S., ... & Randerson, J. T. 'Black carbon aerosol dynamics and isotopic composition in Alaska linked with boreal fire emissions and depth of burn in organic soils', *Global biogeochemical cycles*, pp. 1977–2000. doi: 10.1002/2015GB005247

Mouteva, G. O. *et al.* (2017) 'Using radiocarbon to constrain black and organic carbon aerosol sources in Salt Lake City', *Journal of Geophysical Research: Atmospheres*, 122(18), pp. 9843–9857. doi: 10.1002/2017JD026519

National Park Service and Sequoia and Kings Canyon National Parks 2017 *Sequoia Groves of the Sierra Nevada California* (available at: https://irma.nps.gov/DataStore/Reference/Profile/2259632on) (Accessed 20 February 2023)

National Park Service 2021 *Native Americans of the Southern Sierra* (available at: www.nps.gov/seki/learn/historyculture/native-americans.htmon) (Accessed 21 February 2023)

Nydal, R. (1963) 'Increase in radiocarbon from the most recent series of thermonuclear tests', *Nature*, 200, pp. 212–214. doi:10.1038/200212a0

Olsen, Y., Nøjgaard, J. K., Olesen, H. R., Brandt, J., Sigsgaard, T., Pryor, S. C., ... & Hertel, O. (2020). Emissions and source allocation of carbonaceous air pollutants from wood stoves in developed countries: A review. *Atmospheric Pollution Research*, *11*(2), 234-251. doi: 10.1016/j.apr.2019.10.007

Pataki, D. E. *et al.* (2003) 'The application and interpretation of Keeling plots in terrestrial carbon cycle research', *Global Biogeochemical Cycles*, 17(1). doi: 10.1029/2001GB001850

Pausas, J. G. and Keeley, J. E. (2019) 'Wildfires as an ecosystem service', *Frontiers in Ecology and the Environment*, 17(5), pp. 289–295. doi: 10.1002/fee.2044

Pellegrini, A. F., Caprio, A. C., Georgiou, K., Finnegan, C., Hobbie, S. E., Hatten, J. A., & Jackson, R. B. (2021). Low-intensity frequent fires in coniferous forests transform soil organic matter in ways that may offset ecosystem carbon losses. *Global change biology*, *27*(16), 3810-3823. doi: 10.1111/gcb.15648

Petron, G., Crotwell, A.M., Crotwell M.J., Dlugokencky, E., Madronich M., Moglia, E., Neff D., Thoning, K., Wolter, S., Mund, J.W. (2022). Atmospheric Carbon Monoxide Dry Air Mole Fractions from the NOAA GML Carbon Cycle Cooperative Global Air Sampling Network, 1988-2021, Version: 2022-07-28, doi: 10.15138/33bv-s284

Reid, C. E. *et al.* (2016) 'Critical review of health impacts of wildfire smoke exposure', *Environmental Health Perspectives*, 124(9), pp. 1334–1343. doi: 10.1289/ehp.1409277

Safford, H. D., Paulson, A. K., Steel, Z. L., Young, D. J., & Wayman, R. B. (2022) 'The 2020 California fire season: A year like no other, a return to the past or a harbinger of the future?', *Global Ecology and Biogeography*, 31(10), pp. 2005–2025. doi: 10.1111/geb.13498

Safford, H. D. and Stevens, J. T. (2017) 'Natural range of variation for yellow pine and mixed-conifer forests in the Sierra Nevada, southern Cascades, and Modoc and Inyo National Forests, California, USA.', *General Technical Report - Pacific Southwest Research Station, USDA Forest Service. PSW-GTR-256*, (PSW-GTR-256), p. 229.

Schweizer, D. W. and Cisneros, R. (2017) 'Forest fire policy: change conventional thinking of smoke management to prioritize long-term air quality and public health', *Air Quality, Atmosphere and Health*. Air Quality, Atmosphere & Health, 10(1), pp. 33–36. doi: 10.1007/s11869-016-0405-4

Shive, K. L. *et al.* (2022) 'Ancient trees and modern wildfires: Declining resilience to wildfire in the highly fire-adapted giant sequoia', *Forest Ecology and Management*, 511, p. 120110. doi: 10.1016/j.foreco.2022.120110

Stephens, S. L., Moghaddas, J. J., Edminster, C., Fiedler, C. E., Haase, S., Harrington, M., ... & Youngblood, A. (2009) 'Fire treatment effects on vegetation structure, fuels, and potential fire severity in western U.S. forests', *Ecological Applications*, 19(2), pp. 305–320. doi: 10.1890/07-1755.1

Stephens, S. L., Bernal, A. A., Collins, B. M., Finney, M. A., Lautenberger, C., & Saah, D. (2022) 'Mass fire behavior created by extensive tree mortality and high tree density not predicted by operational fire behavior models in the southern Sierra Nevada', *Forest Ecology and Management*, 518(April), p. 120258. doi: 10.1016/j.foreco.2022.120258

Stephenson, N. and Brigham, C. (2021) 'Preliminary Estimates of Sequoia Mortality in the 2020 Castle Fire', *National Park Service*, pp. 1–32.

Stevens, J. T. (2017a) 'Scale-dependent effects of post-fire canopy cover on snowpack depth in montane coniferous forests', *Ecological Applications*, 27(6), pp. 1888–1900. doi: 10.1002/eap.1575

Stevens, J. T. *et al.* (2021) 'Tamm Review: Postfire landscape management in frequent-fire conifer forests of the southwestern United States', *Forest Ecology and Management*, 502(September), p. 119678. doi: 10.1016/j.foreco.2021.119678

Stevens, J. T. *et al.* (2017b) 'Changing spatial patterns of stand-replacing fire in California conifer forests', *Forest Ecology and Management*. Elsevier, 406(August), pp. 28–36. doi: 10.1016/j.foreco.2017.08.051

Stuiver, M. and Polach, H. A. (1977) 'Discussion: Reporting of 14C Data', *Radiocarbon*, 19(3), pp. 355–363. doi: 10.1017/S0033822200003672

Swetnam, T. W. *et al.* (2009) 'Multi-millennial fire history of the giant forest, Sequoia National Park, California, USA', *Fire Ecology*, 5(3), pp. 120–150. doi: 10.4996/fireecology.0503120

Swetnam, W. (1993) 'Fire History and Climate Change in Giant Sequoia Groves' *Science*, *262*(5135), pp. 885-889. doi: 10.1126/science.262.5135.885

Taylor, A. H. *et al.* (2016) 'Socioecological transitions trigger fire regime shifts and modulate fire-climate interactions in the Sierra Nevada, USA, 1600-2015 CE', *Proceedings of the National Academy of Sciences of the United States of America*, 113(48), pp. 13684–13689. doi: 10.1073/pnas.1609775113

Tubbesing, C. L., Martinez, D. J. and Smith, J. (2021) 'Prioritizing Forest Health Investments: Recommendations from the Science Advisory Panel to the Forest Management Task Force'

Walker, B. D. and Xu, X. (2019) 'An improved method for the sealed-tube zinc graphitization of microgram carbon samples and 14C AMS measurement', *Nuclear Instruments and Methods in Physics Research, Section B: Beam Interactions with Materials and Atoms*, 438, pp. 58–65. doi: 10.1016/j.nimb.2018.08.004

Wang, D. *et al.* (2021) 'Economic footprint of California wildfires in 2018', *Nature Sustainability*. 4(3), pp. 252–260. doi:10.1038/s41893-020-00646-7

Wiggins, E. B. *et al.* (2018) 'Smoke radiocarbon measurements from Indonesian fires provide evidence for burning of millennia-aged peat', *Proceedings of the National Academy of Sciences of the United States of America*, 115(49), pp. 12419–12424. doi: 10.1073/pnas.1806003115

Williams, A. P. *et al.* (2019) 'Observed Impacts of Anthropogenic Climate Change on Wildfire in California', *Earth's Future*, 7(8), pp. 892–910. doi 10.1029/2019EF001210

Wu, T., Kim, Y. S. and Hurteau, M. D. (2011) 'Investing in Natural Capital: Using Economic Incentives to Overcome Barriers to Forest Restoration', *Restoration Ecology*, 19(4), pp. 441–445. doi: 10.1111/j.1526-100X.2011.00788.x

Yañez, C. C. *et al.* (2022) 'Reductions in California's Urban Fossil Fuel CO2 Emissions During the COVID-19 Pandemic', *AGU Advances*, 3(6), e2022AV000732. doi: 10.1029/2022AV000732

Chapter 4

Large-diameter dead fuel classes as drivers of $PM_{2.5}$ emissions from prescribed fire in California

Odwuor, A., Welch, A. M., Czimczik, C. I., Randerson, J.T., Xu, X., York, R., and Banerjee, T.

4.1. Introduction

Over the last several decades, large wildfires in western North America have increased in frequency and become more destructive, threatening public health and safety, the economy, and ecosystems (Abatzoglou and Williams, 2016; Brookes *et al*., 2021; Safford *et al.*, 2022). Increasing fire activity in western forests is often attributed to the cumulative effects of climate warming (Williams *et al.*, 2019; Gutierrez *et al.*, 2021; Hagmann *et al.*, 2021) and management practices during the 20th century that emphasized fire suppression (Kalies and Kent, 2016; Keeley and Syphard, 2019; Foster *et al.*, 2020; Prichard *et al*., 2021). Together, a suite of climate and land use changes have contributed to a change in forest structure, including a higher tree density and drier fuels, which promote more severe wildfires (Pausas and Keeley, 2019; Prichard *et al*., 2021).

In California, much of the increase in forest fire severity and burned area has been observed in the Sierra Nevada mountains. Once characterized by frequent, low-intensity surface fires, many forests in the Sierra Nevada now experience unprecedented high-severity, stand-replacing crown fires (Steel, Koontz and Safford, 2018; Levine *et al.*, 2020; Odwuor *et al.*, 2023). Shrubs and shade-tolerant species in the understory not removed mechanically or burned can outcompete larger, fire-tolerant species (Pollet and Omi, 2002). Increases in understory vegetation combined

with the accumulation of coarse woody debris and other dead fuels on the forest floor provide for greater horizontal and vertical fuel continuity and longer flame lengths that, in turn, allow fires to burn into the crown (Pollet and Omi, 2002; Graham et al., 2004). Higher levels of tree mortality associated with crown fires (Hantson *et al.*, 2022) threaten regional carbon stocks (Wang *et al.*, 2022), and endemic species, such as the endangered giant sequoia (*Sequoiadendron giganteum* (LINDL.) J. BUCHHOLZ), which are adapted to a regime of frequent, low-intensity surface fires (Swetnam *et al.*, 2009; Shive *et al.*, 2022). Crown fires also spread faster (Levine *et al.*, 2020), making them more difficult to contain, and increasing damages in nearby communities (Brown *et al.*, 2023).

Recent extremes in fire behavior observed in western North America provide strong motivation for ramping up management efforts to reduce fuel build up and limit fire intensity. Key strategies in this context include expanded use of mechanical fuel treatments and prescribed fire (Prichard *et al*., 2021). Mechanical fuel treatments include crown thinning, thinning from below, and mastication (Stephens and Moghaddas, 2005) while prescribed burning involves intentionally applying fire to a landscape under specific conditions to achieve specific goals (Kalies and Kent, 2016). Prescribed burning is commonly used in conjunction with (after) mechanical treatments (e.g., burning of logging slash). When used on its own, prescribed burning can be similar to cultural burning, commonly practiced by Indigenous people during the pre-settlement era in California (Gorte, 2009; Taylor *et al.*, 2016; Marks-Block and Tripp, 2021) to mitigate wildfire hazard, enhance habitats and natural resources, and meet cultural needs (Anderson and Moratto, 1996;

Marks-Block and Tripp, 2021). After Native American depopulation in the Sierra Nevada in the late 18th century and the subsequent colonization by Euro-American settlers (Taylor *et al.*, 2016), prescribed burning became essentially banned and aggressive fire suppression policy was applied to all forests (Agee and Skinner, 2005; Stephens and Moghaddas, 2005). In more recent decades, prescribed fire policy was reintroduced to western U.S. forests (Stephens *et al.*, 2012) and there is strong evidence that, especially when combined with mechanical treatments, it can effectively reduce fuel loads and, thereby, fire intensity and severity (Kalies and Kent, 2016; Prichard *et al*., 2021). In California, a key management goal is to expand use of prescribed fire each year by a factor or ten or more (California Wildfire and Forest Resilience Task Force, 2021). However, prescribed burning is not appropriate for all forests, including moist mixed-conifer stands with thin-barked species, and is less feasible in remote areas (Pritchard *et al*., 2021). Further, prescribed fires require adequate personnel (Quinn-Davidson and Varner, 2012) and they produce smoke that can negatively impact visibility and endanger both local and remote ecosystems and communities (May *et al.*, 2015), creating barriers to its widespread implementation.

The impact of prescribed fire smoke on human health depends on a variety of factors, including fire intensity and smoke transport, which is strongly influenced by meteorological conditions (Williamson *et al.*, 2016; Huang *et al.*, 2023). Smaller, lower-intensity surface fires, like prescribed fires, are typically associated with cooler temperatures and more stable atmospheric conditions that reduce the ability for smoke to disperse, thereby increasing the risk of smoke exposure for local communities (Williamson *et al.*, 2016; Reisen *et al.*, 2018). However, prescribed fires in the U.S. are sometimes conducted during periods of low- to moderate steady winds to encourage

smoke dispersal (Reisen *et al.*, 2018), but these conditions also promote larger, more intense fires, a greater risk of escape, a longer burn, and more emissions that can be transported farther and impact larger populations (Williamson *et al.*, 2016). When planning a prescribed fire, land managers must consider both the ecological and social objectives of the treatment, which often require tradeoffs for smoke exposure (Schweizer *et al.*, 2019).

The potential for smoke to affect communities is further influenced by the composition and concentration of pollutants, which are determined in part by fire processes that regulate fuel consumption (May *et al.*, 2015; Williamson *et al.*, 2016). Prescribed fires, like wildfires, are often characterized by incomplete combustion which results in the production of gaseous pollutants like nitrous oxides, ozone, methane, etc. and particulate matter (PM) and its precursors (Akagi *et al.*, 2011). Previous work has found that prescribed fires during the wildfire season are less efficient than wildfires (i.e., are characterized by a higher proportion of smoldering combustion) and produce more emissions (Urbanski, 2013). Of special concern is fine airborne PM ($PM_{2.5}$), which is a major component of wildfire smoke and especially impactful for climate, air quality and visibility, and public health (Reisen *et al.*, 2018; Burke *et al.*, 2021). A significant component (20-50%) of $PM_{2.5}$ is carbonaceous aerosol (Hand *et al*., 2012; Ahangar *et al*., 2021), which is commonly differentiated according to thermo-optical properties into light-scattering organic carbon (OC) and light-absorbing black carbon (BC) (Andreae and Gelencsér, 2006). BC can reduce atmospheric visibility and negatively impact air quality (Bond *et al.*, 2013). High-temperature flaming combustion, commonly seen in uncontrolled wildfires, is linked to the more

complete consumption of fuels and rapid production of gaseous pollutants, but also more BC (Andreae and Gelencsér, 2006; Williamson *et al.*, 2016). Lower-temperature smoldering typical of prescribed fires and associated with the combustion of larger fuel classes tends to result in less complete fuel consumption, longer burn duration, and more particulate pollution with lower BC/OC ratios (Bond *et al.*, 2013; Williamson *et al.*, 2016).

In this study, we characterized the composition of fuels and emissions for a prescribed fire in the Sierra Nevada mountains of California. Specifically, we focused on a prescribed fire at the Blodgett Forest that was conducted as part of a Smart Practices and Architectures for Rx Fire in California (SPARx) field campaign. We measured the amounts of different fuel classes before and after the prescribed fire to calculate fuel consumption. We also measured the radiocarbon content (mean age, reported in $\Delta^{14}C$) of different fuel classes and $PM_{2.5}$ to understand how different fuels contributed to observed emissions. We hypothesized that the organic soil horizons (needle litter and duff) and small-diameter surface fuels would dominate the fuel load and total fuel consumption and that this would be reflected in the $\Delta^{14}C$ of $PM_{2.5}$, which we expected to represent the average of the $\Delta^{14}C$ of contemporary atmospheric carbon dioxide (CO_2) over the past one to two decades.

4.2. Methods

4.2.1. Study site

Prescribed fire was applied to a 10-acre (0.05 km^2) unit (Fig. 4.1) within the University of California Blodgett Forest Research Station (Blodgett Forest), located near Georgetown, CA, USA (38.91ºN, 120.06ºW). Blodgett Forest spans 4000 acres (16.2 km^2) and is a mid-elevation (1200-1500 m) mixed-conifer second-growth forest with some portions of oak forest and shrubland (Levine *et al.*, 2020). Tree species are dominated by white fir (*Abies concolor* (GORD. & GLEND.) LINDL. EX HILDEBR.), incense cedar *(Calocedrus decurrens* (TORR.) FLORIN), sugar pine *(Pinus lambertiana* DOUGLAS), ponderosa pine *(P. ponderosa* LAWSON & C. LAWSON), Douglas-fir (*Pseudotsuga menziesii* (MIRB.) FRANCO), and black oak (*Quercus kelloggii* NEWBERRY) (Stephens and Moghaddas, 2005). The median fire return interval in this area was approximately 13 yr (8-15 yr; Stephens and Collins, 2004; Foster *et al.*, 2020) before the implementation of widespread fire suppression in the early 20th century. Due primarily to the legacy of fire suppression and intensive logging, much of the forest has moderate to high canopy cover, high tree density, younger trees, fewer large trees, and heavy fuel loads (Stephens and Moghaddas, 2005; Foster *et al.*, 2020).

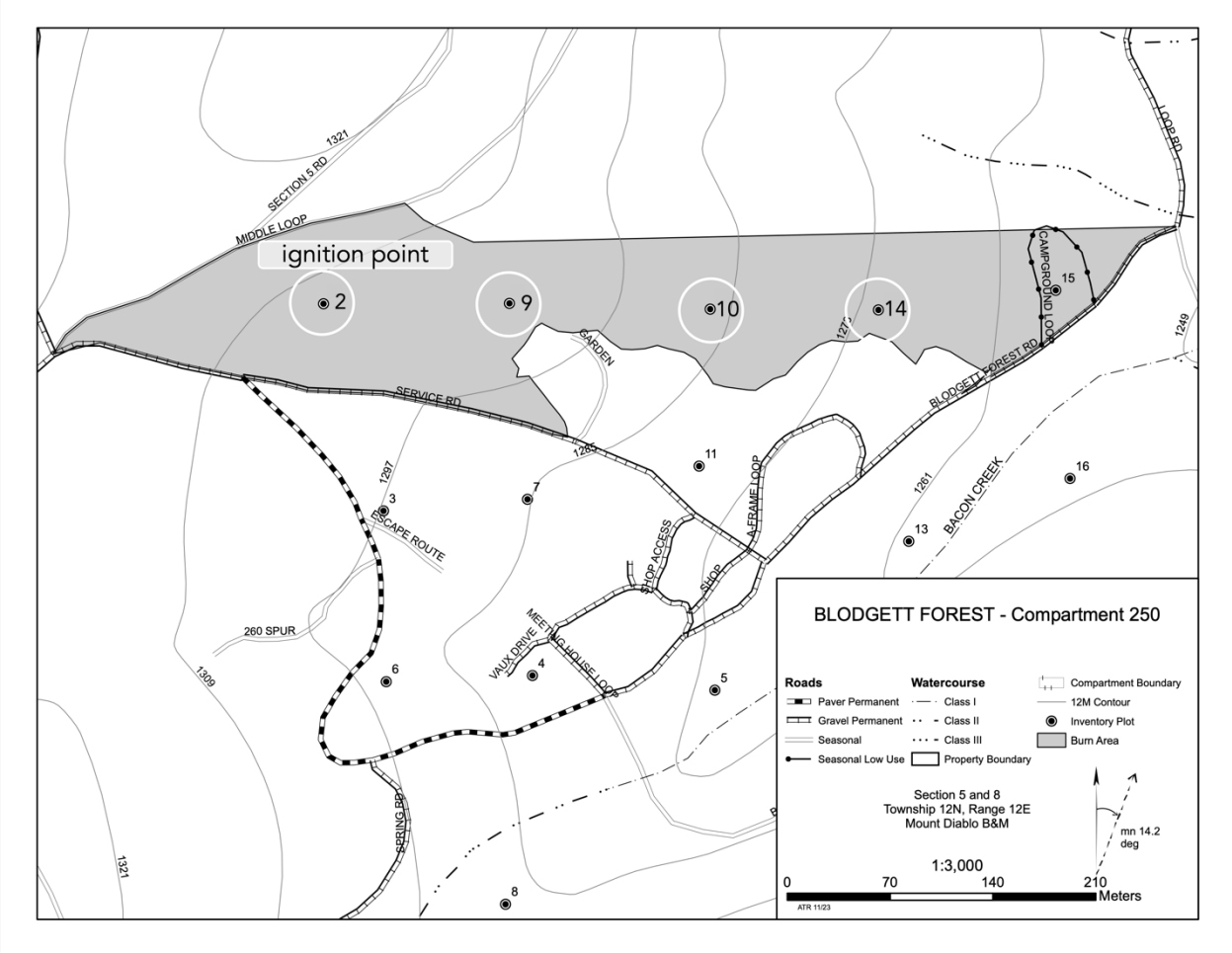

Figure 4.1. Map of the unit at the Blodgett Forest Research Station where a prescribed burn occurred in May 2022. Each number enclosed in a white circle (not to scale) represents one of the unit's four plots (Plot 2, 9, 10, 14). On 14 May, the initial ignition occurred to the northeast of plot 2, with subsequent ignitions occurring in strips between the northeastern and southwestern boundaries of the unit. The fire burned from 14-15 May.

4.2.2. Prescribed fire

The fire was ignited using a strip-head ignition pattern on 14 May 2022 at approximately 11:20 am local time (PDT) with a standard forestry drip torch and a diesel-gasoline mix. Ignitions began

at the highest elevation point (Plot 2; Fig. 4.1) and continued northwest downhill to the lowest point (Plot 14) in a strip pattern, with strips ignited between the northern and southern boundaries of the plot. Occasionally, dot ignitions were employed according to fuel conditions and fire behavior. Active flaming continued until 14 May at approximately 5:45 pm and smoldering occurred for the remainder of the sampling duration on 15 May.

4.2.3. Field observations of fuels and $PM_{2.5}$

4.2.3.1. Fuel inventory and collection

To estimate fuel loads and consumption, we collected measurements of fuels at each of four plots located within the experimentally burned unit (Fig. 4.1) before and after the fire. The plots were established by R. York to measure forest composition and biomass. Each plot contained two 10 m long transects separated by 60º. We used a line-intersect method to measure woody detritus along each of these transects for a total of eight transects measured (two per plot). To estimate needle litter and duff consumption, we measured duff layer thickness at 1 m increments along each transect prior to and after burning and also established two side-by-side 1 × 1 m quadrats at each plot.

To estimate consumption of small and large diameter dead fuels, we measured the diameter of each piece of woody detritus that intersected each 10 m transect before and after the fire. We recorded the number of pieces of fuel before and after the fire to report the total number and percentage of pieces consumed. We converted the number of pieces of woody detritus to a volume

and mass using the line-intersect equations from van Wagner (1968) and assuming an average wood density of 0.4 g cm^{-3} for western conifers (Meier, 2015). We calculated consumption as the difference in woody detritus mass before and after the fire.

We separated woody detritus mass and fuel consumption estimates according to fuel classes defined by the U.S. National Fire-Danger Rating System dead fuel moisture classification system (Deeming *et al.,* 1977). The fuel classes are defined by the number of hours (timelag) required for a fuel to respond to changes in precipitation, relative humidity, and temperature, which is proportional to its diameter. With this system, 1-hour fuels have diameters (d) less than 0.25 in (d < 0.6 cm), 10-hour fuels have diameters between 0.25 and 1.0" ($0.6 \leq d < 2.5$ cm), 100-hour fuels have diameters between 1.0 and 3" ($2.5 \leq d < 7.6$ cm), 1000-hour fuels have diameters between 3 and 8" ($7.6 \leq d < 20.3$ cm).

To quantify duff load and consumption, we collected needle litter and duff from one of the two 1 m^2 quadrats per plot before and after the fire. The material was dried at 55°C to constant mass, weighed, and consumption and combustion completeness was calculated by difference. We define combustion completeness as the percentage of the fuel mass that was consumed. To provide additional information on needle litter and duff consumption, we also measured the depth of the organic horizons along each transect before and after the fire and estimated consumption by difference (Fig. 4.2a, b). We used a tile probe to measure organic horizon depth in cm at every 1

m along the transect. To do this, we vertically inserted a tile probe until we felt resistance, which we assumed to be the beginning of the mineral soil.

Figure 4.2. Photos taken at the Blodgett Forest Research Station during a prescribed fire in May 2022. Photos at the top show a transect (a) before and (b) after the fire (Plot 2). By comparing the before and after photos, it is evident that most of the pinecones and smaller-diameter dead fuels were consumed. Bottom photos show (c) active flaming in plot 14 of the unit on 14 May 2022 and the (d) AirMetrics Tactical Air Sampler with $PM_{2.5}$ impactor mounted on top (right), with a PurpleAir PA-II sensor secured to its back.

We also collected fuel samples to determine the $\Delta^{14}C$ of each fuel type (see Section 4.2.4). Needles, duff, and 1- and 10-hour woody fuels were obtained from the 1 m^2 quadrats, and 100-hour fuels, pinecones, and live grass and shrub leaves at each plot outside the transects. All fuel samples were stored in a refrigerator.

4.2.3.2. $PM_{2.5}$ measurement and collection

We continuously monitored $PM_{2.5}$ concentrations before, during, and after the prescribed fire. *In situ* $PM_{2.5}$ mass concentration (μg $PM_{2.5}$ m^{-3} air) was measured at an inlet height of approximately 1.2 m above ground with a PurpleAir PA-II air quality sensor, which collects measurements via laser particle counting at a two-minute time resolution (PurpleAir, Draper, UT, USA). We analyzed the PA-II Channel A data, which is appropriate for outdoor conditions.

To characterize the $PM_{2.5}$ isotopic composition, we collected filter samples of $PM_{2.5}$ by relocating the sampler to follow the active flaming fire front (Fig. 4.2c). We used an AirMetrics Tactical Air Sampler (AirMetrics, Springfield, OR, USA; Fig. 4.2d) with a $PM_{2.5}$ impactor (#202-100) following the methods described in Odwuor *et al*. (2023) and summarized here. The flow rate of the sampler was adjusted between 4.50 to 4.75 liters per minute (lpm) according to ambient pressure and temperature conditions to maintain a uniform volume flow. We collected samples on quartz fiber filters with a loaded area of 11.95 cm^2 (GE Healthcare Life Sciences, #1851-047). The filters were pre-combusted at 500°C for 3 hours, wrapped individually in aluminum foil, and stored in plastic bags prior to sampling. A blank filter was mounted on the inside of the sampler housing

with no active air flow to collect background PM simultaneously with the $PM_{2.5}$ sample. After collection, filters were wrapped in aluminum foil, sealed in plastic bags, and stored at -20°C. A total of 11 $PM_{2.5}$ samples and 2 blanks were collected for durations ranging from 1.2 to 12.1 h. Blanks were collected concurrently with samples AMS #270187 and 270190 (Table 4.1).

Table 4.1. Summary of total carbon (TC) concentration and radiocarbon content ($\Delta^{14}C$) of $PM_{2.5}$ collected on 12-15 May 2022 within the smoke plume of a prescribed fire at the Blodgett Forest Research Station in Georgetown, CA, USA. Uncertainty in TC_{sample} and $\Delta^{14}C_{sample}$ represent the propagated uncertainty in the collection of these measurements. All samples were measured in 2022. Values denoted by an asterisk (*) are derived from elemental analysis.

Start Date (PDT)	End Date (PDT)	Sample duration (h)	TC_{sample} (µg cm^{-2} filter)	TC_{sample} (µg m^{-3} air)		$\Delta^{14}C_{sample}$ (‰)		TC_{sample} (µg m^{-3} air)*	TN_{sample} (µg m^{-3} air)*	UCI AMS #
			Mean	Mean	Uncer-tainty	Mean	Uncer-tainty			
12-May 00:10	12-May 07:00	6.7	0.8	3.2	0.3	-167	25	NA	NA	270183
12-May 11:40	12-May 18:40	7.0	0.6	1.9	0.3	-513	47	NA	NA	270184
12-May 19:37	13-May 07:37	12.1	0.9	2.0	0.2	-261	20	NA	NA	270185
13-May 08:03	13-May 20:03	12.0	1.1	2.8	0.3	-263	19	NA	NA	270186
14-May 11:11	14-May 13:11	2.0	136.2	2869.1	202.6	97	2	2984.6*	37.4*	270187
14-May 13:12	14-May 14:24	1.2	51.8	1813.6	129.9	124	3	570.5*	14.3*	270188
14-May 14:25	14-May 15:48	1.4	28.0	837.7	59.8	143	4	309.0*	3.5*	270189
14-May 15:49	14-May 17:59	2.1	27.7	550.6	39.4	151	4	341.6*	1.9*	270190
14-May 19:10	14-May 21:32	2.4	3.5	56.1	4.3	74	6	NA	NA	270195
14-May 21:32	15-May 06:31	9.0	9.8	44.8	3.2	82	3	NA	NA	270196
15-May 06:32	15-May 11:12	4.2	16.5	162.7	11.7	88	2	NA	NA	270197

NA = not applicable

4.2.4. Laboratory analysis of fuels and $PM_{2.5}$ samples

To prepare fuel samples for $\Delta^{14}C$ analysis, each sample was first dried at 55ºC to constant mass (48 h to 35 d) and then homogenized (i.e., ground) using the following methods: Grass samples

were cut using shears. Shrub leaves, pinecones, and organic horizons were ground using a Wiley mill (Thomas Scientific, Swedesboro, NJ, USA) with a 20-mesh sieve, coffee grinder (Black and Decker, New Britain, CT, USA), and universal mill (IKA Works Inc, Wilmington, NC, USA) with hard metal cutter (part no. 0000521800), respectively. Woody fuels were homogenized using a combination of shears, Wiley mill, coffee grinder, universal mill, and a hacksaw. Smaller-diameter pieces were first cut with shears and then ground in Wiley mill or coffee grinder. Larger-diameter pieces were first cut radially with a hacksaw and then ground with the coffee grinder or universal mill. The sawdust from cutting was also collected. For longer pieces, a part (1-3 cm width) was first cut and then homogenized. Approximately 4 mg of each sample was used for ^{14}C analysis.

For each sampled $PM_{2.5}$ filter, a portion (1.5 cm^2) was first analyzed for carbon and nitrogen elemental composition with an elemental analyzer (EA, NA 1500 NC, Thermo Scientific, Waltham, MA, USA). The remaining filter area (9.9 cm^2) was used for ^{14}C analysis. Blank filters were not analyzed using EA and the entire filter area (17.3 cm^2) was used for ^{14}C analysis.

Radiocarbon samples were analyzed at the W. M. Keck Carbon Cycle Accelerator Mass Spectrometry (KCCAMS) laboratory at the University of California, Irvine. All samples were sealed with 60 mg cupric oxide in pre-combusted 6 mm OD quartz tubes and oxidized to CO_2 at 900°C for 3 h. The evolved CO_2 was purified on a vacuum line and converted to graphite using a sealed-tube zinc reduction method for the fuels (Xu *et al*., 2007) and modified method for the $PM_{2.5}$ filter samples (Walker and Xu, 2019). Samples were measured with accelerator mass

spectrometry with a measurement uncertainty of < 3‰ from processing standards and blanks. The data are reported as Δ14C, which is corrected for isotope fractionation, so that differences reflect changes in mean age (Odwuor *et al*., 2023). By convention, $\Delta^{14}C \geq 0‰$ indicates carbon assimilated by photosynthesis since 1950 and < 0‰ indicates carbon assimilated before 1950.

To account for extraneous carbon introduced during filter handing in the laboratory and field, the measured $\Delta^{14}C$ of each filter ($\Delta^{14}C_{meas}$) was corrected using blank filters and a simple isotopic mass balance equation (Eqn. 4.1):

$$\Delta^{14}C_{sample} = \frac{\Delta^{14}C_{meas} \times TC_{meas} - \Delta^{14}C_{blank} \times TC_{blank}}{TC_{meas} - TC_{blank}} \quad \text{(Eqn. 4.1)}$$

where "sample" refers to the sampled filter and "blank" refers to the blank filter. The mean blank TC was 0.3 μg C cm^{-2} with a $\Delta^{14}C$ of -192 ± 89‰. The uncertainty (unc) in $\Delta^{14}C_{sample}$ was calculated by propagating the standard deviation (SD) of filter $\Delta^{14}C$ measurements according to Eqn. 4.2:

$$unc\ in\ \Delta^{14}C_{sample} = \sqrt{\left(\frac{TC_{meas}}{TC_{sample}} \times err\ in\ \Delta^{14}C_{meas}\right)^2 - \left(\frac{TC_{blank}}{TC_{sample}} \times err\ in\ \Delta^{14}C_{blank}\right)^2} \quad \text{(Eqn. 4.2)}$$

4.2.5. Estimation of $PM_{2.5}$ and combusted fuel composition

4.2.5.1. Bottom-up estimation of fire-emitted $PM_{2.5}$ radiocarbon content

To estimate the $\Delta^{14}C$ of the smoke produced by combustion of these fuels ($\Delta^{14}C_{PM2.5,\ predicted}$), we first multiplied the mean $\Delta^{14}C$ of each fuel class ($\Delta^{14}C_{sample}$) by its estimated mass consumption

(mass consumed$_{sample}$), producing an isoflux for each fuel class. For 1000-hour fuels, since $\Delta^{14}C$ was not measured, we assigned a mean value computed using the steady-state one box ecosystem model described in section 4.2.5.3 for a mean age of 50 yr. We then divided the sum of the isofluxes by the total fuel consumption to estimate the $\Delta^{14}C$ of $PM_{2.5}$ (Eqn. 4.3):

$$\Delta^{14}C_{PM_{2.5},predicted} = \frac{\Sigma\,(\Delta^{14}C_{sample} \times\ mass\ consumed_{sample})}{total\ mass\ consumed} \qquad \text{(Eqn. 4.3)}$$

4.2.5.2. Keeling plot analysis for $PM_{2.5}$ filters

Using a Keeling plot fit with a Model-II regression (Keeling, 1958; Pataki *et al.*, 2003), we estimated the mean $\Delta^{14}C$ of the combusted fuel from the $PM_{2.5}$ TC and $\Delta^{14}C$ measurements (Mouteva *et al.*, 2015; Wiggins *et al.*, 2018; Odwuor *et al.*, 2023). We first assume that the mass and $\Delta^{14}C$ composition of each sampled $PM_{2.5}$ filter represents a different mixture of two endmembers, fire (i.e., combusted fuel) and the background atmosphere. This approach assumes that the combustion source and background do not change during the course of sampling.

The Keeling plot equation is derived from the linear relationship between $\Delta^{14}C_{sample}$ and $1/TC_{sample}$. The fire $\Delta^{14}C$ end member is identified as the y-intercept of the geometric mean regression computed for the 11 sampled filter measurements of 1/TC and $\Delta^{14}C$. The regression was calculated

using the 'lsqfitgm' function in Matlab developed by E. T. Peltzer at the Monterey Bay Aquarium Research Institute[4].

4.2.5.3. Estimating the mean age of combusted fuels

The age distribution of each fuel class was estimated by calculating its mean $\Delta^{14}C$ and standard deviation and linearly matching these years to the corresponding set of years on the on the time series of atmospheric $\Delta^{14}CO_2$ (Table 4.2).

[4] lsqfitgm function by E. T. Peltzer, Monterey Bay Aquarium Research Institute.

Table 4.2. Summary table of measurements for each fuel type collected at the Blodgett Forest Research Station on 12-15 May 2022. Uncertainty in pre-burn fuel load, post-burn fuel mass, and fuel mass consumed per fuel type is represented by the standard deviation (SD). Uncertainty in the total pre-burn fuel load, post-burn fuel mass, and mass consumed (**bolded values**) is the propagated uncertainty for each fuel type. The $\Delta^{14}C$ of needles, 1-, 10-, and 100-hour fuels is the mean of all samples per fuel type measured in the laboratory and corresponding ages reported were estimated by direct comparison to the historical record of atmospheric $\Delta^{14}CO_2$. Because $\Delta^{14}C$ of 1000-hour fuels was not measured, it was modeled using a one-box steady-state ecosystem model assuming a mean age of 50 yr.

Fuel Type	**Diameter (cm)**	**Pre-burn (g m^2)**		**Post-burn (g m^2)**		**Consumed (g m^2)**			**$\Delta^{14}C$ (‰)**		**Age (yr)**
		Mean	SD	Mean	SD	Mean	SD	%	Mean	Uncer-tainty	
Needles		311	112	135	106	176	54	57	9	2	5
1-hour	<0.635	15	7	3	3	13	7	82	55	9	14-17
10-hour	0.635 - 2.54	165	66	108	68	56	72	34	65	20	13-21
100-hour	2.54 - 7.62	1158	277	653	542	451	381	39	215	46	34-40
1000-hour	7.62-20.32	1893	1980	1028	963	865	1202	46	107	NA	50
Total		3542	**2003**	1926	**1112**	1561	**1264**	NA	NA	NA	NA

NA = not applicable

To estimate the $\Delta^{14}C$ and age of the 1000-hour fuel class, we used a steady-state one-box ecosystem model forced with a time series of historical atmospheric $\Delta^{14}CO_2$ from observations by Hua *et al*. (2022) from 1950 to 2019 for 30ºN to 60ºN and by X. Xu[5] from 2003-2021 at Pt. Barrow, AK, USA. The model sets the ^{14}C composition of net primary production equal to the atmospheric record. Losses from the ecosystem carbon pool (i.e., combusted fuel) are assumed to be first order and only due to decomposition and radioactive decay and controlled by a single turnover time parameter. For this system, we assume that the turnover time is equal to the mean age of the carbon pool. Given a user-prescribed mean age of the carbon pool, the model simulates the evolving $\Delta^{14}C$ of the pool from 10,000 yr before present to 2021 with inputs and losses each year. Here we ran the model for a prescribed mean age of 50 yr to simulate the $\Delta^{14}C$ of the 1000-hour fuel class in 2021.

4.3. Results

4.3.1. Fuel consumption

We estimated that total consumption for all surface fuels was 1561 ± 1264 g m^{-2} (Fig. 4.3; Table 4.2). Much of the uncertainty in this estimate originates from the consumption of large-diameter dead fuels, with 24% and 69% of the uncertainty originate from the uncertainty of the 100- and 1000-hour fuels, respectively.

[5] X. Xu, personal communication 2022.

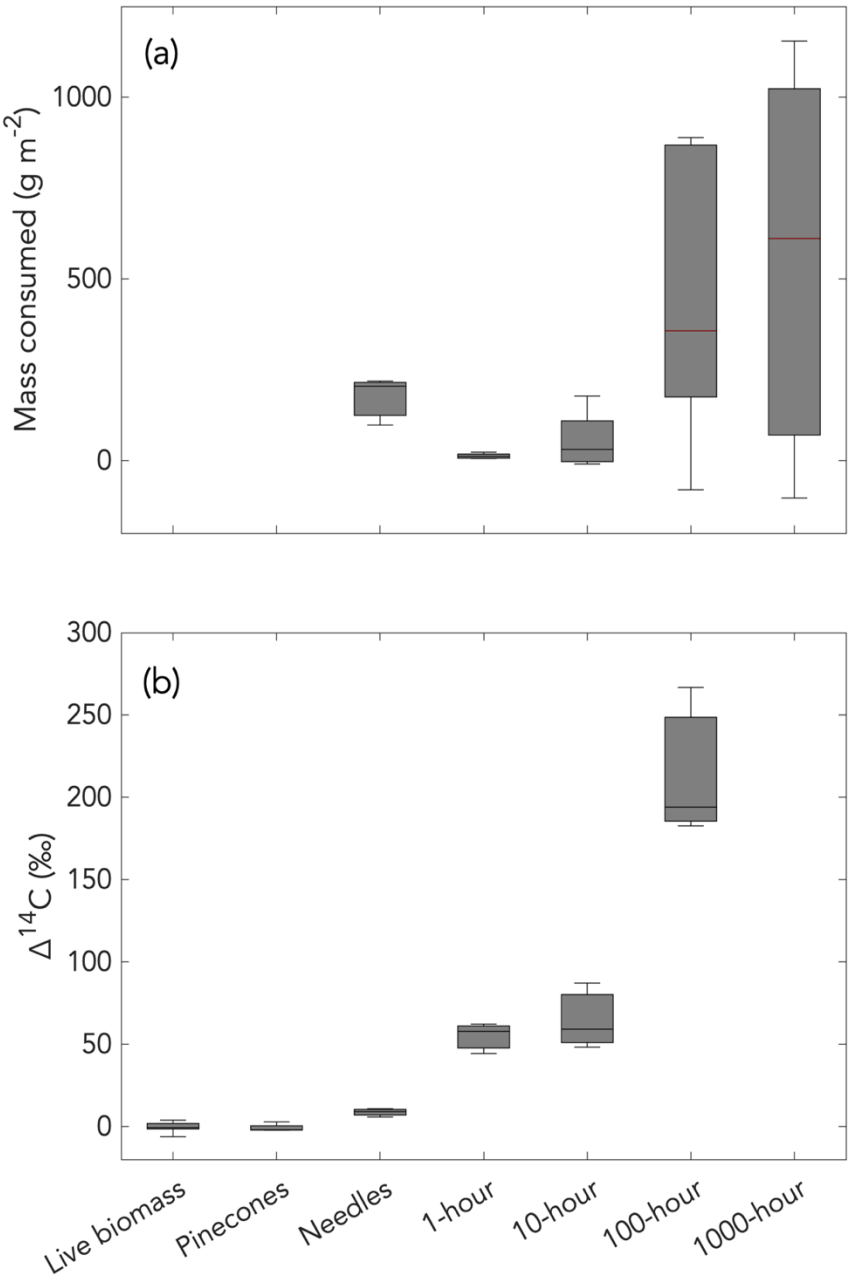

Figure 4.3. Box and whisker plots of (a) mass consumed and (b) radiocarbon content ($\Delta^{14}C$) of fuel classes burned during the prescribed fire at the Blodgett Forest Research Station on 14 May 2022. The central mark in each box represents the median value and the top and bottom whiskers are the 25th and 75th percentiles, respectively. Outliers are not shown, but one exists for 1000-hour fuel mass consumption at 3613 g m^{-2}. The consumption of live biomass and pinecones and the $\Delta^{14}C$ of 1000-hour fuels was not quantified.

Needle litter and duff comprised one of the most continuous layers in the fuel bed at the experimental forest. From our four 1 m^2 quadrats, the mass on the forest floor was 311 ± 112 g m^{-2} prior to burning. The fire consumed about 57% of this pool, yielding a fuel consumption for this layer of 176 ± 54 g m^{-2} (Fig. 4.4).

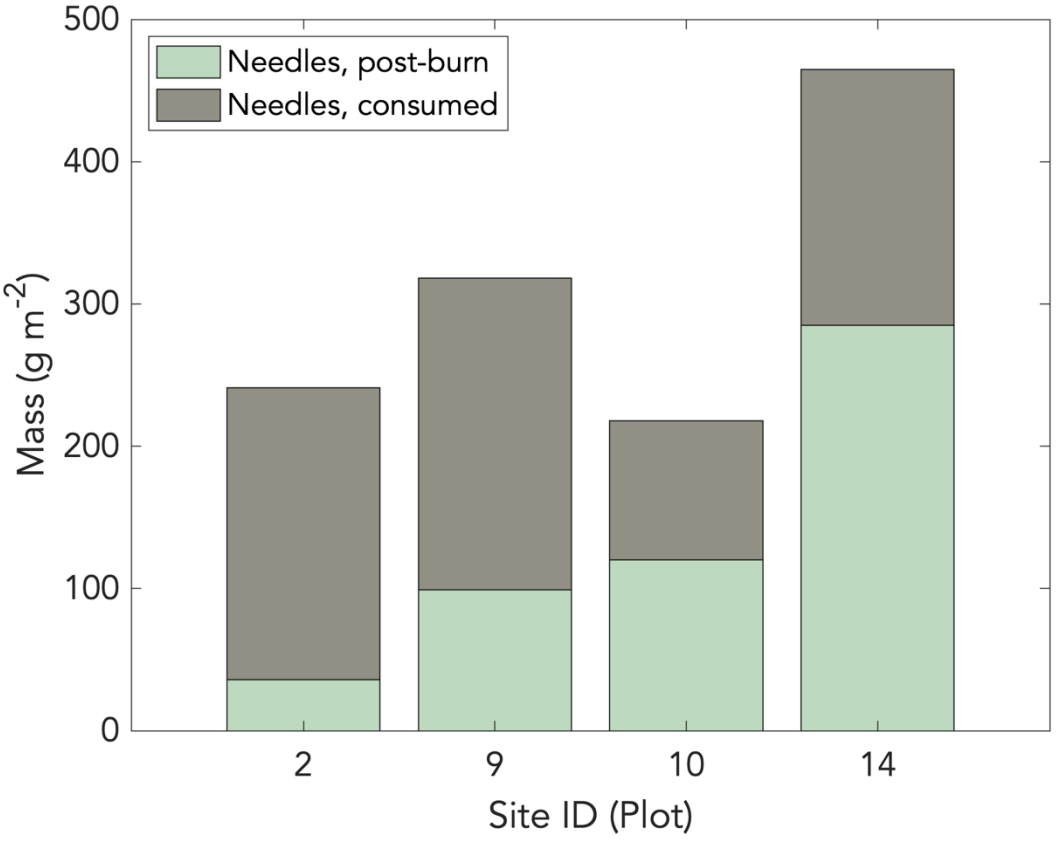

Figure 4.4. Mass of needle litter pre-burn (total height of bar), post-burn (size of green bar) and consumed (size of grey bar) for the prescribed fire observed in this study.

The consumption of fine dead woody fuels, estimated using the line-intersect method, varied considerably as a function of fuel class. 1-hour fuels on the forest floor contributed only modestly to the total fuel load, with a pre-fire density of 15 ± 7 g m^{-2}. The fire consumed nearly all of these fine fuels (82%), yielding a contribution to fuel consumption of 13 ± 7 g m^{-2}.

Ten-hour fuels had a larger pre-fire pool size (165 ± 66 g m^{-2}) but a lower level of combustion completeness (34%), yielding a fuel consumption of 56 ± 72 g m^{-2}. Consumption for larger dead fuel classes was 451 ± 381 g m^{-2} for 100-hour fuels and 865 ± 1202 g m^{-2} for 1000-hour fuels (Fig. 3a). Combustion completeness ranged from 34% to 82% across all surface fuels, with the lowest combustion completeness observed for larger fuels and highest for finer fuels (Table 4.2).

We also estimated the number of pieces of each dead moisture fuel class consumed. The percentage of pieces consumed was generally greater than the combustion completeness (by mass). In general, a greater number of pieces was consumed for smaller fuel classes, but percentage consumption varied across fuel classes: 11 ± 9 pieces (73% of pre-fire mass) for 1-hour fuels, 9 ± 11 pieces (44% of pre-fire mass) for 10-hour fuels, 5 ± 5 pieces (51% of pre-fire mass) for 100-hour fuels, and 1 ± 1 pieces (38% of pre-fire mass) for 1000-hour fuels.

From tile probe measurements, we observed a mean duff depth consumed of 3.2 ±1.0 cm (Table 4.3).

Table 4.3. Summary table of duff depth measurements collected in 4 plots (Plot 2, 9, 10, 14) within a 10-acre unit at the Blodgett Forest Research Station on 12-15 May 2022.

Site	Pre-burn	Post-burn	Consumed	
		cm		%
Plot 2	7.9	5.6	2.4	37.3
Plot 9	12.3	8.9	3.4	38.1
Plot 10	8.4	5.9	2.5	44.5
Plot 14	11.0	6.4	4.6	43.7
Mean	9.9	6.7	3.2	45.1

4.3.2. Fuel $\Delta^{14}C$ measurements and expected $PM_{2.5}$ $\Delta^{14}C$ composition

The mean $\Delta^{14}C$ of the fuel types (live to 100-hour fuels) ranged from -6.1‰ to 215.0‰. Live fuels and pinecones had the lowest observed $\Delta^{14}C$. Live grasses had a $\Delta^{14}C$ of -6.1 ± 1.6‰ that was close to atmospheric levels in 2021 (-3.2 ± 1.4‰). Pinecones had a similar isotopic composition (-0.7 ± 2.5‰). For live shrub fuels, we measured 0.6 ± 2.1‰. Fuels became more enriched with increasing diameter among dead fuels (Fig. 4.3b). We estimated that the mean $\Delta^{14}C$ was 9 ± 2‰ for the needle liter and duff, 55 ± 9‰ for 1-hour fuels, 65 ± 20‰ for 10-hour fuels, and 215 ± 46‰ for 100-hour fuels. The corresponding fuel ages for the organic horizon, 1-, 10-, and 100-hour fuels are approximately 5, 14-17, 13-21, and 34-40 yr, respectively (Table 4.2). We assigned a mean $\Delta^{14}C$ of 107‰ to 1000-hour fuels, computed using the steady-state one-box ecosystem model assuming a mean age of 50 yr. Using the $\Delta^{14}C$ values and consumption for each fuel class in a bottom-up approach, we estimated a value of 125‰ for the fire-emitted $PM_{2.5}$.

4.3.3. $PM_{2.5}$ and TC concentrations and isotopic composition

Before the fire was ignited, $PM_{2.5}$ concentrations were relatively low, ranging from 0 to 40 μg m^{-3} between 12 May at 12:17 am and 14 May 11:30 am (Table 4.1; Fig. 4.5a). Following ignition, $PM_{2.5}$ levels began to rise around 11:30 am on 14 May, reaching a maximum of 3000 μg m^{-3} around 12:28 pm on 14 May before declining through the afternoon and into the evening of 14 May. Although low in comparison to the afternoon of 14 May, $PM_{2.5}$ concentrations overnight oscillated between 1 μg m^{-3} and 845 μg m^{-3} until the end of the sampling period around 11:12 am on 15 May while the fire was still smoldering. The 24-hour average $PM_{2.5}$ burden ranged between 1.8 μg m^{-3} for the pre-ignition period to 347.3 μg m^{-3} during the active flaming period of the fire.

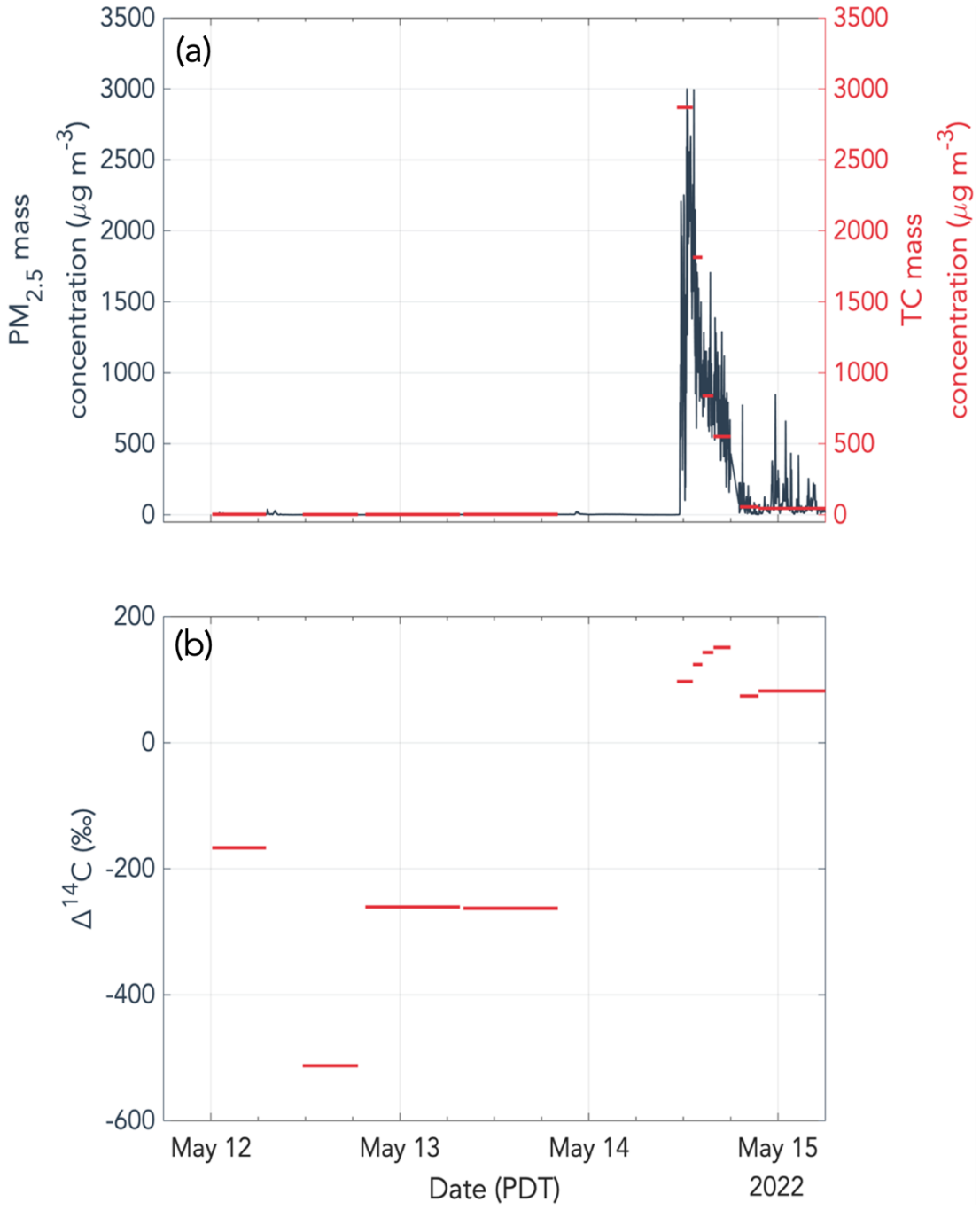

Figure 4.5. Time series measurements of $PM_{2.5}$ during a prescribed forest fire: (a) *In situ* $PM_{2.5}$ mass concentration (left axis, blue) and total carbon (TC) mass concentration of $PM_{2.5}$ (right axis, red) and (b) corresponding $\Delta^{14}C$ signatures of $PM_{2.5}$.

TC concentrations closely tracked optical $PM_{2.5}$ measurements, ranging from 1.9 μg C m^{-3} to 3.2 μg C m^{-3} during the period before the fire was ignited around 11:20am (Fig. 4.5a). After ignition, TC concentrations were very high, ranging from 44.8 μg C m^{-3} for the sample collected from 9:32 pm on 14 May to 6:31 am on 15 May to 2869.1 μg C m^{-3} for the sample collected from 11:11 am to 1:11 pm on 14 May. Our data suggests that the $PM_{2.5}$ burden was dominated (60-100%) by organic carbon during the fire.

Radiocarbon signatures of TC were lower before the fire and became more enriched and relatively constant after the fire was ignited (Fig. 4.5b), ranging from -513 ± 47‰ to -167 ± 25‰ before the fire, and 74 ± 6‰ to 151 ± 4‰ during the fire.

Using the Keeling plot approach, we estimated the mean $\Delta^{14}C$ of combusted fuel to be 122 ± 22‰ (Fig. 4.6), corresponding to a mean fuel age of 45 yr with a range of 27-62 yr computed using the steady-state one-box ecosystem model. This is within the error of $\Delta^{14}C$ computed using the bottom-up approach (125‰).

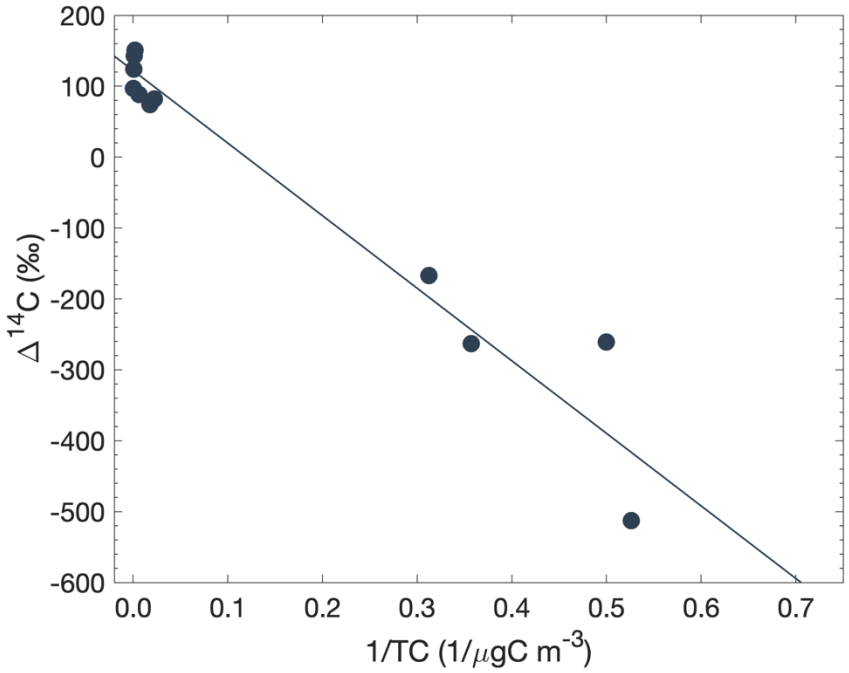

Figure 4.6. Keeling plot showing the relationship between the $\Delta^{14}C$ signature and the total carbon (TC) mass concentration of $PM_{2.5}$ collected during a prescribed forest fire. The y-intercept of the regression represents the mean observed $\Delta^{14}C$ signature of the combusted fuel (122 ± 22‰, R^2 = 0.97).

4.4. Discussion

In this study, we combined measurements of fuel ^{14}C composition and consumption with the ^{14}C composition of fire-emitted $PM_{2.5}$ to characterize the smoke burden associated with a prescribed forest fire in California's Sierra Nevada mountains. This represents the first study to directly compare the $\Delta^{14}C$ signature of fuels to that of fire-emitted $PM_{2.5}$ for California forests – an approach commonly used to understand wildfire (Gustafsson *et al*., 2009; Mouteva *et al*., 2015; Wiggins *et al*., 2018; Odwuor *et al*., 2023).

Few studies have quantified fuel consumption during prescribed fires at Blodgett Forest (Kauffman, 1989; Stephens and Moghaddas 2005; Levine *et al*., 2020; York *et al*., 2022), California's Sierra Nevada mountains (Knapp *et al*., 2005; Keeley and McGinnis, 2007; Walker *et al*., 2006; Cansler *et al.,* 2019;), and other western North American forests (Prichard *et al*., 2017; Agee and Lolley, 2006; Hunter *et al*., 2011). Further, while prescribed burning was the only treatment studied here, most previous work combined burning with mechanical treatment.

Other studies of prescribed fire in the Sierra Nevada, are typically focused on the combination of mechanical thinning and prescribed fire (Walker *et al*., 2004; Knapp *et al.,* 2017; Cansler *et al*., 2019). For other forests of the western United States, studies typically observe a combination of mechanical and prescribed fire treatments (Brown *et al*., 1991; Agee and Lolley, 2006). One study by Prichard *et al.* (2017) only applied fire treatment and found that while litter and duff dominated pre-fire fuel loading across the experimental site, larger-diameter woody debris constituted a significant portion of pre-fire fuel loading at some locations within the site. They also estimated a combustion completeness of about 50% (Prichard *et al.,* 2017).

In this study, the combustion completeness of ground and surface fuels reported here (44%) closely matches the average value observed (45%) across 3 burns that occurred over 14 yr in a recent study of prescribed fire at Blodgett Forest (Levine *et al.*, 2020). For the most recent burn in 2017 (8 yr

elapsed since the previous burn), Levine *et al*. (2020) observed a mean combustion completeness of only 29 ± 31%. In our study, approximately 3 yr had elapsed since the last prescribed burn.

We observed the greatest percent consumption in the organic horizon and 1-hour fuel classes, whereas Levine *et al*. (2020) observed the greatest consumption in organic horizon and 1000-hour fuels. While we expected organic horizon and smaller diameter (1- and 10-hour) fuels to dominate the fuel load, we observed relatively small fuel loads for these finer surface fuels (14% of total) compared to previous studies (56-85%) (Kauffman and Martin, 1989, Levine *et al.*, 2020) and to larger-diameter (100- and 1000-hour) fuel loads in this study (86%). One possible reason for the discrepancy in O-horizon fuel load and consumption might be the time elapsed between burns. Our study observed the first prescribed fire at the site in only 3 yr, while the most recent prescribed fire observed by Levine *et al*. (2020) occurred approximately 8 yr after the last burn, allowing more time for the accumulation of finer surface fuels.

In our study, 1000-hour fuels represented approximately 53% of the surface fuel load, compared to only 30% observed for the most recent fire in the study by Levine *et al*. (2020) and 30% by Kauffman and Martin (1989). Further, we observed a greater contribution from larger-diameter fuels (1372 ± 1263 g m^{-2}) to total fuel consumption (1561 ± 1264 g m^{-2}). While we did expect some accumulation of large-diameter fuels at this site, what we observed was greater than previous studies at Blodgett Forest. Whereas larger fuels (e.g., 1000-hour fuels) are typically slow to ignite, requiring high intensity fire that is often sustained by combustion of smaller-diameter fuel (Gorte,

2009), we found that a large portion (46%) of the 1000-hour fuels were consumed in the prescribed fire. It is likely tree mortality induced by prolonged drought in the Sierra Nevada (2012-2015; Goulden and Bales, 2019; Kim *et al*., 2022) contributed to the accumulation of larger-diameter fuels via the input of fuels but also by constraining fuel moisture.

We assume that larger fuel classes are older and have been incorporating carbon over a greater lifetime, which is reflected in the $\Delta^{14}C$ measurements of our fuel samples and $PM_{2.5}$ filters. From our ^{14}C-based assessments, we estimated a mean age for fuels combusted in the prescribed burn of 45 years, further supporting the notion that larger-diameter dead fuels contributed significantly to total fuel consumption and emissions. Further, we observed agreement between the expected $\Delta^{14}C$ of fire-emitted $PM_{2.5}$ computed using the $\Delta^{14}C$ and consumption estimates for different fuel classes (125‰) and the observed $\Delta^{14}C$ of emissions from the Keeling plot approach (122 ± 22‰). This indicates that the fuel composition is reflected in the isotopic composition of $PM_{2.5}$ emissions and, therefore, we suggest that burning of smaller-diameter fuels would result in $\Delta^{14}C$ of fire-emitted $PM_{2.5}$ that more closely matches the contemporary atmosphere because we found that smaller-diameter dead fuels generally had lower $\Delta^{14}C$ values (Fig. 4.7).

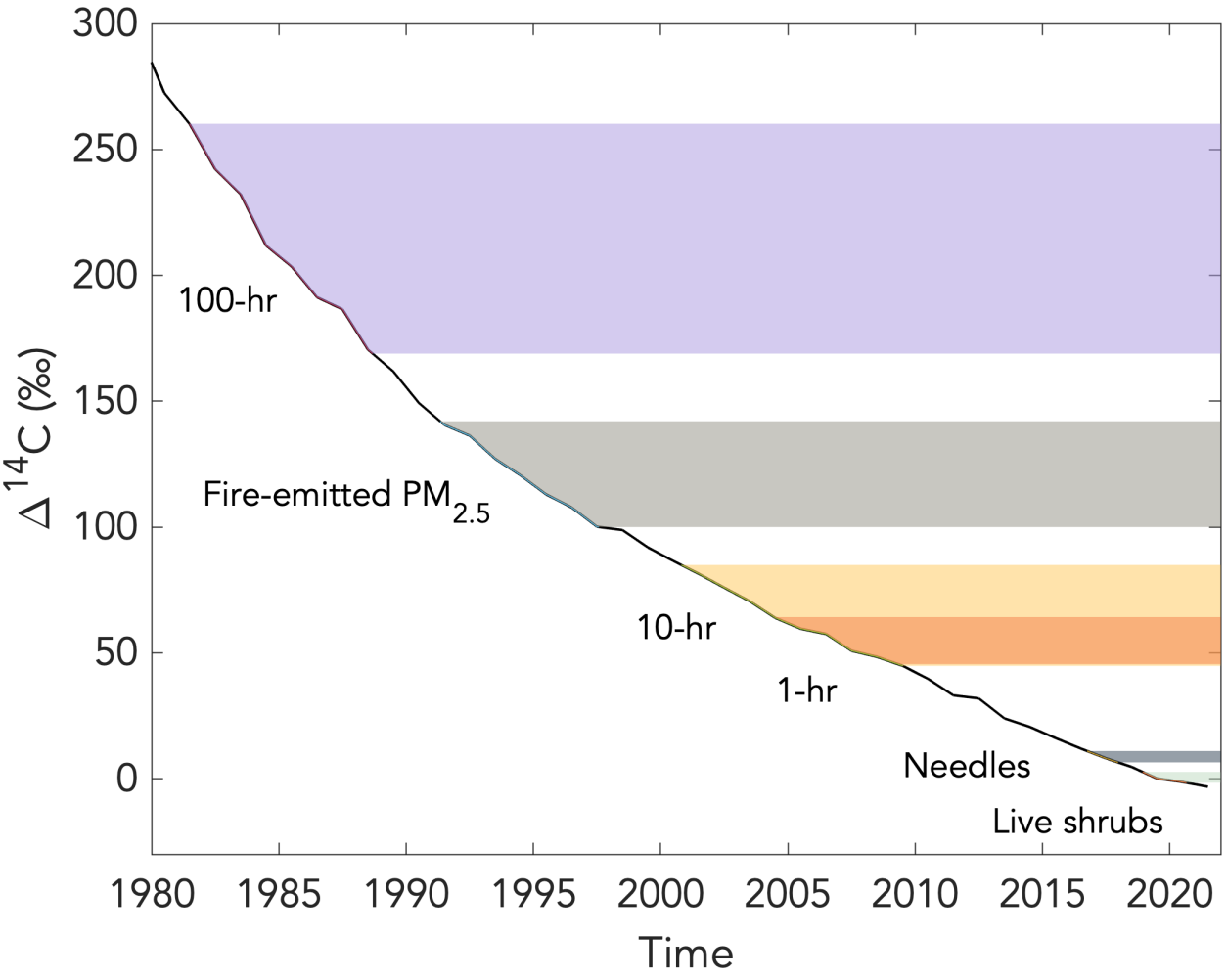

Figure 4.7. Atmospheric $\Delta^{14}CO_2$ (black line). Each shaded region represents the distribution of $\Delta^{14}C$ values measured for each fuel type and for fire-emitted $PM_{2.5}$ (mean ± SD). The age distribution of each fuel class was estimated by matching the $\Delta^{14}C$ distribution to the corresponding set of years on the on the time series of atmospheric $\Delta^{14}CO_2$.

Regional patterns in particulate matter concentrations in the western U.S. have been associated with fire activity (Hand *et al.,* 2013). While fuel composition partially influences the composition and concentration of emissions, the impact of those emissions on public health is also determined

by smoke transport, the duration of smoke exposure, and the number of people who are exposed, particularly those with underlying health conditions (Williamson *et al.*, 2016). As smoke is transported, $PM_{2.5}$ undergoes chemical and physical transformations to produce secondary particulates (Akagi *et al.*, 2011), so the impact of $PM_{2.5}$ on a regional scale is further influenced by the species it interacts with downwind of the fire. However, our study was limited to the observation of primary fire-emitted $PM_{2.5}$, rather than secondary particulates. Lower intensity fires are associated with more immediate local effects, as the height at which smoke is injected into the atmosphere (i.e., plume injection height) is typically lower, preventing the large-scale dispersion of smoke and encouraging the concentration of pollutants over small areas (Williamson *et al.*, 2016; Reisen *et al.*, 2018). However, higher intensity fires typically have a higher plume injection height and would have greater effects on remote communities (Williamson *et al.*, 2016). Further, $PM_{2.5}$ from wildfires has been shown to have a more significant impact on remote communities, in part because of the absence of other major sources of $PM_{2.5}$ (Ahangar *et al.,* 2021). Larger fuels contribute primarily to fire intensity, whereas smaller fuels contribute mainly to fire spread (Gorte, 2009). Therefore, we might expect the sustained use of prescribed fire to result in lower intensity fires and more local effects, but initially we expect higher intensity fires with more impact on remote communities initially with the consumption of larger fuel classes.

The consumption of larger fuel classes is typically associated with smoldering combustion (Fig. 4.8; Williamson *et al.*, 2016). Previous studies have found that the majority of fuels (72%; Kauffman and Martin, 1989) are consumed during the smoldering phase of a prescribed fire.

Although all landscape fires (e.g., wildfires, prescribed fires) are characterized by incomplete combustion, smoldering is characterized by less complete combustion than flaming, is promoted by densely packed fuels and larger fuel diameters (Williamson *et al.,* 2016), and is associated with higher levels of $PM_{2.5}$ (Akagi *et al.*, 2011; Reisen *et al.*, 2018). Therefore, we expect more $PM_{2.5}$ emitted during the smoldering phase of combustion, when most of the larger-diameter fuels are consumed.

Figure 4.8. Downed sugar pine trunk smoldering (a) on 14 May 2022 and (b) on 15 May 2022.

Although we initially expected litter and smaller-diameter fuels to dominate the fuel load and total fuel consumption, our findings that larger-diameter dead fuels contributed significantly to

emissions during this prescribed fire can be useful for understanding better the effects of prescribed fire on smoke composition.

4.5. Conclusions

Based on our findings from this prescribed burn at Blodgett Forest, we conclude that as prescribed fire becomes widespread across the state, larger fuels classes will initially dominate the fuel load, and carbonaceous $PM_{2.5}$ concentrations will be greatly elevated due to smoldering combustion. We propose that mechanical thinning could help reduce the input of large-diameter fuels over time by removing smaller trees that compete with larger trees, so that fewer large trees die, and that the removal of saw logs and/or mastication could further reduce 1000-hour fuel loads. Evidence suggests that when combined, mechanical treatments and prescribed fire have the greatest effect on reducing fire severity (Stephens and Moghaddas, 2005; Stephens *et al.*, 2012; Kalies and Kent, 2016; Prichard *et al.,* 2021). As larger fuels are removed mechanically and/or by prescribed fire, smaller-diameter fuels, which are largely consumed during flaming combustion, will then dominate the fuel load and $PM_{2.5}$ concentrations in smoke will decrease. Further, because we found that smaller-diameter dead fuels generally had lower $\Delta^{14}C$ values than larger-diameter fuels, we expect $\Delta^{14}C$ of fire-emitted $PM_{2.5}$ to be lower and more closely match atmospheric $\Delta^{14}CO_2$ with repeated applications of prescribed fire, reflecting the combustion of younger, smaller fuels. This represents the first direct comparison of fire-emitted $PM_{2.5}$ isotopic composition to a bottom-up estimate from fuel $\Delta^{14}C$ and consumption, and agreement in the findings between these two assessments suggests that our methods have the potential to allow the monitoring of fuel

consumption using $PM_{2.5}$ $\Delta^{14}C$ measurements as the used of prescribed fire is expanded across California.

4.6 Acknowledgements

The field work for this study was conducted on unceded Nisenan lands, which was stewarded for thousands of years prior to colonization by the Nisenan, Washoe, Miwok, and Maidu peoples. This material is based upon work supported by the National Science Foundation Graduate Research Fellowship under Grant No. DGE-2039655 to AO. JTR received funding support from the NASA's Modeling, Analysis, and Prediction (MAP) and Earth Information System – Fire research programs and the U.S. Dept of Energy Office of Science's RUBISCO Science Focus Area. Funding from the Ralph J. and Carol. M. Cicerone Chair in the Department of Earth System Science supported the field campaign and laboratory measurements. We thank the KCCAMS staff for supporting the elemental and isotopic analyses.

4.7. References

Abatzoglou, J. T. and Williams, A. P. (2016) 'Impact of anthropogenic climate change on wildfire across western US forests', *Proceedings of the National Academy of Sciences,* 113(42), 11770-11775. doi: 10.1073/pnas.1607171113.

Agee, J. K. and Skinner, C. N. (2005) 'Basic principles of forest fuel reduction treatments', *Forest Ecology and Management*, 211(1–2), pp. 83–96. doi: 10.1016/j.foreco.2005.01.034.

Agee, J. K., & Lolley, M. R. (2006). Thinning and prescribed fire effects on fuels and potential fire behavior in an eastern Cascades forest, Washington, USA. *Fire Ecology*, *2*, 3-19. doi: 10.4996/fireecology.0202003

Ahangar, F. E., Pakbin, P., Hasheminassab, S., Epstein, S. A., Li, X., Polidori, A., & Low, J. (2021). Long-term trends of PM2. 5 and its carbon content in the South Coast Air Basin: A focus on the impact of wildfires. *Atmospheric Environment*, *255*, 118431. doi: 10.1016/j.atmosenv.2021.118431

Akagi, S. K. *et al.* (2011) 'Emission factors for open and domestic biomass burning for use in atmospheric models', *Atmospheric Chemistry and Physics*, 11(9), pp. 4039–4072. doi: 10.5194/acp-11-4039-2011.

Anderson, M. K. and Moratto, M. J. (1996) *Native American Land-Use Practices and Ecological Impacts*. In *Sierra Nevada ecosystem project: final report to Congress* (Vol. 2, pp. 187-206). Davis, CA: University of California, Centers for Water and Wildland Resources Davis.

Andreae, M. O. and Gelencsér, A. (2006) 'Atmospheric Chemistry and Physics Black carbon or brown carbon? The nature of light-absorbing carbonaceous aerosols', *Atmos. Chem. Phys*, 6, pp. 3131–3148. doi: 10.5194/acp-6-3131-2006

Bond, T. C. *et al.* (2013) 'Bounding the role of black carbon in the climate system: A scientific assessment', *Journal of Geophysical Research Atmospheres*, 118(11), pp. 5380–5552. doi: 10.1002/jgrd.50171.

Brown, P. T. *et al.* (2023) 'Climate warming increases extreme daily wildfire growth risk in California', *Nature*. 1-7. doi: 10.1038/s41586-023-06444-3.

Brookes, W., Daniels, L. D., Copes-Gerbitz, K., Baron, J. N., & Carroll, A. L. (2021). A disrupted historical fire regime in central British Columbia. *Frontiers in Ecology and Evolution*, *9*, 676961. doi: 10.3389/fevo.2021.676961

Burke, M. *et al.* (2021) 'The changing risk and burden of wildfire in the United States', *Proceedings of the National Academy of Sciences of the United States of America*, 118(2), pp. 1–6. doi: 10.1073/PNAS.2011048118.

California Wildfire and Forest Resilience Task Force (2022) *California's Strategic Plan for Expanding the Use of Beneficial Fire* (available at: https://wildfiretaskforce.org/wp-content/uploads/2022/05/californias-strategic-plan-for-expanding-the-use-of-beneficial-fire.pdf) (Accessed 3 November 2023)

Cansler, C. A., Swanson, M. E., Furniss, T. J., Larson, A. J., & Lutz, J. A. (2019). Fuel dynamics after reintroduced fire in an old-growth Sierra Nevada mixed-conifer forest. *Fire Ecology*, *15*, 1-17. https://doi.org/10.1186/s42408-019-0035-y

Deeming, John E.; Burgan, Robert E.; Cohen, Jack D. 1977. The National Fire-Danger Rating System - 1978. Gen. Tech. Rep. INT-GTR-39. Ogden, UT: U.S. Department of Agriculture, Forest Service, Intermountain Forest and Range Experiment Station. 63 p

Foster, D. E. *et al.* (2020) 'Potential wildfire and carbon stability in frequent-fire forests in the Sierra Nevada: trade-offs from a long-term study', *Ecosphere*, 11(8). doi: 10.1002/ecs2.3198.

Gorte, R. W. (2009) 'Wildfire fuels and fuel reduction', *Congressional Research Service, Library of Congress*, pp. 1–16.

Goulden, M. L., & Bales, R. C. (2019). California forest die-off linked to multi-year deep soil drying in 2012–2015 drought. *Nature Geoscience*, *12*(8), 632-637 doi: 10.1038/s41561-019-0388-5

Graham, R.T., McCaffrey, S., Jain, T.B., 2004. Science basis for changing forest structure to modify wildfire behavior and severity. USDA Forest Service General Technical Report, RMRS- 120, Rocky Mountain Research Station, Ogden, Utah, 43 p.

Gustafsson, O., Krusa, M., Zencak, Z., Sheesley, R. J., Granat, L., Engstrom, E., ... & Rodhe, H. (2009). Brown clouds over South Asia: biomass or fossil fuel combustion?. Science, 323(5913), 495-498. doi: 10.1126/science.1164857

Gutierrez, A. A. *et al.* (2021) 'Wildfire response to changing daily temperature extremes in California's Sierra Nevada', *Science Advances*, 7(47), pp. 1–11. doi: 10.1126/sciadv.abe6417.

Hagmann, R. K. *et al.* (2021) 'Evidence for widespread changes in the structure, composition, and fire regimes of western North American forests', *Ecological Applications*, 31(8). doi: 10.1002/eap.2431.

Hand, J. L., B. A. Schichtel, M. Pitchford, W. C. Malm, and N. H. Frank (2012), Seasonal composition of remote and urban fine particulate matter in the United States, *J. Geophys. Res*., *117*, D05209, doi:10.1029/2011JD017122.

Hantson, S. *et al.* (2022) 'Human-ignited fires result in more extreme fire behavior and ecosystem impacts', *Nature Communications*. Springer US, 13(1), pp. 1–8. doi: 10.1038/s41467-022-30030-2.

Huang, X. *et al.* (2023) 'Smoke-weather interaction affects extreme wildfires in diverse coastal regions', *Science*, 379(6631), pp. 457–461. doi: 10.1126/science.add9843.

Kalies, E. L. and Kent, L. L. Y. (2016) 'Tamm Review: Are fuel treatments effective at achieving ecological and social objectives? A systematic review', *Forest Ecology and Management*. Elsevier B.V., 375, pp. 84–95. doi: 10.1016/j.foreco.2016.05.021.

Kauffman, J. B., & Martin, R. E. (1989). Fire behavior, fuel consumption, and forest-floor changes following prescribed understory fires in Sierra Nevada mixed conifer forests. *Canadian Journal of Forest Research*, *19*(4), 455-462. doi: 10.1139/x89-071

Keeling, C. D. (1958) 'The concentration and isotopic abundances of atmospheric carbon dioxide in rural area', *Geochimica et Cosmochimica Acta*, 13, pp. 1–13. doi: 10.1016/0016-7037(58)90033-4

Keeley, J. E., & McGinnis, T. W. (2007). Impact of prescribed fire and other factors on cheatgrass persistence in a Sierra Nevada ponderosa pine forest. *International Journal of*

Wildland Fire, *16*(1), 96-106. doi: 10.1071/WF06052
Keeley, J. E., & Syphard, A. D. (2019). Twenty-first century California, USA, wildfires: fuel-dominated vs. wind-dominated fires. *Fire Ecology*, *15*(1), 1-15. doi: 10.1186/s42408-019-0041-0
Kim, Y., Grulke, N. E., Merschel, A. G., & Uyeda, K. A. (2022). Assessing Role of Drought Indices in Anticipating Pine Decline in the Sierra Nevada, CA. *Climate*, *10*(5), 72. doi: 10.3390/c
Knapp, E. E., Keeley, J. E., Ballenger, E. A., & Brennan, T. J. (2005). Fuel reduction and coarse woody debris dynamics with early season and late season prescribed fire in a Sierra Nevada mixed conifer forest. *Forest Ecology and Management*, *208*(1-3), 383-397. doi: 10.1016/j.foreco.2005.01.016
Levine, J. I. *et al.* (2020) 'Forest stand and site characteristics influence fuel consumption in repeat prescribed burns', *International Journal of Wildland Fire*, 29(2), pp. 148–159. doi: 10.1071/WF19043.
Marks-Block, T. and Tripp, W. (2021) 'Facilitating prescribed fire in northern california through indigenous governance and interagency partnerships', *Fire*, 4(3). doi: 10.3390/fire4030037.
May, A. A. *et al.* (2015) 'Observations and analysis of organic aerosol evolution in some prescribed fire smoke plumes', *Atmospheric Chemistry and Physics*, 15(11), pp. 6323–6335. doi: 10.5194/acp-15-6323-2015.
Meier, E. W. (2015). Identifying and using hundreds of woods worldwide. *Wood Database*.
Mouteva, G. O. *et al.* (2015) 'Black carbon aerosol dynamics and isotopic composition in Alaska linked with boreak fire emissions and depth of burn in organic soils', *Global biogeochemical cycles*, pp. 1977–2000. doi: 10.1111/1462-2920.13280.
Odwuor, A., Yañez, C. C., Chen, Y., Hopkins, F. M., Moreno, A., Xu, X., ... & Randerson, J. T. (2023). Evidence for multi-decadal fuel buildup in a large California wildfire from smoke radiocarbon measurements. *Environmental Research Letters*, *18*(9), 094030. doi: 10.1088/1748-9326/aced17
Pataki, D. E. *et al.* (2003) 'The application and interpretation of Keeling plots in terrestrial carbon cycle research', *Global Biogeochemical Cycles*, 17(1). doi: 10.1029/2001GB001850.
Prichard, S. J., Hessburg, P. F., Hagmann, R. K., Povak, N. A., Dobrowski, S. Z., Hurteau, M. D., ... & Khatri-Chhetri, P. (2021). Adapting western North American forests to climate change and wildfires: 10 common questions. *Ecological applications*, *31*(8), e02433. doi: 10.1002/eap.2433
Prichard, S. J., Kennedy, M. C., Wright, C. S., Cronan, J. B., & Ottmar, R. D. (2017). Predicting forest floor and woody fuel consumption from prescribed burns in southern and western pine ecosystems of the United States. *Forest Ecology and Management*, *405*, 328-338. doi: 10.1016/j.foreco.2017.09.025
Pausas, J. G. and Keeley, J. E. (2019) 'Wildfires as an ecosystem service', *Frontiers in Ecology and the Environment*, 17(5), pp. 289–295. doi: 10.1002/fee.2044.
Pollet, J., & Omi, P. N. (2002). Effect of thinning and prescribed burning on crown fire severity

in ponderosa pine forests. *International Journal of Wildland Fire*, *11*(1), 1-10. doi: 10.1071/WF01045.

Quinn-Davidson, L. N., & Varner, J. M. (2011). Impediments to prescribed fire across agency, landscape and manager: an example from northern California. *International Journal of Wildland Fire*, *21*(3), 210-218. doi: 10.1071/WF11017

Reisen, F. *et al.* (2018) 'Ground-Based Field Measurements of PM2.5 Emission Factors From Flaming and Smoldering Combustion in Eucalypt Forests', *Journal of Geophysical Research: Atmospheres*, 123(15), pp. 8301–8314. doi: 10.1029/2018JD028488.

Safford, H. D. *et al.* (2022) 'The 2020 California fire season: A year like no other, a return to the past or a harbinger of the future?', *Global Ecology and Biogeography*, 31(10), pp. 2005–2025. doi: 10.1111/geb.13498.

Schweizer, D., Preisler, H. K., & Cisneros, R. (2019). Assessing relative differences in smoke exposure from prescribed, managed, and full suppression wildland fire. *Air Quality, Atmosphere & Health*, *12*, 87-95. doi: 10.1007/s11869-018-0633-x

Shive, K. L. *et al.* (2022) 'Ancient trees and modern wildfires: Declining resilience to wildfire in the highly fire-adapted giant sequoia', *Forest Ecology and Management*. Elsevier B.V., 511(February), p. 120110. doi: 10.1016/j.foreco.2022.120110.

Steel, Z. L., Koontz, M. J. and Safford, H. D. (2018) 'The changing landscape of wildfire: burn pattern trends and implications for California's yellow pine and mixed conifer forests', *Landscape Ecology*. Springer Netherlands, 33(7), pp. 1159–1176. doi: 10.1007/s10980-018-0665-5.

Stephens, S. L. *et al.* (2012) 'The effects of forest fuel-reduction treatments in the United States', *BioScience*, 62(6), pp. 549–560. doi: 10.1525/bio.2012.62.6.6.

Stephens, S. L. and Collins, B. M. (2004) 'Fire Regimes of Mixed Conifer Forests in the North-Central Sierra Nevada at Multiple Spatial Scales', *Northwest Science*, 78(1), pp. 12–23. available at: https://nature.berkeley.edu/stephenslab/wp-content/uploads/2018/01/Stephens-Collins-2004_NWSci-781-pp12-23.pdf

Stephens, S. L. and Moghaddas, J. J. (2005) 'Experimental fuel treatment impacts on forest structure, potential fire behavior, and predicted tree mortality in a California mixed conifer forest', *Forest Ecology and Management*, 215(1–3), pp. 21–36. doi: 10.1016/j.foreco.2005.03.070.

Swetnam, T. W. *et al.* (2009) 'Multi-millennial fire history of the giant forest, Sequoia National Park, California, USA', *Fire Ecology*, 5(3), pp. 120–150. doi: 10.4996/fireecology.0503120.

Taylor, A. H. *et al.* (2016) 'Socioecological transitions trigger fire regime shifts and modulate fire-climate interactions in the Sierra Nevada, USA, 1600-2015 CE', *Proceedings of the National Academy of Sciences of the United States of America*, 113(48), pp. 13684–13689. doi: 10.1073/pnas.1609775113.

Urbanski, S. P. (2013) 'Combustion efficiency and emission factors for wildfire-season fires in mixed conifer forests of the northern Rocky Mountains, US', *Atmospheric Chemistry and Physics*, 13(14), pp. 7241–7262. doi: 10.5194/acp-13-7241-2013.

Walker, R. F., Fecko, R. M., Frederick, W. B., Murphy, J. D., Johnson, D. W., & Miller, W. W.

(2006). Thinning and prescribed fire effects on forest floor fuels in the east side Sierra Nevada pine type. *Journal of Sustainable Forestry*, *23*(2), 99-115. doi: 10.1300/J091v23n02_06

Walker, B. D. and Xu, X. (2019) 'An improved method for the sealed-tube zinc graphitization of microgram carbon samples and 14C AMS measurement', *Nuclear Instruments and Methods in Physics Research, Section B: Beam Interactions with Materials and Atoms*. Elsevier, 438(January 2018), pp. 58–65. doi: 10.1016/j.nimb.2018.08.004.

Wang, J. A. *et al.* (2022) 'Losses of Tree Cover in California Driven by Increasing Fire Disturbance and Climate Stress', *AGU Advances*, 3(4). doi: 10.1029/2021AV000654.

Wiggins, E. B. *et al.* (2018) 'Smoke radiocarbon measurements from Indonesian fires provide evidence for burning of millennia-aged peat', *Proceedings of the National Academy of Sciences of the United States of America*, 115(49), pp. 12419–12424. doi: 10.1073/pnas.1806003115.

Williams, A. P. *et al.* (2019) 'Observed Impacts of Anthropogenic Climate Change on Wildfire in California', *Earth's Future*, 7(8), pp. 892–910. doi: 10.1029/2019EF001210.

Williamson, G. J. *et al.* (2016) 'A transdisciplinary approach to understanding the health effects of wildfire and prescribed fire smoke regimes', *Environmental Research Letters*. IOP Publishing, 11(12). doi: 10.1088/1748-9326/11/12/125009.

Chapter 5

Conclusion

5.1. Summary of results

The goal of my dissertation was to explore fuel consumption and its influence on emissions in California's Sierra Nevada mountains. I accomplished this by combining field and laboratory techniques, centered around radiocarbon (^{14}C) analyses of fuels and fire-emitted fine particulate matter ($PM_{2.5}$), to estimate fuel consumption for wildfires and understand the influence of fuel composition on emissions in wildfire and prescribed fire.

In Chapter 2, I analyzed the relationships among fire growth, climate variables, firefighting resources, and damages from wildfires to better understand some of the challenges to fire suppression in California. Specifically, I aimed to investigate the drivers of fire growth in the Sierra Nevada when multiple large fires occur at once and understand how this influences the allocation of firefighting resources and damages from fires. I found that wildfires occurring simultaneously in the Sierra Nevada responded to similar broad-scale weather patterns, resulting in synchronized growth between the Dixie and Caldor Fires, two of the largest wildfires during California's 2021 fire season. The greatest damages from fires occurred shortly after the instances of greatest fire growth. Further, resources were allocated similarly across the the Dixie and Caldor Fires, suggesting that already-limited resources are spread even farther, rather than concentrated, in response to extreme fire growth in fires burning across different socioecological landscapes. However, the KNP Complex Fire, which burned through more forested area and threatened fewer

structures but more natural resources, received fewer firefighting resources This provides insight into some of the challenges to fire suppression efforts to protect life, property, and natural resources when multiple large fires burn simultaneously, highlighting the need for fuel management strategies as climate conditions become more conducive to extreme fire behavior.

In Chapter 3, I measured the total carbon and ^{14}C composition of fire-emitted $PM_{2.5}$ in the 2021 KNP Complex Fire to estimate the mean age of combusted fuels and better understand the influence of fuel composition on fire-emitted $PM_{2.5}$. I observed a mean age of 40 years for the fuel combusted in the fire, suggesting a significant contribution from larger dead fuel classes, which accumulated over multiple decades, to $PM_{2.5}$ emissions. These findings support previous work suggesting that the legacy of fire suppression in California has contributed to increased fire severity in the Sierra Nevada by allowing fuel accumulation over several decades.

In Chapter 4, I estimated fuel consumption and characterized the composition of $PM_{2.5}$ emissions and fuels for a prescribed fire in the central Sierra Nevada mountains to further understand the influence of fuel composition on the ^{14}C composition of $PM_{2.5}$ from landscape fires. From my ground-based fuel inventories, I found a significant contribution from larger dead fuel classes to total fuel consumption, which was also reflected in the ^{14}C composition of fire-emitted $PM_{2.5}$ estimated from a Keeling plot approach. This suggests that larger dead fuel classes may contribute significantly to $PM_{2.5}$ emissions during initial applications of prescribed fire in landscapes with similar fuel composition, resulting in elevated concentrations of $PM_{2.5}$ that is associated with

combustion of larger-diameter dead fuels. I also measured the ^{14}C composition of different fuel classes and combined it with my estimates of fuel consumption to calculate a bottom-up estimate of fire-emitted $PM_{2.5}$. This represents the first comparison of the observed ^{14}C composition of fire-emitted $PM_{2.5}$ in California to the ^{14}C composition of fire-emitted $PM_{2.5}$ estimated using ^{14}C measurements of actual fuels combusted. Agreement between in fuel mean $\Delta^{14}C$ and age inferred from these different approaches suggests that these methods can effectively be used to monitor fuel consumption in prescribed fires.

My work helps us better understand the influence of fuel composition on emissions in landscape fires in the Sierra Nevada, which is critical to quantifying the impacts of wildfires and fuel treatments. Together, these chapters conclude that fuel accumulation in the Sierra Nevada contributes to fires that are harder to contain and that we can infer fuel consumption from the ^{14}C composition of fire-emitted $PM_{2.5}$.Further, these methods have the potential to help evaluate the effectiveness of prescribed fire, reducing a barrier to its rapid and widespread implementation so that we can effectively manage fuels as a control on fire severity in a warming climate.

5.2. Future research directions

5.2.1. Radiocarbon analyses of other carbonaceous $PM_{2.5}$ fractions

In this work, I focused my analyses on $PM_{2.5}$ not only because of its relevance to air quality and public health concerns, but also because, compared to many other species found in smoke, it is relatively easy to sample, requiring only a short sampling duration to collect sufficient mass, and

it easier to prepare for ^{14}C analysis. We were able to collect massive enough $PM_{2.5}$ samples to analyze total carbon (TC) for ^{14}C but not enough to split TC into its organic carbon (OC) and black carbon (BC) fractions. However, OC and TC have very similar ages in heavy smoke because TC is composed primarily of TC (Mouteva *et al.*, 2015). BC is especially important for public health concerns (Reisen *et al.*, 2018; Burke *et al.*, 2021), so understanding the influence of fuel composition specifically on the ^{14}C of BC could be helpful for further quantifying the effects of landscape fires on public health. Further, BC is typically associated with flaming combustion (Andreae and Gelencsér, 2006), therefore analyzing the fractions of $PM_{2.5}$ separately could help strengthen the linkages among fuel composition, combustion phase (e.g., smoldering versus flaming), and emissions. Future work in this research area should therefore include radiocarbon analysis not only of TC, but also of other carbonaceous components of $PM_{2.5}$ including OC and BC.

5.2.2. Collecting $PM_{2.5}$ samples using a higher volume aerosol sampler

As outlined in Section 5.2.1, one of the main advantages to measuring the TC of $PM_{2.5}$ is that sufficient mass can be sampled over a short duration. Further, one of the limitations to splitting sampled $PM_{2.5}$ into its carbonaceous fractions is the mass collected. While our methods allow extraction and ^{14}C analysis of TC quantities as small as 2 μgC and particularly because TC typically comprises only a small fraction of BC, more massive samples must be obtained to perform OC/BC analyses. Smaller samples are also associated with larger uncertainties in ^{14}C analysis, so larger samples confer the additional advantage of reducing measurement uncertainty.

While samples could be collected over a longer period of time with the low-volume aerosol sampler used in these studies, this can result in samples that represent a mixture of different sources, rather than just the fire. I propose that a high-volume aerosol sampler would be more effective for collecting larger samples. Currently available high-volume aerosol samplers are more costly and less portable, but could be especially useful with sufficient planning and access to an adequate power supply.

5.2.3. Sampling a fire from multiple locations simultaneously

In Chapter 3 of this dissertation, $PM_{2.5}$ was collected using a sampler at a stationary location for a period of 26 hours. In Chapter 4, the sampler was relocated over the course of the fire. In both cases, only one sample was collected at a time. We assume that the observed $PM_{2.5}$ represents a mixture of the background atmosphere and the wildfire endmember (combusted fuel). The Keeling plot approach, which is used to estimate the mean $\Delta^{14}C$ of the combusted fuel, assumes that these sources remain constant. The strong correlation observed for the Keeling plot regressions in Chapters 3 and 4 give us confidence that the background and combusted fuel actually remained constant over the course of sampling, but this could be further verified by measuring the ^{14}C of $PM_{2.5}$ and applying the Keeling plot approach to samples collected at multiple sites downwind of the fire simultaneously. Additionally, analyzing the OC and BC fractions separately as proposed in Section 5.2.1, could confirm that the OC/BC ratio does not change (significantly) during smoke transport, further suggesting that selection of a sample site downwind of the fire is the main

requirement for collecting representative samples of the fire and that transport distance does not influence observations.

5.2.3. Extending methods to other forested ecosystems

In addition to collecting more samples over the course of a fire and sampling from multiple locations, sampling in different types of forested ecosystems could help elucidate the differences in the relationships between fuel composition and emissions for other parts of California that experience wildfire. The work in this dissertation was focused on the dry mixed-conifer forests of the Sierra Nevada, but other important fire-prone ecosystems in California include the conifer forests of the San Gabriel and San Bernardino Mountains (Southern California mountain ranges) and the moist-conifer forests of the coastal mountain ranges. Wildfires are a pervasive event across the state, and understanding the impacts of the legacy of fuel suppression on fuel composition and emissions in the Sierra Nevada is a key part of mitigating the effects from wildfires, but more work should be done to further quantify the relationships between fuels and emissions for the rest of the state.

5.2.4. Systematizing ground-based fuel inventories to complement ^{14}C analyses

An important consideration for interpreting the $\Delta^{14}C$ of fire-emitted $PM_{2.5}$ is that more enriched $\Delta^{14}C$ signatures like those observed in Chapter 3 and 4 can be associated with both larger fuel classes and older material in the organic soil layer of forested ecosystems. Unless the area was burned frequently (which consumes the deeper organic soil horizons and lowers the mean age of

the more shallow organic horizons; Pellegrini *et al*., 2021), we must assume that organic horizons were consumed in the KNP Complex Fire along with larger dead fuel classes. However, for Chapter 3, we were limited in our ability to apportion fuel consumption between large dead fuel classes and organic soil layers because we did not collect depth of burn measurements. In Chapter 4, we did collect depth of burn measurements, but we were unable to confidently convert depth of the organic layers consumed to a mass of fuel and estimate its contribution to observed $PM_{2.5}$ $\Delta^{14}C$, as we did with other fuel classes. Additionally, our mass consumption estimates for larger fuel classes were associated with large errors, which could be avoided by collecting more samples in the field. Future work using these methods should consider a more systematized approach for sampling fuels in the field to bolster mass consumption estimates and ^{14}C analyses.

5.2.5. Monitoring the $\Delta^{14}C$ of $PM_{2.5}$ from repeat applications of prescribed fire

Lastly, I propose that these methods be applied to repeat applications of prescribed fire to understand the relationship more thoroughly between fuel composition and fire-emitted $PM_{2.5}$ and further enhance estimates of fuel consumption.

In this work, I propose that the $\Delta^{14}C$ of $PM_{2.5}$ emissions from prescribed fire should decreased as larger fuel classes are removed from the landscape. However, as described in Section 5.2.4, the contribution from the combustion of organic soil layers remains uncertain without estimates of the mass of fuel corresponding to the depth of organic layers burned. If future fires burn through landscapes with fewer large dead fuels on the surface but $PM_{2.5}$ remains the same, this might

suggest that organic soil combustion is significant to emissions in a way that my work has not been able to investigate.

The State of California recently invested $1.5 billion to enhance forest health and resilience to wildfire, including funding to increase the capacity of the California Department of Forestry and Fire Protection to respond to wildfires but also for expanding fuel treatments like mechanical thinning and prescribed fire. With the improvements to my methods proposed in this Section 5.2, I believe that they can help reduce one of the barriers to the rapid and widespread implementation of prescribed fire, which is a means to evaluate its effectiveness. Another barrier to this expansion is an understanding of the air quality and public health implications of prescribed fire. My methods may allow us to better understand the fuel sources of fire-emitted $PM_{2.5}$, and therefore the composition and expected concentrations of this pollutant. Overall, I hope that these methods can be a useful complement to ground- and satellite-based approaches for estimating fuel consumption and understanding its influence on emissions in wildfire and prescribed fire across California.

5.3. References

Andreae, M. O. and Gelencsér, A. (2006) 'Atmospheric Chemistry and Physics Black carbon or brown carbon? The nature of light-absorbing carbonaceous aerosols', *Atmos. Chem. Phys*, 6, pp. 3131–3148. Available at: www.atmos-chem-phys.net/6/3131/2006/.

Burke, M. *et al.* (2021) 'The changing risk and burden of wildfire in the United States', *Proceedings of the National Academy of Sciences of the United States of America*, 118(2), pp. 1–6. doi: 10.1073/PNAS.2011048118.

Mouteva, G. O. *et al.* (2015) 'Black carbon aerosol dynamics and isotopic composition in Alaska linked with boreal fire emissions and depth of burn in organic soils', *Global biogeochemical cycles*, pp. 1977–2000. doi: 10.1002/ 2015GB005247.

Pellegrini, E., Boscutti, F., Alberti, G., Casolo, V., Contin, M., & De Nobili, M. (2021). Stand age, degree of encroachment and soil characteristics modulate changes of C and N cycles in dry grassland soils invaded by the N2-fixing shrub Amorpha fruticosa. *Science of the Total Environment*, *792*, 148295

Reisen, F. *et al.* (2018) 'Ground-Based Field Measurements of PM2.5 Emission Factors From Flaming and Smoldering Combustion in Eucalypt Forests', *Journal of Geophysical Research: Atmospheres*, 123(15), pp. 8301–8314. doi: 10.1029/2018JD028488.

Appendix A

$PM_{2.5}$ Sampling Procedure Using MiniVol Tactical Air Sampler

Adapted from MiniVol Tactical Air Sampler (TAS) manual (available at: https://d3pcsg2wjq9izr.cloudfront.net/files/1356/download/311370/4.pdf) by A. Odwuor (December 2023)

Materials

- Tripod
- MiniVol sampler and parts
    - Charged battery pack
    - Inlet assembly
    - Filter holder
    - Filter cassette
    - $PM_{2.5}$ impactor
    - PM_{10} impactor
    - Impactor adaptor
- 47 mm diameter quartz fiber filters, pre-combusted at 500ºC for 3 h and stored in clean aluminum foil envelopes inside zippered plastic bags
- Small forceps
- Deionized (DI) water
- Compressed air duster
- Kimwipes

- Aluminum foil
- Computer and spreadsheet software

Preparing the sampler

1. Mount sampler on tripod.
2. Place charged battery pack in sampler. Record the number of the battery pack.
    a. The sampler comes with 2 battery packs.
3. Set the real-time clock
    a. DAY SET: Hold down the CLOCK button and press the WEEK button until the correct day appears at the top of the display.
    b. TIME SET (Hour): Hold down the CLOCK button and press the HOUR button until the display indicates the correct hour. You may have to cycle through the hours twice to obtain the proper AM or PM (on the left side of the display). Seconds will automatically reset to zero.
    c. TIME SET (Minutes): Hold down the CLOCK button and press the MIN button until the display indicates the correct minutes. Seconds will automatically reset to zero.
4. Calculate flow rate according to the following equation:

$$I_{sp} = \frac{5.0 \times \sqrt{\frac{P_{act}}{P_{std}} \times \frac{T_{std}}{T_{act}}) - b_{vol}}}{m_{vol}}$$

where I_{sp} = flowmeter set point, liters/minute (lpm)

P_{std} = standard atmospheric pressure, 760 mmHg

T_{std} = standard temperature, 298 K°

P_{act} = actual ambient pressure, mmHg

T_{act} = actual ambient temperature, K°

m_{vol} = the sampler's calibration slope, supplied by the MiniVol Portable Sampler NIST Traceable Flow Calibration" that came with the sampler

b_{vol} = the sampler's calibration intercept

This ensures that actual flow rate is maintained at 5 lpm.

5. Set flow rate on sampler by slowly turning the Flow Rate Adjustment Knob until the air flow is set at the desired level.
6. Record ambient conditions and set flow rate for each sample in spreadsheet. See Fig. A1 for example of spreadsheet fields.

Installing the filter for sampling

All filter handling should be done while wearing latex gloves and on clean surfaces covered in aluminum foil. Make note of which filter holder assembly is being used (the sampler comes with 2 filter holder assemblies).

1. First clean forceps, inlet assembly, impactors and adaptor, and entire filter holder except for the mesh screen of the filter cassette using DI water and Kimwipes. Dry using duster.
2. For mesh screen in filter cassette, dry using duster only.
3. Using forceps, place pre-combusted quartz fiber filter in the filter cassette on top of clean mesh screen. Limit contact with the filter to its edge. Avoid bending or folding filter.
4. Re-assemble filter cassette and place in filter holder according to Fig. A2.
5. Assemble inlet, impactors, and filter holder according to Fig. A2.
6. Attach filter assembly to MiniVol^{TM}. The fully assembled sampler is shown in in Fig. A3.
7. Ensure that foil envelope and plastic bag are labeled with the sample ID.
    a. Select a descriptive but concise sample ID, ideally including the sample location or campaign, sequential number, date, and sample length.
8. Record sample information in spreadsheet.

Sample/Blk #	Sample ID	intended sample length (hr)	Filter assembly	Battery #	start								
					time (PT)	time (UTC)	batt elapsed time (hr)	AirTemp_Avg (C)	temp used (C)	temp (K)	BP (pressure, mbar)	pressure (mmHg)	calculated set flow rate (lpm)

end								total run time
time (PT)	time (UTC)	batt elapsed time (hr)	temp (C)	temp (K)	pressure (mbar)	pressure (mmHg)	flow rate (lpm)	h

Figure A1. Suggested fields for spreadsheet for collecting sample information.

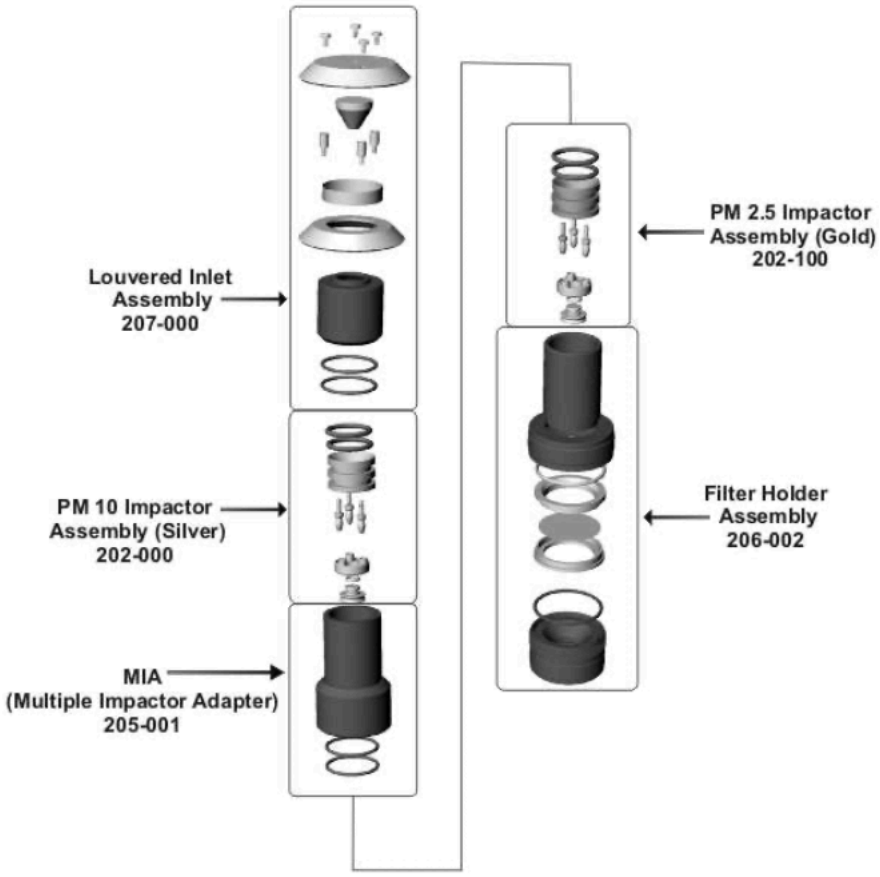

Figure A2. Filter holder assembly and inlet for sampling (from MiniVol TAS manual)

Figure A3. MiniVol sampler fully assembled and mounted on tripod.

Installing a blank filter (field blank)

1. Open foil envelope containing filter along one edge.
2. Place foil envelope in zippered plastic bag and leave bag open.
3. Secure plastic bag to the inside of the sampler door using tape.
4. Record blank filter information in spreadsheet.

Collecting a $PM_{2.5}$ sample

1. Set the desired sample start (power-on) and end (power-off) times
    a. Press the PROG button once. 1^{ON} will appear near the lower left corner of the display indicating that the
    b. Press the HOUR and MIN buttons to enter the power-on time for the first cycle.
    c. Press the WEEK button to select the desired day.
    d. After you have entered the power-on time and date for the first cycle, press the PROG button. 1^{OFF} now appears on the display to indicate that the power-off time for the first cycle is ready to be programmed. Repeat steps 2a-c to enter the desired power-off time.

2. Place the sampler in “Auto” mode by pressing the “ON/AUTO/OFF” button twice (until the bar is above the "AUTO" legend). The sampler will turn on at the desired time and the sample will be collected until the programmed end time.
3. Record sample start time, battery elapsed time, and intended sample length in spreadsheet.

Removing the sampled filter

1. Make sure that the sampler is off before removing filter holder assembly and inlet.
2. Unscrew filter holder and remove filter cassette.
3. Using clean forceps, remove filter from filter holder cassette. Replace in its original foil envelope.
4. Store sampled filters in foil envelopes inside zippered plastic bags in the freezer until analysis.
5. Record sample end time, flow rate, battery elapsed time, ambient conditions, and total run time in spreadsheet.
6. Once all samples have been collected, clean entire inlet and filter assembly, cover in aluminum foil, and store in a plastic bag until next use.

MiniVol storage and maintenance

Do not store sampler with battery pack in place.

Replace O-rings as necessary (at first signs of wear).

Refer to manual for further maintenance and service instructions.